Strategies for Effective Membrane Distillation Operation during Treatment of High Strength Industrial Wastewater

Maedeh Nadimi

BSc, MSc

Thesis submitted for the fulfilment of the requirements for the degree of

Doctor of Philosophy

Victoria University, Australia

Institute for Sustainable Industries and Liveable Cities (ISILC)

August 2024

Abstract:

Membrane distillation (MD) is a promising technology for producing high-quality distillate from highly concentrated industrial process wastewater streams containing dyes (e.g. from textile industries, paper and pulp industries, and pharmaceutical industries). Despite its potential, MD faces significant challenges, including organic fouling and feed liquid breakthrough (wetting), exacerbated by the presence of the high-strength dye solutions containing substantial amounts of salts. These challenges can be addressed by either oxidation of the dyes to increase their hydrophilicity or enhancing the hydrophilicity of the membrane surface. This research, therefore, explores these two primary methods to overcome these MD performance challenges involving the integration of sulphate radical-based advanced oxidation processes (SR-AOPs) and the development of hydrophilic surface modifications on commercial MD membrane.

The initial focus of this research is the integration of SR-AOPs with MD to enhance system performance. Oxone was applied as an oxidant under various conditions, including without pH adjustments, with pH adjusted to approximately 6.7, and considering the isolated effects of acidic conditions induced by hydrochloric acid. A key observation was that while the addition of Oxone delays the onset of wetting, it fails to improve MD flux or reduce fouling. This limited effect can be attributed to the high salinity and high organic concentrations in the feed, leading to the identification of a likely effect known as salting-out. Further testing by increasing Oxone dosing or reducing the organic load could potentially enhance the degradation of MB and potentially improve MD performance even at higher salt concentrations, but the dose amounts became impractically high.

In another approach to address dye fouling and wetting challenges, this study applied hydrophilic surface modifications using polydopamine (PDA). This was guided by literature as a means to increase hydrophilicity and decreasing foulant adhesion. The success of PDA modification was confirmed by water contact angle and identification of functional groups by FTIR analysis. Despite the confirmed functional surface improvement, MD testing found wetting was only delayed and not prevented. This corroborated with the Oxone testing results that the challenge is further complicated by the diverse interactions among ions, water molecules, and nonelectrolytes (e.g. organic material) in high salinity environments. This can outweigh any changes (even major changes) to either solute or membrane surface chemistry, giving motivation towards an investigation into salting-out effect.

The dedication towards understanding the science behind the salting-out effect was therefore due to its demonstrated significant role in MD performance, acting to decrease the solubility of organics and causing them to precipitate in high-salt solutions. This phenomenon has not previously been investigated within the context of MD. The influence of salting-out was quantitatively assessed by measuring the Setschenow/salting-out constant for a specific MD foulant. Another key finding of this research is the direct correlation established between MD flux, the solubility of MB, and the mass of MB aggregates. Additionally, the identification of a critical mass threshold for these aggregates that triggers wetting provided a new and practical means to predict the impact of salting-out on both flux behaviour and wetting in MD processes.

In conclusion, this study confirmed that SR-AOPs and hydrophilic modifications provide limited mitigation against wetting while concentrating high salinity industry dye wastes where MD is likely to be practically applied. Salting-out was confirmed to be a dominant effect influencing MD performance. Future work should integrate reactive processes with MD using salting-out theory and explore its applicability to other compounds and membranes. These efforts aim to advance technologies for economically viable zero liquid discharge (ZLD) of highly concentrated wastewaters, enhancing sustainability and efficacy across various industries.

Declaration of Authenticity

“I, Maedeh Nadimi, declare that the PhD thesis entitled “Strategies for Effective Membrane Distillation Operation during Treatment of High Strength Industrial Wastewater ” is no more than 80,000 words in length including quotes and exclusive of tables, figures, appendices, bibliography, references and footnotes. This thesis contains no material that has been submitted previously, in whole or in part, for the award of any other academic degree or diploma. Except where otherwise indicated, this thesis is my own work”. “I have conducted my research in alignment with the Australian Code for the Responsible Conduct of Research and Victoria University’s Higher Degree by Research Policy and Procedures.”

[redacted]

01/08/2024

Dedicated to my Family

Acknowledgements

This dissertation has been completed thanks to the guidance and support of many individuals who provided their invaluable assistance in various capacities.

My PhD journey has been a profound and challenging experience, particularly as this research was conducted during the COVID-19 pandemic, a time that I could not have navigated alone. First and foremost, I would like to express my deepest gratitude to my supervisors, Professor Mikel Duke, Professor Xing Yang, and Professor Rong Wang. Their unwavering support, insightful guidance, and encouragement have been pivotal in shaping my research and helping me grow as a scholar. Mikel’s mentorship has significantly honed my critical thinking skills, while Xing’s early and continuous support, even from KU Leuven, has been instrumental in directing and refining my work. Rong’s thorough insights and meticulous feedback from proposal to final manuscript have consistently enhanced the quality of my research.

I am immensely grateful to my parents, Mohammad and Masoumeh, and my siblings, Elham and Elaheh, for their unconditional love and support. Their encouragement and belief in my abilities have been a constant source of motivation, helping me overcome numerous challenges along the way.

Special thanks to my colleagues, whose wisdom and camaraderie have been invaluable. I appreciate the insights and opinions shared by Stephen Gray, who has supported me whenever I reached out to him. Thanks also to Noel Dow, Jianhua Zhang, Marlene Cran, and Khalid Moinuddin for their assistance at different project stages. I extend my gratitude to Stacey Lloyd, Nishantha Illangantilaka, Larruceo (Larry) Bautista, and Mary Marshall for their technical assistance and support in providing facilities, equipment, and going above and beyond with lab-related issues.

I am also thankful to Mahdi Shahrooz, Afshin Ziarati, and Mona Ghorbani for their invaluable support in critical moments.

I extend my sincere thanks and appreciation to the South East Water Organization, both the research and development team and the planning and delivery team, for their

continuous support. Special thanks to Li Gao, David Bergmann, and Joel Segal, both as mentors and as my managers, for supporting me during this challenging journey.

Lastly, this journey would not have been the same without the companionship and inspiration from friends like Derrick D'Souza, Malavika Arun, Davor Daniloski, Elaheh Ahmadi, Laryssa Pereira, Marta Vasconcelos, Sarani Kannangara, Lavern Nyamutswa, Charleston Bezerra. Their engaging discussions and encouragement have been a source of strength throughout my PhD journey.

I extend my gratitude to the Australian Research Council (ARC) (DP170102391) for their financial support, which made this research possible.

To everyone who has been a part of this journey, thank you for your support, guidance, and friendship. This accomplishment would not have been possible without you.

MAEDEH NADIMI

DETAILS OF INCLUDED PAPERS: THESIS WITH PUBLICATION

Chapter No.	Publication Title	Publication Status	Publication Details
		Published **Accepted for publication** **In revised and resubmit stage** **Under review** **Manuscript ready for submission**	**Citation, if published** **Title, Journal, Date of acceptance letter and Corresponding editor's email address** **Title, Journal, Date of submission**
2	Process intensification with reactive membrane distillation: A review of hybrid and integrated processes	Published	M. Nadimi, M. Shahrooz, R. Wang, X. Yang, M.C. Duke, Process intensification with reactive membrane distillation: A review of hybrid and integrated processes, Desalination. 573 (2024) 117182. https://doi.org/10.1016/j.desal.2023.117182.

Declaration by: Maedeh Nadimi **Signature:** Maedeh Nadimi **Date: 14/08/2024**

CONFERENCE PROCEEDINGS

1. Maedeh Nadimi, Mahdi Shahrooz, Rong Wang, Xing Yang, Mikel C. Duke, Unravelling the Impact of Salting-Out Phenomena on Fouling and Wetting in Membrane Distillation for High-Salinity Waste Streams, 6th International Conference on Desalination using Membrane Technology (MEMDES2023) (19-22 November 2023), Meliá Sitges Hotel Congress Centre, Sitges, Spain. (Oral presentation)
2. Maedeh Nadimi, Mahdi Shahrooz, Rong Wang, Xing Yang, Mikel C. Duke, Unravelling the Impact of Salting-Out Phenomena on Fouling and Wetting in Membrane Distillation for High-Salinity Waste Streams, The International Workshop on Membrane in Kobe (iWMK2023) (16-17 Nov 2023), Kobe University, Japan. (Poster presentation)
3. Maedeh Nadimi, Mahdi Shahrooz, Rong Wang, Xing Yang, Mikel C. Duke, Membrane distillation of high-strength saline dye solution: effects of salting-out, solution chemistry, and oxidation, 11th International membrane science& technology conference (IMSTEC2022) (4-8 DEC 2022), Monash University, Melbourne, Australia. (Oral presentation)
4. Maedeh Nadimi, Mahdi Shahrooz, Rong Wang, Xing Yang, Mikel C. Duke, Experimental and theoretical study of salting-out effect during membrane distillation for treating high salinity dye solutions, The 13th conference of Aseanian Membrane Society (AMS13) (4-6 July 2022), Nanyang Technological University, Singapore. (Oral presentation)
5. Maedeh Nadimi, Mahdi Shahrooz, Rong Wang, Xing Yang, Mikel C. Duke "Reactive membrane distillation for treatment of challenging organics in wastewaters", 8th MSA early career researcher (ECR) membrane symposium, 25 November 2021. (Oral presentation)
6. Maedeh Nadimi, Mahdi Shahrooz, Rong Wang, Xing Yang, Mikel C. Duke, "Membrane distillation coupled with oxidation processes for water/wastewater treatment: enhanced treatment capabilities, and future opportunities", The International Workshop on Membrane in Kobe (iWMK2021), 18th November 2021, Kobe University, Japan. (Poster presentation)
7. Maedeh Nadimi, Mahdi Shahrooz, Rong Wang, Xing Yang, Mikel C. Duke, "Process intensification with reactive membrane distillation for wastewater reclamation: a review", Membrane Desalination 2021 (MEMDES2021), 5th International Conference on Desalination using Membrane Technology, 14-17 November 2021. (Poster presentation)
8. Maedeh Nadimi, "Novel Integration of Membrane distillation and Advanced Oxidation Processes for Wastewater Treatment", Institute for Sustainable Industries and Liveable Cities (ISILC) HDR Student Research Conference, 3rd Dec 2020, Victoria University, Melbourne, Australia. (Oral Presentation)

Table of content

List of Figures

List of Tables

Chapter 1

Introduction

1.1 Background

Pollutant-free water is key to the motivation for development of water treatment technologies, including membrane and oxidation processes [10]. Importantly, due to population growth and industrialization, the associated increased water pollution must be addressed to ensure the public health and clean environment [11,12]. One of the most important organic pollutants is the residual dyes from various industries (e.g., textile industries, paper and pulp industries, and pharmaceutical industries), which are discharged into the water sources and cause harm to the environment and human health [13]. Also, inorganic compounds (e.g., NaCl) can increase the salinity of water and affect the quality of water used for drinking, irrigation, and industry [14]. Therefore, the development of a membrane technology which is resistant to highly concentrated solutes is particularly important given the increasing pressure on water resources.

Desalination technologies have been employed to meet the freshwater need, in which membrane distillation (MD) has been considered to be a promising technology for water recovery and has received a strong focus on high salinity water treatment (including zero liquid discharge (ZLD)) applications [15]. The MD concept of operation, specifically the ‘direct contact’ mode, is shown in **Figure 1-1.** As can be seen, MD is a thermally driven membrane process involving a hydrophobic porous membrane, for the transport of vapour molecules through the membrane pores. Water evaporates at the membrane surface on the hot feed side before going through the pores of the membrane and condensing at the cooler permeate side. One of the main advantages of MD is a 100% theoretical rejection of non-volatile substances, making it a promising separation process for treating extreme concentrated solutions [16]. Due to this unique feature, MD has been implemented for the rejection of organics, producing high-quality distillate from wastewater, and/or recovery of valuable components in the remaining concentrate [17–19]. However, membrane fouling and wetting are major problems in MD occurring due to the high concentration of organic pollutants in the feed wastewater [16,20,21]. The chemistry of the membranes is one of the critical factors that affect the foulant-membrane surface interactions during fouling formation.

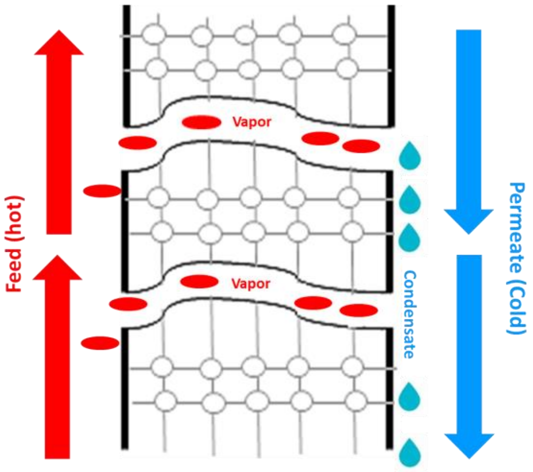

Figure. 1-1. The concept of the DCMD process.

Most of the membranes implemented for MD applications come from commercially available microfiltration membranes that have hydrophobic properties, or are tailored to be hydrophobic/superhydrophobic [22]. However, the hydrophobic nature of the membranes used in MD makes them susceptible to contamination when treating feed waters containing hydrophobic compounds due to hydrophobic-hydrophobic interactions, resulting in decreased membrane performance in terms of water throughput (flux) and solute rejection. Additionally, the presence of low-surface-tension organics such as surfactants eventually leads to membrane wetting by their unfavourable accumulation on the membrane surface [23].

Therefore, intensive research has been carried out to improve the membrane performance used in MD. In recent years, several strategies to actively prevent the fouling deposition on the membrane surface are emerging including oxidation and more robust membranes.

Introduction of oxidation processes to MD

Incorporating oxidation processes into MD has been an effective strategy to improve the fouling resistance of membranes through the decomposition/degradation of hydrophobic organic molecules or functional groups. Oxidation processes such as photochemical, chemical (e.g., ozonation), electrochemical oxidations, as well as biological processes have been integrated to MD. In oxidation processes, the degradation takes place by the generated reactive radicals such as OH° or other strong oxidizing agents. The radicals are formed via oxidants such as hydrogen peroxide (H_2O_2)) or the oxidation of water. To facilitate the generation of radicals, heterogeneous (the use of catalyst in a different phase from the solution, e.g., solid catalysts) or homogeneous catalysts (the use of catalyst in the same phase as the solution, e.g., metal ions) have been utilized [24,25].

As an alternative to other advanced oxidation processes (AOPs) utilizing photoactivated catalysts which normally pair with the OH^o radicals, the sulphate radical-based advanced oxidation processes (SR-AOPs) is an emerging concept, involving the introduction of sulphate radicals (SO_4^o) via persulphate (PS) or peroxymonosulphate (PMS). The SO_4^o radical offers many advantages such as better degradation efficiency, higher selectivity, longer lifetime, and higher oxidative potential, as compared to OH^o. Moreover, PMS and PS, as the origin of SO_4^o radicals, are relatively stable, and environmentally friendly [26–28]. Therefore, considering the ability of oxidation processes in transforming/degrading the organics, a synergistic coupled process design can further intensify the MD performance. However, despite their potential, the integration of SR-AOPs in MD, especially for handling high-strength wastewater, remains underexplored, revealing a gap in the current research.

Developing robust MD membranes

Another strategy to advance MD membrane technology focuses on developing membranes resistant to both fouling and wetting. This approach often involves the fabrication of a hydrophilic layer on top of a hydrophobic substrate, which significantly enhances the membrane's antifouling capabilities [29,30]. The application of a thin hydrophilic layer on the hydrophobic surface is believed to foster the formation of a hydration layer on the membrane, effectively minimizing foulant adsorption and thereby improving performance [30–32]. Inspired by the strong binding affinity of polydopamine (PDA) toward substrates of varying wettability, there has been a growing interest in using PDA for surface modification [33,34]. The PDA layer, rich in hydroxyl and amine groups, enhances hydrophilicity of membrane, thereby enhancing the MD performance.

The interaction between PDA and different substrates is primarily attributed to non-covalent interactions such as hydrogen bonding [34–36], coordination [33,37], and hydrophobic interactions [34,38]. However, the PDA deposition on most material surfaces has been reported to be a time-consuming process [30,33]. To address this problem, the use of oxidants [30,39–41] was considered to accelerate the dopamine polymerization. However, PDA-modified MD membranes offer many advantages in creating adhesion resistant membranes due to the hydrophilic properties, but they have not been thoroughly studied for treating high-strength wastewater containing organic matters. The novelty of this study lies in applying PDA-modified membranes to treat high-salinity dye wastewater, which presents greater challenges in terms of fouling and wetting. This approach extends the application of PDA-modified membranes to more complex, industrially relevant conditions, offering insights into their effectiveness under these demanding scenarios.

The effect of high salinity and solubility of organic compounds on MD performance:

In the presence of typical inorganic salts such as sodium and calcium minerals, the complexes formed by organic-inorganic components adjacent to the membrane surface may accelerate fouling formation, leading to severe flux reduction [12,15,16,21,42]. Meanwhile, with foulants of a high concentration (e.g., protein, dye), or foulants with less solubility (e.g., minerals such as calcium ions (containing Ca^{2+})), the concentration polarization can cause a foulant to go beyond its solubility and form a scale or gel layer and deteriorate the membrane flux over time [43,44].

A key factor that exacerbates fouling in high-salinity environments is the salting-out effect. This phenomenon occurs when high salt concentrations reduce the solubility of organic compounds, causing them to precipitate onto the membrane. Setschenow [45] first described an empirical relationship to explain this effect, which further complicates membrane fouling under high-salinity conditions. While salting out effect has yet to be extensively studied in MD research, it is commonly applied in fields like homogeneous liquid-liquid extraction, protein separation, and reactive dye isolation [46–48]. Additionally, membranes used in these applications, such as those for protein or dye separation, have exhibited reductions in flux or rejection rates.

This phenomenon is particularly of interest in high-strength wastewaters containing organics such as dyes. Methylene blue (MB) is a model organic dye due to its widespread use in industries such as textiles, pharmaceuticals, and paper, which generate significant volumes of wastewater containing organic dyes. The strength of the solutions is high, where textile industries for instance, discharge wastewater with high inorganic salt content (up to 6.0 wt% NaCl) from neutralization reactions during dye synthesis or as additives to enhance dye uptake in dyeing processes [44,49].

A study by Van der Bruggen et al. [50] explored an intensified hybrid process integrating nanofiltration (NF), reverse osmosis (RO), and MD for treating textile wastewater, highlighting MD's role in managing high-concentration waste. In their approach, NF is first used to remove and concentrate organic components which are fed to MD to concentrate prior to incineration. The dye-depleted NF permeate is followed by a second NF or RO to concentrate the remaining salts.

This aligns with the strategic choice in this study to simulate the targeted MD conditions with high concentrations of dyes and salts, providing a realistic setting for testing MD's capabilities for high-strength wastewater treatment. The goal is to assess MD's effectiveness in treating concentrated waste, while exploring its potential for recovering valuable products and minimizing waste volumes. Therefore, investigating how the salting-out effect influences fouling and wetting behaviours in MD systems will be critical for advancing MD's practical applicability in treating high-strength wastewater streams. This understanding will help broaden the capabilities of MD, particularly in applications such as zero-liquid discharge (ZLD), where high concentrations of salts and organics must be effectively managed.

1.2 Research objective

The primary aim of this research is to study the critical challenges and address the gaps identified in the field of MD, specifically those related to the treatment of high-strength wastewater streams. To achieve this aim, this study will develop a comprehensive understanding of how SR-AOPs and membrane surface modifications can mitigate issues of membrane fouling and wetting in MD, particularly when processing high-strength wastewater containing organic dyes and inorganic salts. Additionally, the study will investigate the impact of high-salinity conditions on the performance of MD, focusing on the phenomena of salting-out and its implications for flux decline and membrane wetting. Commercial membranes, including PVDF (native hydrophobic polymer) and Versapor (native omniphobic polymer), will be utilized to evaluate the efficiency and product quality of the MD process.

Through these approaches, the main objectives of this research are to:

1. Integrate SR-AOPs with MD to demonstrate the effectiveness to reduce membrane fouling;

2. Develop hydrophilic membrane surface modifications using PDA and test their effectiveness in improving the antifouling properties and wetting resistance of MD membranes in high-salinity conditions; and

3. Investigate the role of the salting-out effect in MD by quantifying its impact on the overall performance and enable prediction of performance limiting effects.

The study will utilize synthetic feeds containing a mix of organic contaminant and inorganic salt, with MB chosen as the model organic dye. A concentration of 3750 mg/L MB has been selected as it aligns with Van der Bruggen's research on the intensification textile wastewater processing, where the MD feed is from NF concentrate [50]. In terms of salinity, representative NaCl solutions should be in the range of 35 to 100 g/L.

1.3 Thesis outline

This dissertation is structured into seven chapters, outlined as follows:

Chapter 1: Introduction – A brief background on the current state of the art, its existing challenges, research gaps, and the objectives of the current research are summarized in this chapter;

Chapter 2: Literature review – This chapter presents a comprehensive analysis of 163 papers, summarizing the current state of the art in reactive MD processes;

Chapter 3: Materials and methods: This chapter provides a detailed overview of the materials, chemicals, and methods employed within this Ph.D. research;

Chapter 4: Limitations of MD in High-Salinity Dye Solutions: This chapter investigates and identifies the performance limitations of MD systems. It provides a preliminary examination of membrane fouling and wetting across a wide range of solution concentrations, including the combination of MB, Orange G, and NaCl. By exploring these conditions, the chapter aims to establish the operational limits and performance benchmarks using different types of membranes including PVDF and PTFE membranes. The results enable a comparison with state-of-the-art membrane technologies and help to identify areas for improvement in MD processes.

Chapter 5: Advanced oxidation assisted MD for wetting mitigation during treatment of high salinity dye solutions: This chapter analyses the integration of DCMD with SR-

AOPs to mitigate fouling in high-salinity dye solutions, particularly focusing on MB as the model pollutant;

Chapter 6: Surface modification to prevent wetting during MD with high salinity dye solutions: This chapter investigates the effects of hydrophilic surface modification on fouling elimination in MD for treating high-salinity dye solutions. The primary focus is on evaluating the performance of PDA-modified MD membranes in treating high salinity MB solution as the model pollutant. Through bench-scale MD experiments, this chapter aims to determine the extent to which PDA modification can enhance membrane resistance to fouling and wetting, comparing the results to those obtained with unmodified commercial PVDF membranes.

Chapter 7: Salting-out effect during MD for treating high salinity dye solution : This chapter investigates the salting-out effect in MD for treating high-salinity dye solutions. Specifically, it focuses on MB as the model organic compound. Through detailed analysis, the chapter aims to understand how the salting-out phenomenon impacts fouling and wetting behaviours in MD processes. The objectives include measuring the Setschenow/salting-out constant for MB, calculating its solubility and mass aggregation during MD operation, and analysing the fouling and wetting behaviours during both batch and continuous operations.

Chapter 8: Conclusions and future work: This chapter summarizes the conclusions drawn from Chapters 4, 5, 6, and 7 and provides detailed recommendations for future research.

Chapter 2

literature review

Section 2.2 is based on the review article from *M. Nadimi, M. Shahrooz, R. Wang, X. Yang, M.C. Duke, Process intensification with reactive membrane distillation: A review of hybrid and integrated processes, Desalination. 573 (2024) 117182,* and mostly contains its content.

2.1 Declaration of co-authorship and co-contribution of the chapter

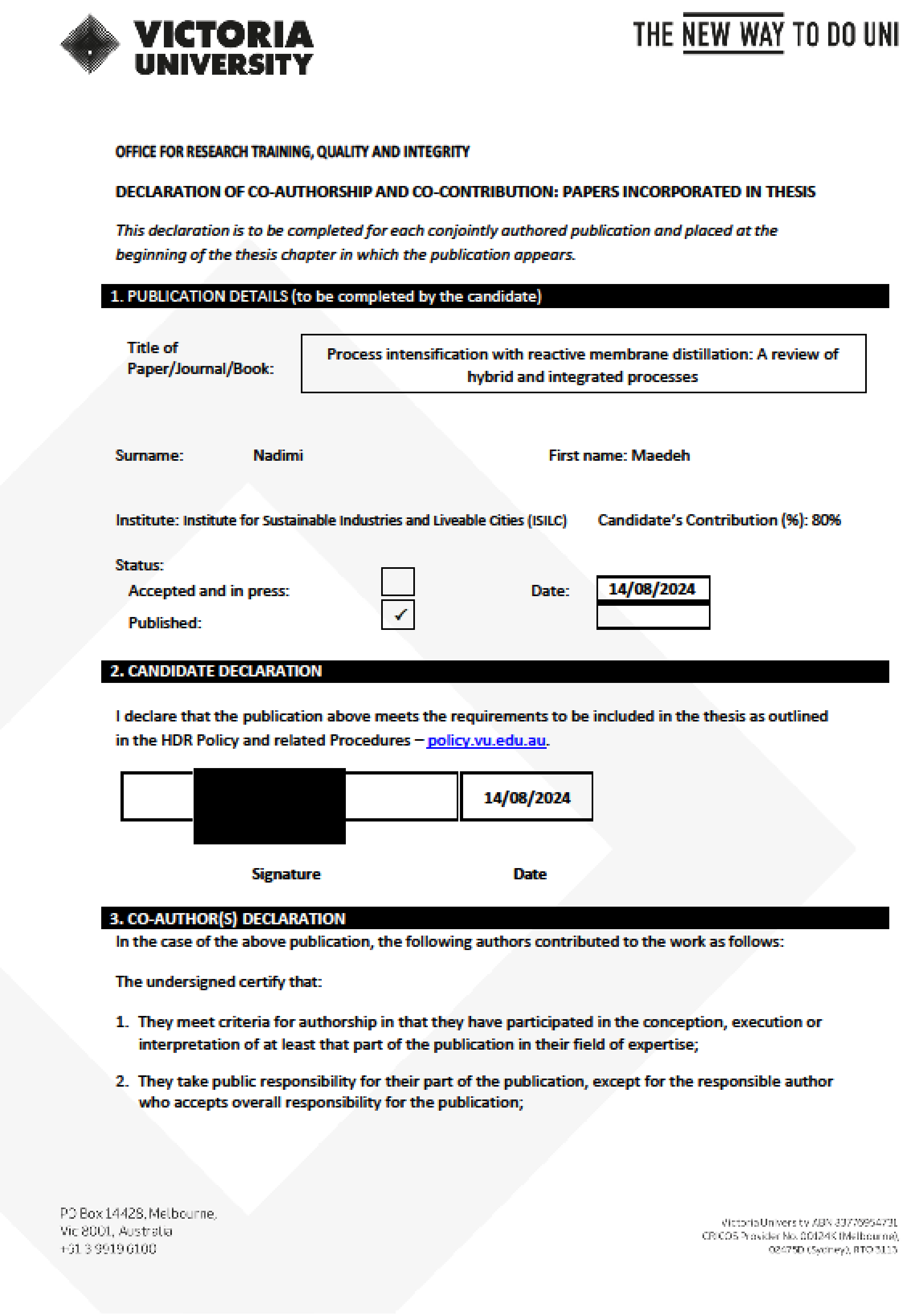

VICTORIA UNIVERSITY

THE NEW WAY TO DO UNI

OFFICE FOR RESEARCH TRAINING, QUALITY AND INTEGRITY

DECLARATION OF CO-AUTHORSHIP AND CO-CONTRIBUTION: PAPERS INCORPORATED IN THESIS

This declaration is to be completed for each conjointly authored publication and placed at the beginning of the thesis chapter in which the publication appears.

1. PUBLICATION DETAILS (to be completed by the candidate)

Title of Paper/Journal/Book: Process intensification with reactive membrane distillation: A review of hybrid and integrated processes

Surname: Nadimi

First name: Maedeh

Institute: Institute for Sustainable Industries and Liveable Cities (ISILC)

Candidate's Contribution (%): 80%

Status:

Accepted and in press: ☐

Published: ☑

Date: 14/08/2024

2. CANDIDATE DECLARATION

I declare that the publication above meets the requirements to be included in the thesis as outlined in the HDR Policy and related Procedures – policy.vu.edu.au.

[redacted]

14/08/2024

Signature **Date**

3. CO-AUTHOR(S) DECLARATION

In the case of the above publication, the following authors contributed to the work as follows:

The undersigned certify that:

1. They meet criteria for authorship in that they have participated in the conception, execution or interpretation of at least that part of the publication in their field of expertise;
2. They take public responsibility for their part of the publication, except for the responsible author who accepts overall responsibility for the publication;

PO Box 14428, Melbourne,
Vic 8001, Australia
+61 3 9919 6100

Victoria University ABN 83776954731
CRICOS Provider No. 00124K (Melbourne),
02475D (Sydney), RTO 3113

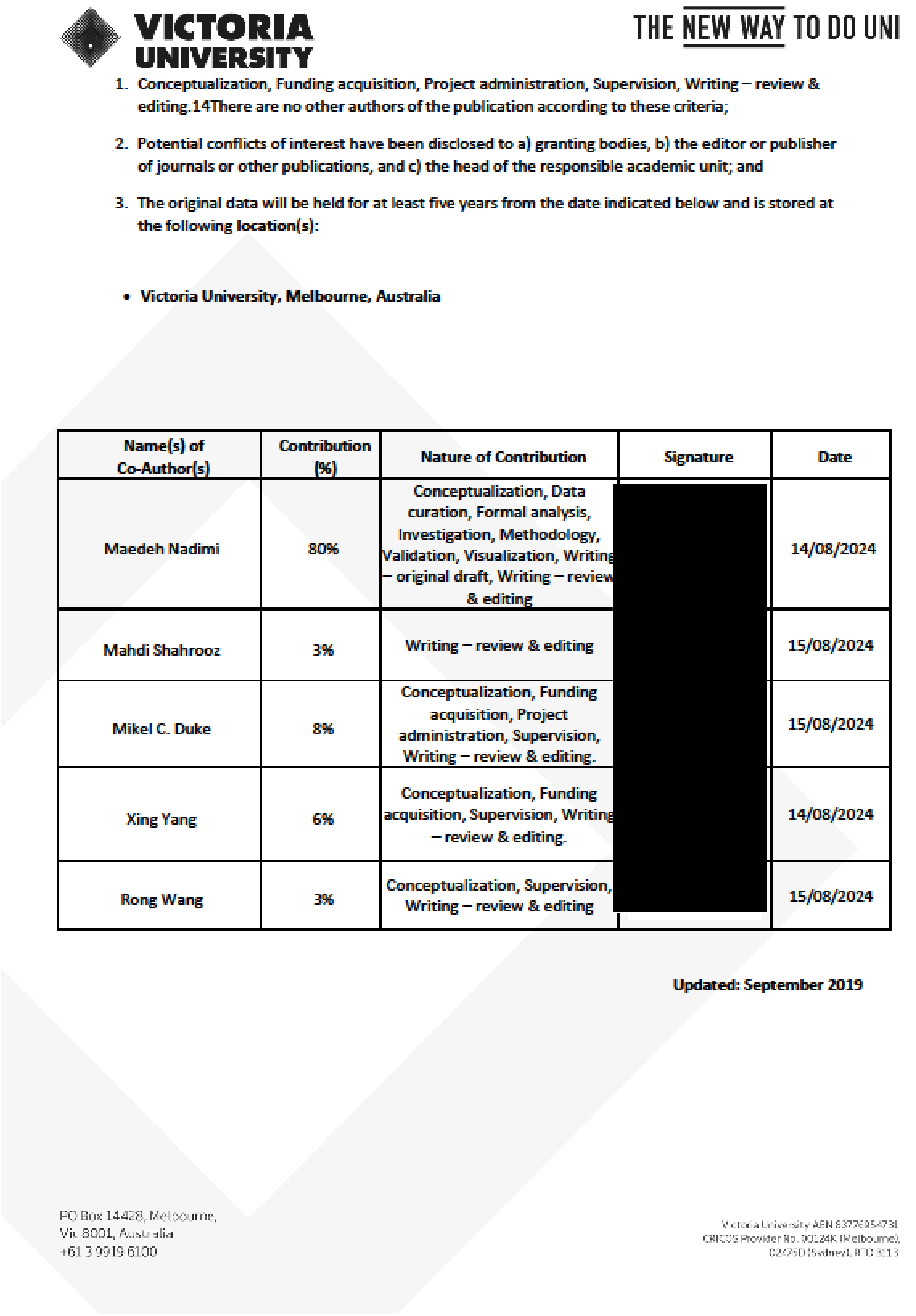

1. Conceptualization, Funding acquisition, Project administration, Supervision, Writing – review & editing.14There are no other authors of the publication according to these criteria;
2. Potential conflicts of interest have been disclosed to a) granting bodies, b) the editor or publisher of journals or other publications, and c) the head of the responsible academic unit; and
3. The original data will be held for at least five years from the date indicated below and is stored at the following **location**(s):

- **Victoria University, Melbourne, Australia**

Name(s) of Co-Author(s)	**Contribution (%)**	**Nature of Contribution**	**Signature**	**Date**
Maedeh Nadimi	80%	Conceptualization, Data curation, Formal analysis, Investigation, Methodology, Validation, Visualization, Writing – original draft, Writing – review & editing	[redacted]	14/08/2024
Mahdi Shahrooz	3%	Writing – review & editing	[redacted]	15/08/2024
Mikel C. Duke	8%	Conceptualization, Funding acquisition, Project administration, Supervision, Writing – review & editing.	[redacted]	15/08/2024
Xing Yang	6%	Conceptualization, Funding acquisition, Supervision, Writing – review & editing.	[redacted]	14/08/2024
Rong Wang	3%	Conceptualization, Supervision, Writing – review & editing	[redacted]	15/08/2024

Updated: September 2019

2.2 Fouling and wetting control strategies in MD involving reactions

While there are numerous recent reviews focusing on fouling and wetting in MD, no literature review has been conducted to categorize the MD processes that include reaction, highlighting the state of the art, identifying the research gaps, and analysing the benefits and limiting factors toward fouling and wetting resistance and pollutant degradation. Therefore, the aim of this review is to categorize the types of MD with reaction, analyse the current developments, limitations and future prospects in the combination of reactive processes with MD.

After reviewing the articles featuring MD and oxidation reactions, three main designs were identified as represented in Figure 2-1: (i) separated design (Figure. 2-1 a1, a2), where MD and oxidation is coupled as two individual processes; (ii) hybrid design (Figure. 2-1 b), where MD is coupled with oxidation in one single process; (iii) integrated membrane design by engineering the reactive membranes (Figure. 2-1 c), where reactive materials such as catalysts or electrically conductive materials are incorporated into/onto the membrane. It should be also noted that researchers have designed Janus membranes to assist in the mitigation of fouling, wetting and scaling [51]. Despite relevant hydrophilic-hydrophobic interfacing chemistry, this term has not so far been adopted by the researchers involved in catalytic MD.

In the first two designs of Figure 2-1 (a1 and a2), MD and oxidation are shown as two separate stand-alone units. Most studies focused on coupling MD with an oxidation step as pre-treatment (Figure 2-1 (a1)), aiming to degrade the pollutants that pose a fouling risk to the membrane surface prior to entering MD [52–56]. In the other design shown in Figure 2-1 (a2), oxidation has been served as the post-treatment unit to MD to decrease the environmental impacts of the concentrated MD feed solution [57]. As these are completely separate unit operations, this review will focus on the hybrid and integrated (Figure 2-1 b, and Figure 2-1 c) to analyse the coupled process where simultaneous degradation and rejection of the organic/inorganic contaminants happens which the MD process plays a role in the reaction behaviour.

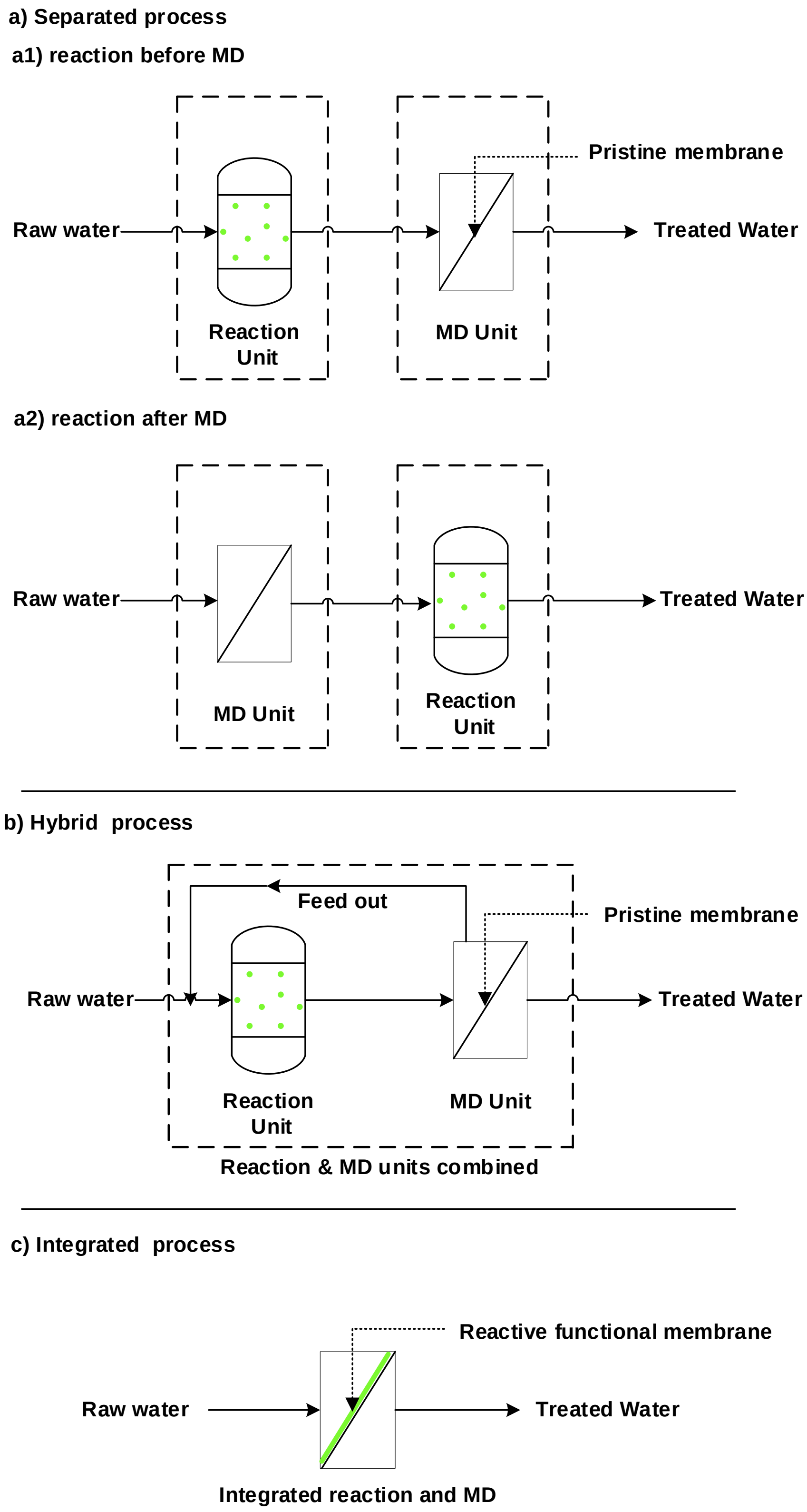

Figure. 2-1. Three main designs for coupling MD and catalytic reaction a) Separated process (reaction before and after MD, catalysts are shown in grown dots), b) Hybrid processes (with the catalyst causing reaction, shown in green colour dots, loaded into the feed tank), and c) Integrated processes (with the catalyst or electrode incorporated into/onto the membrane indicated as green line).

The introduction of reactions to MD in both hybrid and integrated design introduce several advantages at the membrane-water interface due to their overall contribution to (i) higher water recovery by simultaneously rejecting the non-volatile compounds and mitigating foulant deposition via oxidative degrading of organic foulants; (ii) consistent high-quality distillate by mitigating fouling and wetting; and (iii) potentially enhancing the oxidative reactions which can transform/ degrade the organic foulants. Therefore, with the benefits mentioned above, the coupled MD process can surpass the standalone MD in terms of fouling/wetting prevention and the ability to deal with various challenging feed streams that were previously not treatable by MD. For example, solutions containing oil and surfactants where increased flux and enhanced wetting resistance have been demonstrated successfully on coupled systems compared to the traditional DCMD mode [23,58].

2.2.1 Hybrid MD processes

2.2.1.1 MD/photochemical oxidation

Photochemical oxidation (photocatalysis or photolysis) is an important oxidation process studied in combination with MD. Photocatalysis relies on light absorption to generate radicals (e.g., OH° radicals). The reaction between the contaminants and reactive radicals can lead to the oxidation of the pollutants to CO_2 and H_2O, but more commonly to other intermediates [59–62] that has a lower fouling tendency. Photolysis is the decomposition of the target pollutant by light. However, photolysis suffers from the photostability of the contaminants or their by-products which hinders the process of decomposition [63–66]. As degradation of the pollutants is an important factor for intensifying MD performance, MD/photocatalysis is gaining increasing attention due to the more efficient removal of the contaminants than photolysis. **Figure 2-2** shows the basic schematic of MD/photocatalysis hybrid processes studied in the literature in two configurations: a) photocatalytic process before MD unit b) submerged photocatalytic MD reactor.

a) MD/photocatalysis

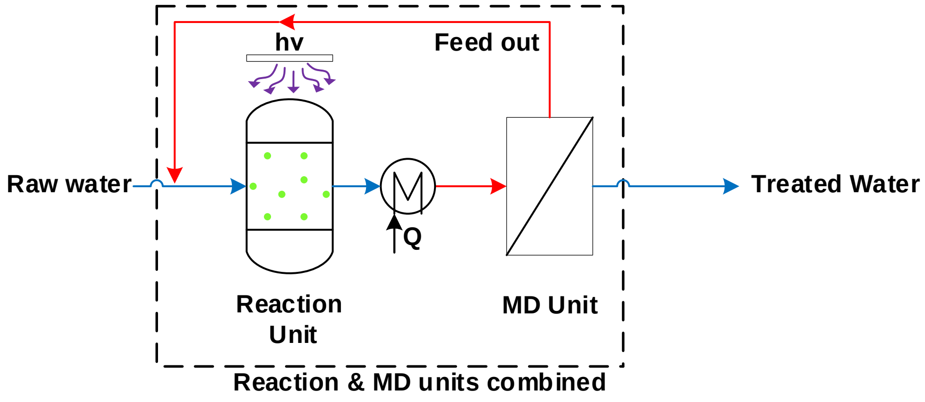

b)Submerged photocatalytic MD reactor

b1) Submerged MD into the reaction unit

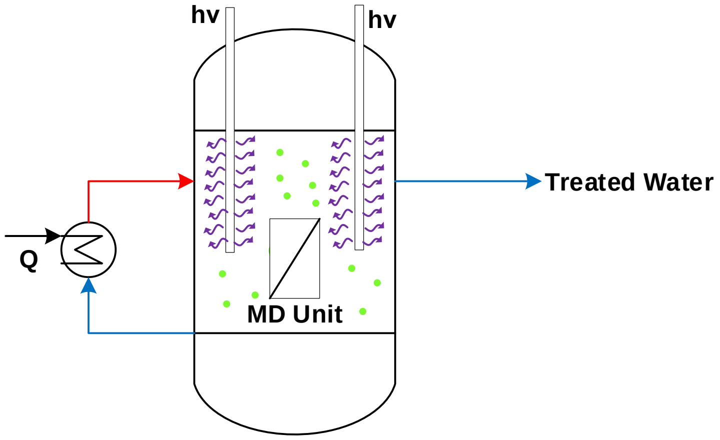

b2) Submerged MD into the feed tank

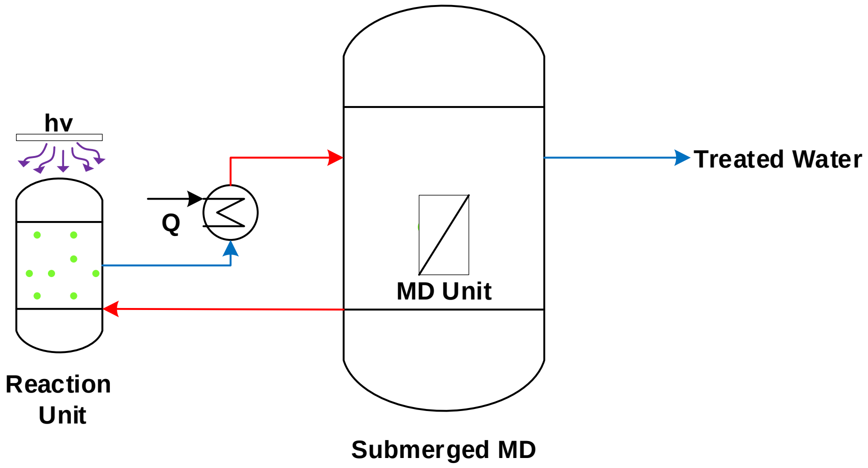

Figure. 2-2. The schematic of MD/photochemical oxidation hybrid process a) photocatalytic process before the MD system b) submerged photocatalytic MD reactor (process concepts redrawn from [65,67–71]). The green dots indicates the catalysts.

The MD/photocatalysis processes benefit from their ability to retain non-volatile compounds to produce high-quality distillate [65–67,69,72–77] and minimal fouling caused by the catalyst deposition on the membrane surface as compared to microfiltration (MF) or ultrafiltration (UF) [66,72,73,75,76,78]. In the currently reported MD/photcatalysis hybrid processes, the majority of foulants were dyes, which are non-volatile compounds. Therefore, they cannot be transported in vapour phase through the membrane pores [65–67,69,72–77]. However, by-products of the degradation during the MD-photocatalysis hybrid process that may become volatile (including CO_2), can now pass through the membrane pores as vapours, affecting the permeate quality [64–66,74–77,79–81]. Moreover, the results obtained from the hybrid process in both modes (Figure 2-2) showed that the presence of the catalyst did not affect the permeate flux, regardless of the catalyst concentration within the range of 0.1-0.5 g/L [68,69,82,83,72–77,79,81]. However, increasing the catalyst concentration above 0.5 g/L led to a reduction in flux [67,73,74,83]. This inconsistency is related to the formation of a catalyst cake layer on the membrane surface in higher catalyst concentration.

In addition to the above-mentioned advantages of the MD/photocatalysis, the performance intensification of the hybrid process in terms of water recovery and distillate quality depends on membrane fouling prevention and the increased degradation efficiency of the organics, which are affected by factors such as: (a) membrane properties (e.g., hydrophobicity and surface charge); (b) feed composition (e.g., chemical structure of the organics, ionic strength, and pH); (c) catalyst characteristics (e.g., crystalline phase, and particle size); and (d) light irradiation. Since the information provided in most of the MD/photocatalysis studies on the membrane properties is not enough to analyse its effect on the fouling prevention in these systems, this review will focus mostly on factors b, c, and d by elaborating how these factors can contribute to the MD performance.

Feed composition:

The feed composition in MD/photocatalysis hybrid processes can contribute to both the extent of fouling and catalytic activity, affecting the wettability of the membrane and its rejection. The feed composition constitutes different aspects as follows:

(i) **Chemical structure of the organics:** The foulant properties (e.g., surface charge and hydrophobicity) can affect degradation efficiency, their tendency for adsorption on the catalyst surface, and their stability and aggregation behaviour in solution [75,84–86]. For example, hydrophilic catalysts tend to adsorb hydrophilic compounds [87]. In addition, negatively charged pollutants would adsorb more favourably on positively charged catalysts. The adsorption of the contaminants on the catalyst surface is important in accelerating their degradation, as most heterogeneous photocatalytic reactions take place at the surface of the catalyst [88–91]. Also, the aggregation of the foulants, which is greatly based on the inherent properties of the contaminants and solution environment, leads to pore blockage [68]. For instance, Laqbaqbi et al. [86] reported that aggregates could be formed from dye molecules containing both positively and negatively charged groups, leading to the pore blockage of the membrane and therefore flux decline. Moreover, negatively charged dyes (e.g., Acid Red 18 (AR 18), Acid Yellow 36 (AY 36)) were reported to have a lower tendency to fouling on negatively charged membranes due to the electrostatic repulsion [92,93].

(ii) **Ionic strength of the solution:** Ionic species can have complex effects on the catalytic activity, foulant-catalyst, inorganic-organic, and foulant-membrane interactions, which have not been fully considered and studied in MD-related literature. One effect is that they can quench the generated radicals, lowering the degradation rate. Another impact of ionic species is that they can neutralize/change the surface charge of the catalyst, affecting electrostatic interaction between the catalyst and pollutants [94,95]. Moreover, ionic strength can shrink the electrical double layer (EDL), hindering the electrostatic repulsive forces [96]. Further, in the presence of ions such as calcium, organic-inorganic complexes formed adjacent to the membrane surface may accelerate the fouling formation, leading to severe flux reduction [12,21,42,97,98]. For example, Wang et al. [68]. Studied the fouling behaviour of HA in MD at different concentrations of Ca^{2+}. It was demonstrated that in the presence of 20 mmol/L Ca^{2+} in HA solution, the normalized fluxes of MD steadily decreased, and the flux was 79.8% of the initial value after 45 h of operation. In contrast, without Ca^{2+}, the normalized flux of the HA solution remained almost constant over the entire experiment [68]. This difference can be attributed to the bridging effect of the Ca^{2+} ions that leads to more aggregation (foulant-foulant attraction) and subsequent fouling (membrane-foulant attraction) [99].

(iii) **pH of the solution:** The pH can play an important role in the generation of radicals, chemical and surface properties, foulant-membrane interaction, etc., in which some has not yet been studied in MD/photocatalysis hybrid processes. For instance, more OH° radicals would be generated at a higher pH, increasing the degradation rate. In contrast, in acidic pH ($pH<5$), the photocatalytic degradation would be reduced due to the higher proton concentration. pH also changes the degree of protonation of different functional groups (such as COOH and amines) on catalysts and foulants (with more protonation at lower pH), which can affect their chemical and surface properties [95,100]. In addition, varying the pH influences the foulant-membrane interaction. With an increase in the concentration of H^+ ions in the system (decrease in pH), the surface charge of the membrane and foulant becomes more positive, leading to a different type of interaction. A study showed that by lowering the pH of the coal gasification wastewater to pH=3.5 to reject ammonium nitrogen (NH^{4+}-N) through MD, fouling was accelerated due to the reduced electrostatic repulsion between HA (having negative charge) and membrane surface (slightly negative charge at low pH) [68].

Catalyst characteristic:

The catalyst characteristic (e.g., crystalline phase and particle size) is another important factor affecting the organic decomposition rate and therefore, its removal efficiency in the hybrid process, which eventually affect their fouling tendency. Mixed crystal catalysts often offer intensified decomposition due to the synergy between two crystalline phases in suppressing the recombination of electron and hole pairs [101–104]. A study employing the MD/photocatalysis hybrid process for treatment of a solution containing azo dye (AR 18) reported that P25 (TiO_2 in anatase and rutile phase) showed the best performance due to its mixed-phase structure, compared to the other two high purity anatase-phase TiO_2 catalysts from commercial source or lab-made [66]. Moreover, the size of the crystals determines their active surface area, which is in contact with the solution. Therefore, with a small crystal size (e.g., less 10 nm for TiO_2 [105–107]), it is expected that the activity should be enhanced due to an increased surface to volume ratio of the catalyst [105–109]. However, in some cases, an optimal particle size was reported that assures high catalytic activity. This contradiction arises from the quantum effects

[110] where normally reducing the particle size enhances the reactive surface area to volume ratio, positively influencing the process. However, this reduction may concurrently escalate the charge-carrier recombination effect, adversely affecting the process. Consequently, there exists an optimal particle size, below which the recombination effects outweigh the benefits, resulting in diminished catalyst activity. For example, an optimal particle size of about 11 nm of TiO_2 photocatalyst for decomposition of chloroform was reported [110].

Light irradiation:

Light irradiation is another important factor in MD/photocatalysis hybrid process. In photocatalysis, due to the high band gap of some widely-used catalysts (e.g., the band gap of TiO_2 is 3.2 eV), UV irradiation is used to increase the rate of the radical generation, which cannot be activated by visible light. However, catalysts with a lower band gap (e.g., BiOBr with a band gap of 2.7-2.9 eV) [111–114] can be activated using visible light, making them a promising candidate for the hybrid process. It is also important to mention that directing the UV-visible light toward the catalyst surface is dependent on the catalyst concentration and feed solution. Under constant light intensity, it is usually expected that by increasing the catalyst concentration, the rate of the radical generation increases. However, in the case of heterogeneous catalysts, the increase in catalyst concentration can also lead to the increased light scattering effect, which hinders light from reaching the catalysts present in the bulk of the solution. In MD/photocatalysis hybrid processes in both modes represented in **Figure 2-2**, the light scattering phenomena was significant [63,66,67,72,73,77,82], and no noticeable change in MD performance was observed by increasing the concentration of the heterogeneous catalysts. To tackle this problem, two alternatives have been studied:

(i) **Coating the catalyst on a substrate:** The first alternative is to coat the catalyst on a substrate (e.g., glass). Hou et al. [115] demonstrated a new hybrid system for treating synthetic wastewater containing picrolonic acid (PC), using Ag/BiOBr films coated on the glass substrate. The main motivation for coating the catalyst on the glass substrate was to address the light-shielding effect reported as one of the main drawbacks in most MD/photocatalysis hybrid systems [66,72,73,75–78,82]. Another approach that effectively addressed this issue involved the use of light-transmitting porous glass substrates combined with a photocatalytic microfiltration membrane made from P25 TiO_2. The simulated sunlight was conveniently directed through the glass substrate to achieve nonchemical solar cleaning of contaminants from nonpotable water [116], and the benefits of this approach could be translated to MD systems.

(ii) **Indirect irradiation:** The second alternative is the application of microwave electrodeless discharge lamps (MEDLs) that emit UV and visible lights upon microwave irradiation [67,68]. The MEDLs are expected to be more practical than UV irradiation, lowering the light's pathway reaching the catalyst surface, as they can be submerged under water, unlike traditional UV lamps. The MEDLs also produce thermal and non-thermal effects. The thermal effect in microwave irradiation can increase the temperature of the reaction mixture, minimizing the temperature polarization in MD [67,68]. Microwave irradiation can also create local hot spots on the catalysts, triggering the oxidation reaction [117,118], for which the mechanism is well described in the literature [119–122]. The non-thermal effect of microwave irradiation involves chemical reactions, which can result in weakening the attachment between the foulant and the membrane, leading to the detachment of the fouling layer [68], although there is still a debate on the existence of the non-thermal effect [119,121,122].

Overall, the MD/photocatalysis hybrid system is shown by researchers to be effective to treat a wide range of solutions, although there are still some challenges associated with their practical application. According to the above discussions, the main advantage of coupling MD with the photocatalysis process is the almost complete retention of non-volatile compounds. However, in the hybrid MD/photocatalysis system, some volatiles resulting from the pollutant decomposition have been identified in permeate, which are mainly responsible for the MD performance impairment, lowering the distillate quality. By focusing on the mechanism of individual processes and the parameters affecting their efficacy (e.g., feed composition, ionic strength) which also has been reviewed in this section, the rejection and the degradation efficiency can be maximized, lowering the semi (volatile) compounds in permeate. Also, previous studies mostly focused on the removal of a sample dye for a short period of time. Compared to the results obtained from works considering model foulants, the flux decline can be more severe in the case of the primary effluent [77,83]. Additionally, the system can show a different behaviour over a longer operation time which might not be observed within the limited time window of most of the lab tests in the order of hours, or days at most. Therefore, despite the improved MD performance, the MD/photocatalysis hybrid process still involves complexities that require further study.

2.2.1.2 MD/chemical oxidation

Ozonation, persulfate-based advanced oxidation processes (PS-AOPs), and H_2O_2-assisted oxidation are the three classes of chemical oxidation that have been coupled with MD. As shown in **Figure 2-3**, these systems involve oxidation which is employed for removing the organic matters as a pretreatment step before MD. In these processes, the oxidation of organics present in the feed solution can be accomplished by: (i) generated oxidizing agents (e.g., OH°, and SO_4° radicals), namely indirect oxidation; (ii) direct reaction with contaminants without involving radicals, namely direct oxidation [123–127]. The oxidation of organics in MD/chemical oxidation could lead to their decreased fouling tendency, and producing low strength concentrate in the feed side [128–132]. The parameters that affect the efficiency of the MD/chemical oxidation hybrid processes are in common with those for the MD/photoctalysis processes (e.g., feed composition such as pH, and ionic strength, membrane properties). Overall, given the additional advantage that can be brought to MD by minimizing the organic content through oxidation, hybrid MD/chemical oxidation can outperform the MD only in terms of water recovery and fouling control.

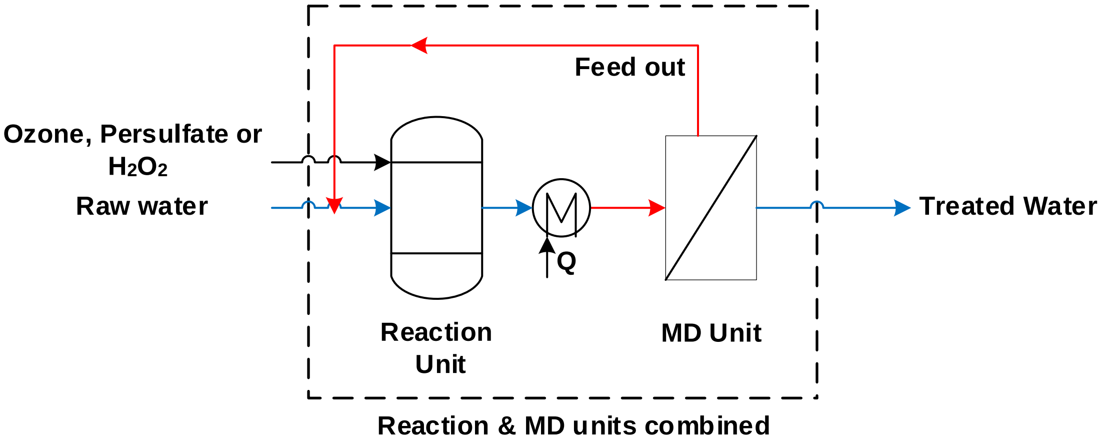

Figure. 2-3. The schematic of MD/chemical oxidation (process concepts redrawn from [128–132])

In MD/chemical oxidation, heat and catalyst have been used for activating oxidants and enhancing radicals generation. The heat from the MD operating temperature can be further utilized to activate the oxidants such as H_2O_2, and persulfate, which are otherwise relatively stable at room temperature [128,130–132]. Han et al. [132] have reported that the increased feed temperature from 55 to 65 °C could improve the PVDF membrane flux and permeate quality while treating feed containing 0.5 mM sodium dodecyl sulfate (SDS) at a persulfate concentration of 3mM. Specifically, in case of the lower feed temperature (55 °C), the flux declined by 72 %; while the flux decline was 20% at 65 °C. In addition, metal ions as homogeneous catalysts that can also be presented in some wastewater as metallic contamination can be completely retained by MD, leading to enhanced radical generation [128,129,131]. Zhang et al. [129] reported the improved flux behaviour of MD/ozonation in the presence of 1mM Cu (II) as the catalyst as shown in **Figure 2-4(a)**, although the permeate quality was slightly compromised due to degradation by-products. It should also be noted that in some cases, with the presence of metal ions, scaling might occur. Asif et al. [131] observed the deposition of iron oxide scales on the PTFE membrane during the treatment of the effluent of membrane bioreactor spiked with micropollutants and their mixture with several sample metals (iron, calcium, magnesium, and lithium).

On the other hand, oxidants and generated radicals can react with polymeric membranes, leading to their alteration. For example, one study reported wrinkles on the PVDF membrane surface after 60 h of the MD/ozonation operation [129]. The SEM images of the membranes are shown in **Figures 2-4 (b), (c), and (d),** displaying the surface morphological changes for the PVDF membrane in pristine state (**Figure 2-4(b)**), after DCMD (**Figure. 2-4(c)**) and after DCMD/ozonation (**Figure 2-4(d)**), respectively.

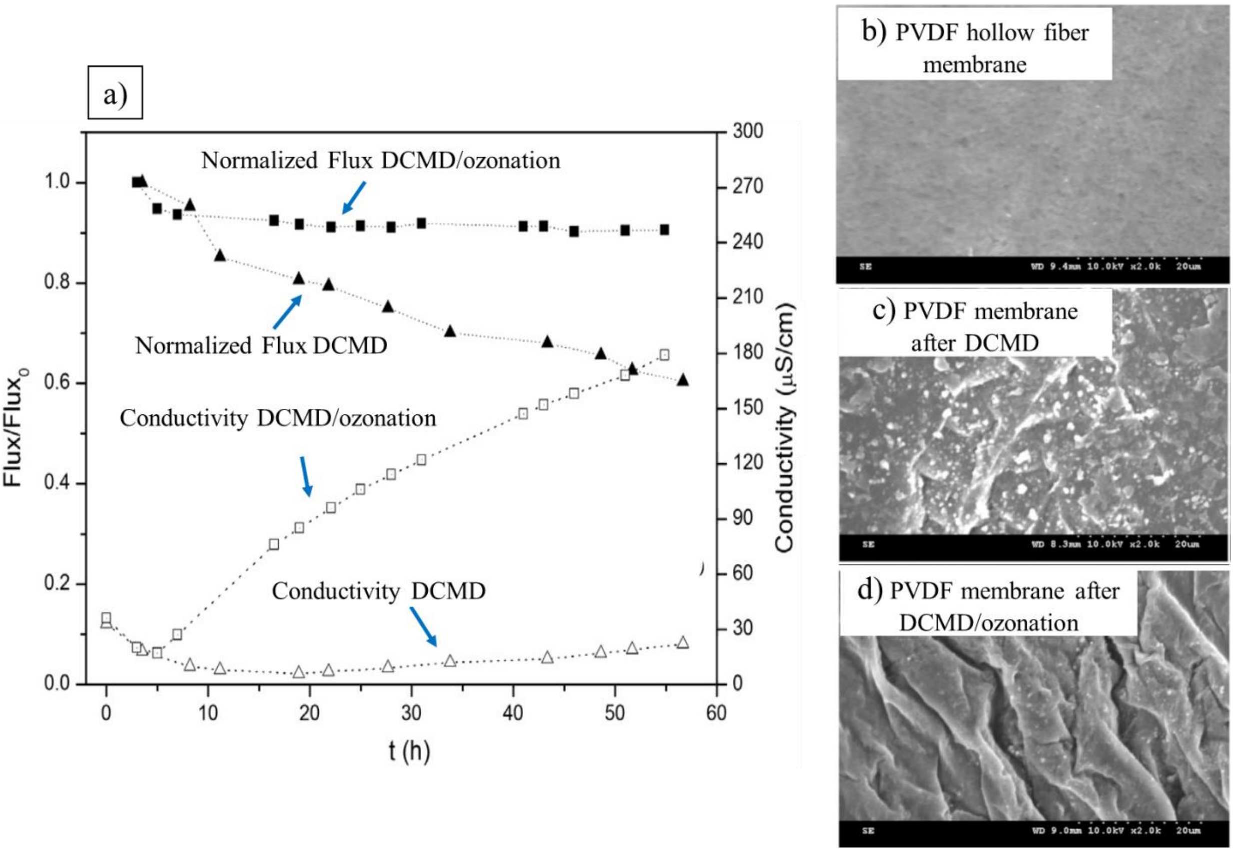

Figure. 2-4. a) DCMD and DCMD/ozonation performance of the PVDF hollow fiber membrane during 60 h operation in treatment of a solution of 1000 mg/L potassium hydrogen phthalate and 1000 mg/L NaCl, SEM images of b) pristine PVDF hollow fiber membrane before MD, c) after 60 h operation of DCMD, and d) after 60 h operation of DCMD/ozonation [129]

Overall, the integration of ozonation, PS-AOPs, and H_2O_2-assisted oxidation with MD was proven effective in degrading the organic containments as well as in recovering/retaining the catalyst, resulting in the improvement of the MD performance in terms of the flux and permeate quality. However, several challenges remain to be investigated such as the possibility of membrane alteration resulting from ozonation, surface scaling due to the use of transition metals as catalysts and potential subsequent wetting effect.

2.2.1.3 MD/electrochemical processes

Several electrochemical oxidation (EO) processes have been studied in combination with MD shown in **Figure 2-5**, namely electrochemical advanced oxidation processes (EAOPs) [23,133,134], fuel cells [135–144], and electroosmotic membrane bioreactor (eOMBR) (combination of electrochemical membrane bioreactors (EMBRs) and forward osmosis (FO)) [145]. The general mechanism and the main components of all studied EO processes are similar. They consist of three main elements: an electrolyte and two electrodes as the anode and the cathode where oxidation and reduction occur, respectively. In EAOPs, a wide range of organics can be oxidized on the anode surface by i) direct electron transfer from the organics to the anode or ii) indirect oxidation through water electrolysis yielding OH° or other reactive radicals [146,147]. In a fuel cell, fuel (e.g., hydrogen) is fed into the anode chamber where oxidation occurs, and the oxygen (or air) is fed into the cathode chamber where reduction occurs [148,149]. Fuel cells can be classified into different types, including proton exchange membrane fuel cell (PEMFC), alkaline fuel cell (AFC)) which have been investigated in the coupled MD process. Apart from fuel cells producing electricity at the cost of consuming fuel, in microbial fuel cells (MFC), the chemical energy stored in the organic/inorganic matter is converted to electricity through the oxidation of organics by microorganisms in the anode chamber (anaerobic conditions) [150–152]. By coupling MFC and membrane bioreactor (MBR), EMBRs have also been developed for water reuse and energy recovery from wastewater [153,154]. Overall, combining the above mentioned processes with MD can improve the MD performance in terms of water recovery and energy efficiency.

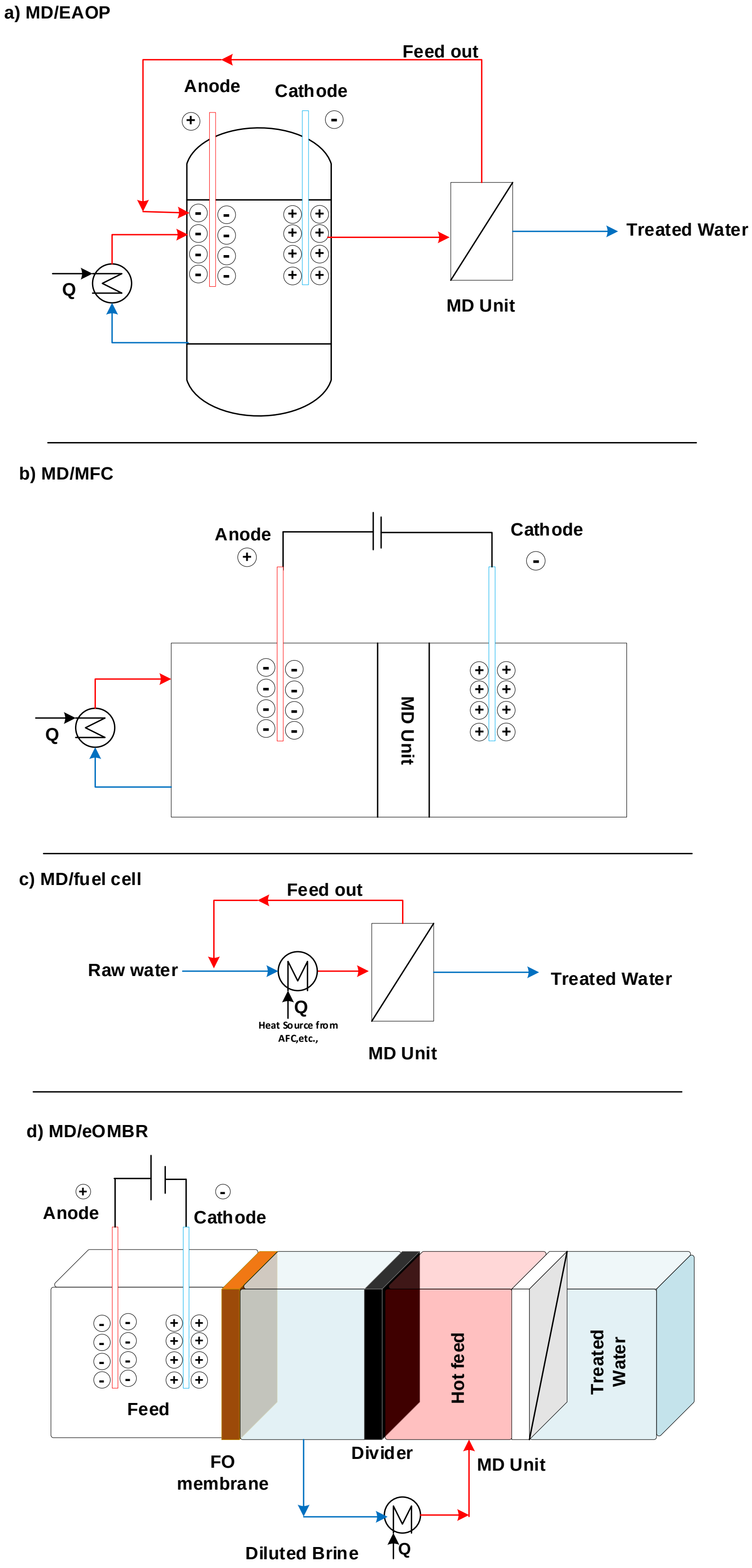

Figure. 2-5. Simplified schematic diagram of a) MD/EAOPs b) MD/MFC, c) MD/ fuel cells, and d) MD/eOMBR (process concepts redrawn from [23,136,137,139,145])

The MD/electrochemical processes have two key advantages. The first advantage of MD/electrochemical processes is to increase the water recovery or water production by minimizing fouling and wetting effect in the MD step [23,135–139,145]. Oxidation can lead to the loss of hydrophobicity or amphiphilic nature of low surface tension contaminants, reducing their favourable tendency to accumulate on the membrane surface due to hydrophobic-hydrophobic interactions. A study [23] reported that compared to MD, where severe wetting happened in 130 min when the SDS concentration reached 0.3 mM, the hybrid process exhibited a steady flux over 240 min operation even when the SDS concentration reached 0.5 mM. Semi volatile organics and SDS were degraded in MD/EAOPs system by the generated sulfate radicals ($SO_4^{-\circ}$). Therefore, the wetting resistance of the membrane in the presence of SDS is attributed to the structural change of the SDS due to the oxidation (loss of the amphiphilic property of SDS) [155,156].

The second advantage of the coupled MD/electrochemical processes is the improved energy efficiency by producing electricity while treating the wastewater, and harvesting the heat energy generated either by fuel cells or electrical resistant heating (Ohmic heating) to drive the separation process [23,135–139,145]. Cao et al. [136] studied the possibility of electricity generation while treating the wastewater by integration of PTFE hydrophobic membrane with MFC. The highest power density was achieved at 45 °C, as 1552 $\mu W/m^3$, although the membrane flux dropped and was below 0.5 L/m^2h after 10 days. In other studies, coupling MD and fuel cells [135,137–139] for utilization of waste heat, modelling results showed the effectiveness of the MD/fuel cell processes in terms of waste heat recovery. Apart from electricity generation or waste heat recovery, *in-situ* heat generation by Ohmic heating (electric resistance heating caused by the passage of electric current) and its utilization can boost the MD energy efficiency. In electrochemical oxidation, low electrolyte concentration is beneficial for generating heat; while it is detrimental for anodic oxidation of organic containments in the system. Therefore, a careful choice of the electrolyte concentration should be made considering this trade-off.

Overall, the MD-electrochemical hybrid processes are still at the early stage of development. However, according to the modelling and experimental results so far, they showed promises in simultaneously capturing energy and performing water purification. There are also a few challenges that can be investigated in future studies, including the potential to achieve high power densities and membrane stability to sulfate-based electrolytes.

2.2.1.4 MD/biological processes

MD/biological processes is another type of MD hybridization processes in which MD is coupled with a membrane bioreactor (MBR) [19,157,158]. MBR can be categorized into aerobic/anaerobic MBR and enzyme-based MBR (EMBR). Aerobic/anaerobic MBR is a technology that combines membrane filtration and a conventional bioreactor. In aerobic MBRs, aeration is required for bacterial growth; while in anaerobic MBR, the breakdown of organic compounds takes place in an oxygen absent environment (no external air is supplied) [159–161]. In EMBR, as the second category of MBR, membrane separation is coupled with enzymatic reaction. Enzymes can be used in both homogeneous (dissolved in feed stream) and heterogeneous (immobilized on a support) forms for the removal of a wide range of pollutants [162–164]. Overall, the potential benefit of enzyme-based MD bioreactor (EMDBR) is to reuse water [165–168], although coupling MBR with MD (MDBR) can broaden its application beyond wastewater treatment, achieving nutrient and biogas recovery at the same time which is also reviewed by other studies [19,157,158]. Therefore, the benefits/limitations of each coupled process are discussed in this current review.

Both MDBR and EMDBR benefit from a longer residence time for the degradation of the pollutants [165–170]. For instance, in MDBR, the organic retention time (ORT) is independent of hydraulic retention time (HRT), leading to the improved biodegradation of the slowly biodegraded organic compounds [169,170]. Moreover, with the ability of MD to completely retain non-volatiles, MDBR systems can effectively concentrate and recover nutrient components such as phosphorus and ammonia [19,171,172]. Besides nutrient recovery and water reuse, biogas can also be recovered from the anaerobic MDBR (AnMDBR) [173–181].

Contrary to the benefits of EMDBR and the aerobic/anaerobic MDBR (its versatility and robustness) mentioned earlier, they both suffer from a relatively low permeate flux. In EMDBR, a lower permeate flux is due to the low feed temperature as increasing the temperature causes the inactivation of enzymes. For instance, a low permeate flux of 4 L/m^2.h was observed during the operation time at the set feed temperature of 30 °C [165–167]. MDBR systems also experience a rapid flux decline due to fouling

[19,158,171,174,178,180,182]. For instance, Yao et al. [180] reported an initial flux of 2-4 L/m^2.h at temperatures of 45-65 °C, which dropped by 16-50% after 7-day of operation.

Overall, the potential water and resource recovery of MD/biological oxidation processes, makes them a promising alternative for water treatment. However, the low permeate flux in general and the potential risk of enzyme inactivation in EMDBR is still a challenge. The limit in the set temperature range of the feed stream due to thermal sensitivity of microbes and enzymes in such biological systems has also hampered the filtration efficiency of MD. Therefore, future investigations should be conducted to study the long-term stability of the hybrid process in terms of the membrane fouling and fouling-induced wetting in MD as well as the enzyme stability.

2.2.2 Integrated MD processes

2.2.2.1 Membrane integrated with photochemical oxidation

Incorporating photochemical oxidation with MD by immobilizing catalysts on the membrane surface is another approach to simultaneous rejection of foulant through MD while minimizing the organic content in the solution through an oxidation reaction. Photochemical oxidation is being increasingly used to degrade organics, as discussed in **Section 2.1**. In this approach, by modifying the membrane surface with catalysts, several studies have been conducted to achieve a photocatalytic membrane with a better fouling resistance functionality and self-cleaning ability [1–9] for wastewater treatment applications. The engineered membranes with catalytic and hydrophobic properties could achieve surface self-cleaning by triggering the photocatalytic activity, via either *in-situ* light irradiation during MD, namely-*in-situ* cleaning as illustrated in **Figure 2-6 (a)**; or exposing the fouled membrane to light for post-cleaning, namely *ex-situ* cleaning as shown in **Figure 2-6 (b)**. The improvement of the process efficiency in terms of fouling resistance and membrane cleaning depends on several factors such as membrane properties, feed composition, catalyst characteristics, which are similar to the hybrid MD/photocatalysis process **(Section 2.1).**

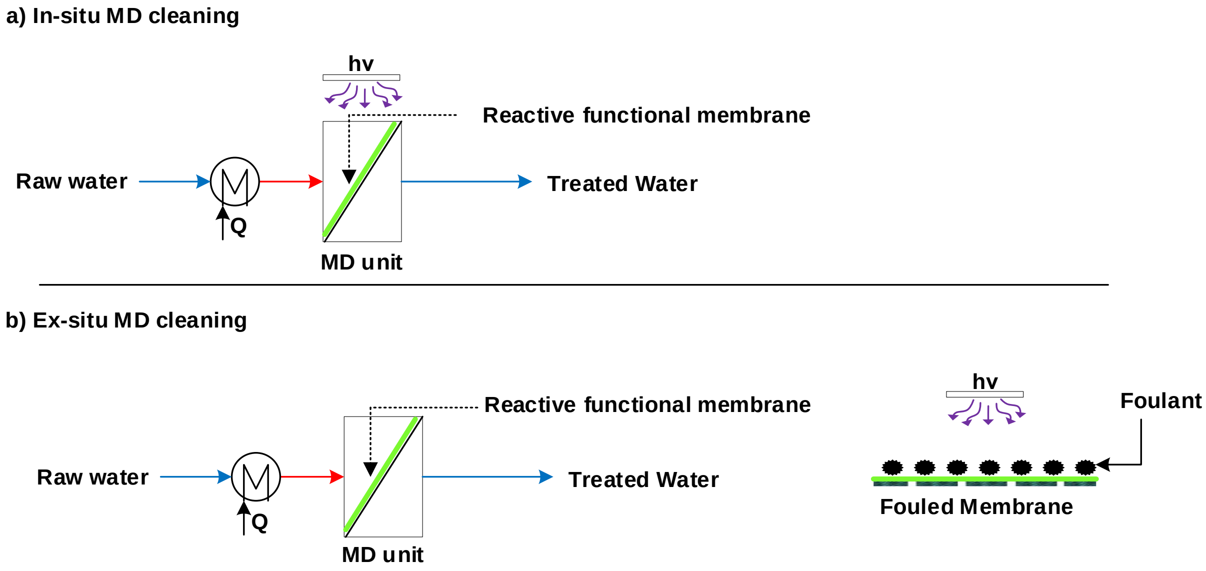

Figure.2-6. Simplified diagram of MD incorporated with photochemical oxidation through a) In-situ MD cleaning b) Ex-situ MD cleaning (process concepts redrawn from [1–9]). The green line indicates the catalysts layer.

In the context of photocatalytic membranes, the loading amount of the catalysts assures their high activity, compared to the hybrid process where increasing the catalyst concentration in the feed may hinder the degradation performance due to the light-shielding effect. Nevertheless, the catalyst immobilization onto the membrane depends on the coating technique (e.g., coating steps), which could potentially impact membrane hydrophobicity.

The choice of catalysts also plays a crucial role in achieving desired reactions. Summary of catalysts used by different researchers have been listed in **Table 2-1**. Various reactive materials, including TiO_2 [1,5,9], ZnO [2,4], BiOBr [3], AgCl [7], and bismuth tungstate (Bi_2WO_6) [6] having catalytic properties, have been employed for membrane surface modification. Some of these studies have reported a decrease in water contact angle after introducing reactive materials compared with the pristine membrane [2,9]. Therefore, further silane modification has been employed to maintain the membrane hydrophobicity to avoid wetting. For example, Hamzah et al. [1,9] reported a superhydrophobic PVDF membrane incorporated with TiO_2 nanoparticles. In the PVDF membrane blended with TiO_2, a lower water contact angle (112.3 ± 1.4 °) was achieved compared to the pristine membrane (121.8 ± 0.7 °) [9]. In contrast, a high contact angle (>150 °) of the membrane was achieved after the silane modification [1,9]. It was reported that tridecafluro-1,1,2,2-tetrahydrooctyl) triethoxysilane could increase the contact angle to above 160°

(superhydrophobicity) [1]. Therefore, maintaining the hydrophobicity of the membrane or support layer is critical to ensure that the membrane stays non-wetted during the operation.

Table. 2-1. Summary of MD incorporated with photochemical oxidation processes reported in literature

MD configuration/ membrane materials	Catalyst	Incorporation method	Pollutant	Efficiency	Ref
VMD/PTFE	ZnO	Mix of electrospinning and sintering	Rhodamine B	• 45% removal after 10h • >94% flux recovery after for 3h UV cleaning	[2]
DCMD/PVDF, PTFE, and BiOBr/Ag	BiOBr/Ag	Electrospray	MB, CV (Crystal Violet), AR18, and AY36	• 99.9% dye rejection over a 5-cycle MD test • 92.2% flux recovery under UV irradiation in Ag/BiOBr membrane	[3]
DCMD/PVDF	TiO_2	Blending	Phenolic solution (Gallic acid)	• less flux decline compared to the pristine PVDF • 99% Gallic acid rejection	[9]
DCMD/PVDF	reduced graphene oxide (RGO)–Bi_2WO_6	Double layer coating	Ciprofloxacin	• 99% flux recovery over 3h UV irradiation	[6]
DCMD/PVDF	TiO_2	Double layer coating	Rhodamine B	• 96% flux recovery after 8h UV irradiation	[5]
DCMD/PVDF	TiO_2	Blending	Gallic acid	• High relative flux (0.9) over 500 min experiment • 99% Gallic acid rejection	[1]
VMD/PVDF	hexagonal boron nitride (h-	Blending	Real Textile Wastewater	• >98% colour removal efficiency	[4]

	BN) nano - ZnO			and increased permeate flux - >85% flux recovered after UV-regeneration cycles	
PTFE/DCMD	AgCl/MIL-100(Fe)	Adhesive-assisted vacuum filtration method	Nitrobenzene (NB)	- Increase NB removal rate from 63.44% to 87.84% in the photocatalytic MD system. - Consistent flux after five MD cycles (600 min).	[7]
PVDF/DCMD	MXene-PVA-TiO_2	Pressure-assisted filtration method.	MB	- Efficient photodegradation capacity (MB removal rate > 95%)	[8]

On the other hand, the degree of fouling on the membrane surface would then be affected by the physicochemical properties of the coating materials such as hydrophilicity/hydrophobicity and surface charge. Therefore, the effectiveness of *in-situ* MD cleaning depends on the fouling tendency of the contaminants. As an example, Huang et al. [2] investigated both *ex-situ* MD and *in-situ* MD cleaning. It was reported that the PTFE/ZnO membrane applied in VMD could effectively degrade the feed solution containing RhB dye up to 45% under UV irradiation during 10 h operation. However, the flux decline was more severe in case of the modified membrane with ZnO compared to the prepared membrane without ZnO, implying that *in-situ* cleaning was not significant due to the serious fouling caused by adsorbing RhB on the modified membrane surface. In contrast to *in-situ* cleaning, the fouled membrane could be cleaned *ex-situ* via 3-h UV irradiation, achieving >94% flux recovery. **Figure 2-7** shows the SEM images of the PTFE/ZnO membrane before MD operation (Figure. 8a), the fouled membrane (**Figure 2-7(b)**), and the membrane cleaned after fouling (**Figure 2-7(c)**). In another study, Guo et al. [3] fabricated BiOBr/Ag photocatalytic membranes for the MD treatment of a mixed dye solution coupled with *in-situ* and *ex-situ* cleaning for regeneration of the fouled membranes. While using *in-situ* UV and visible light irradiation in an intermittent manner (i.e., light irradiation 20 minutes per hour), permeate electrical conductivity and the flux of the BiOBr/Ag photocatalytic membranes remained relatively stable during 24 h of operation. However, without the light irradiation, all the membranes, including the commercial PVDF, PTFE, and the BiOBr/Ag photocatalytic membranes, experienced a rapid flux decline in the first 12 hours when treating a mixed dye solution (200 mg/L). Also, *ex-situ* cleaning under 140 min of 100 W UV irradiation showed an efficient recovery of fouled BiOBr/Ag photocatalytic membrane, with almost unchanged water contact angle as compared to its pristine state.

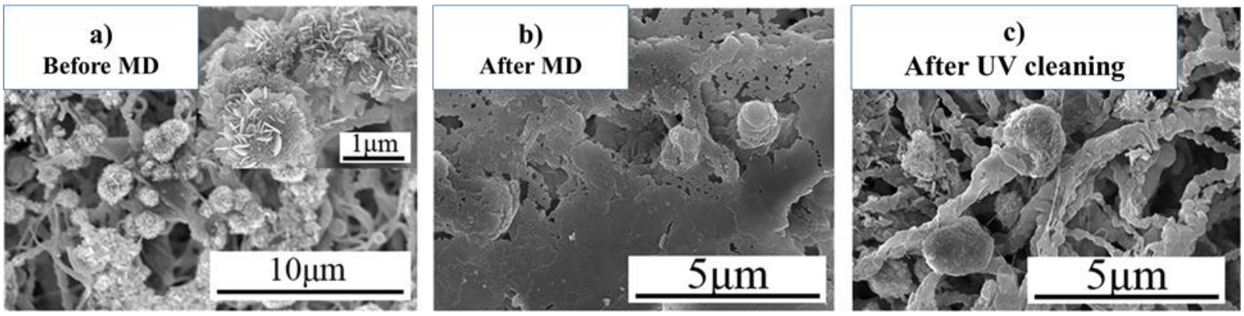

Figure. 2-7. SEM images of PTFE/ZnO membrane a) before MD test b) after 6 h operation of VMD of 20 mg/L RhB and 3.5 wt% NaCl c) after 3 h UV cleaning of the fouled membrane [2]

Overall, the promising self-cleaning properties of the catalytic membranes discussed above make them a potential choice for the water/wastewater treatment processes. However, they are at the early stage of development. In particular, the properties of the chosen catalysts and supporting membrane materials, and water chemistry, including the foulant species, could significantly influence the MD performance [2,3]. In some cases, the fouling tendency may even increase and accelerate the flux decay rate [2]. Therefore, further research is needed for a better operation mechanism of catalytic membranes.

2.2.2.2 Membranes integrated with electrochemical processes

Electric-field-assisted MD system has attracted research interest because of its compact design for enhancing the MD performance in terms of fouling and wetting resistance. Compared to the hybrid MD/electrochemical oxidation reviewed in Section 2.3, which uses conventional MD membranes, the integrated system analysed here follows a similar principle but in a more compact manner by applying electrically conductive membranes (EMs) driven by electric field. In this method, the membrane itself serves as anode or cathode as shown in **Figures 2-8 (a), and (b)** where electrochemical oxidation or reduction occurs, respectively. By utilizing EMs, the energy is delivered to the membrane surface driven by external field, meanwhile separation occurs at the liquid-membrane interface.

To achieve an electrically conductive membrane different supports and conductive layers were studied. Summary of the support layer and the conductive layer along with the incorporation method have been listed in **Table 2-2**. For the development of EMs, several supports have been employed: polymeric [58,183–188], ceramic [189], metallic [190], and superhydrophobic carbon nanotube (CNT) [191]. A conductive layer on the membrane surface was then created using electrically-conductive materials such as graphene, multi-walled carbon nanotubes (MWCNTs), and CNT. The choice of materials and utilization of EMs as anode or cathode will determine MD performance.

Under anodic condition (positive polarization) while the membrane is positively charged, it is hypothesized that oxidation of organics and biofoulants would occur and hence prevent fouling on the membrane surface. However, the membrane performance reduces immediately in terms of flux and salt rejection due to oxidation of positively charged membrane and electrostatic attraction between the positively charged membrane and organics carrying the opposite charge. The schematic of **Figure 2-8 (a)** represents the mechanism of EMs when using as anodes for treating wastewater containing organic components that are mostly negatively charged, based on a critical analysis of several similar studies on the topics [58,189–191]. As an example, while metal-based conductive membrane (stainless steel-CNT) was used as an anode (applying +2V), fouling and membrane degradation were accelerated compared to the open circuit scenario, due to the decreased electrostatic repulsion and increased oxidation of the membrane material. **Figure 2-8 (c)** shows the SEM and the contact angle of the positively charged stainless steel-CNT membrane after 6 h treatment of 70 g/L NaCl solution containing 30 mg/L HA [190]. A highly hydrophilic surface with a water contact angle of 26 °C was observed in the case of the positive polarization, indicating severe membrane fouling and corrosion. Jiang et al. [58] also reported the increase in the permeate conductivity from 2.3 to 2340 μS/cm and the decrease in permeate flux from 10.6 to 1.99 L/m^{2}h in 3.5 h when treating a 10 g/L NaCl solution while graphene-coated PTFE membrane was positively charged, i.e., applied as anode.

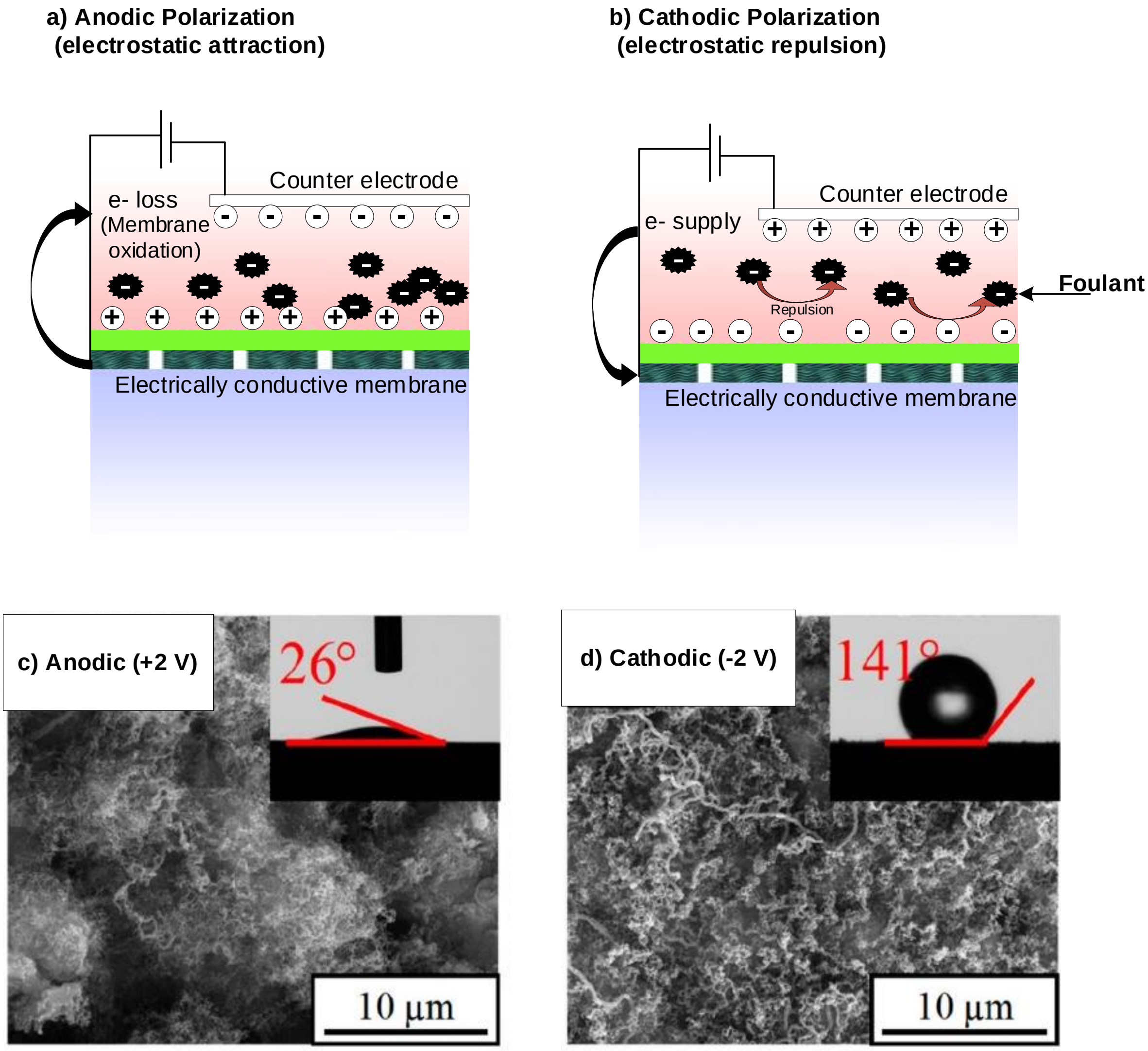

Figure. 2-8. Simplified electrostatic interaction models between the membrane surface and the negatively charged foulant under different applied voltage. a) Anodic polarization (membrane as anode) b) Cathodic polarization (membrane as cathode). The green line indicates the conductive layer. SEM images and water contact angle values (insets) of stainless steel-carbon nanotube membrane at different applied voltage c) +2V (anodic polarization) d) -2V (cathodic polarization) after 6 h operation of electric field-assisted VMD (EVMD) of 70 g/L NaCl solution containing 30 mg/L HA [190].

To prevent membrane oxidation and increase the electrostatic repulsion, some studies employed EMs as the cathode where electrostatic repulsion could prevent the attachment of negatively charged foulant to the membrane surface shown in **Figure 2-8 (b)**. Meanwhile, H_2 and H_2O_2 microbubbles generation and the electrochemical oxidation lead to the detachment and degradation of organics, respectively [58,183–185,189–191]. Under cationic conditions (negative polarization) while the membrane is negatively charged shown in **Figure 2-8 (d)**, membrane fouling was mitigated and the membrane maintained its high water contact angle (reducing from 171°C to 146°C) after 6 hour operation, due to lower fouling as a result of the enhanced electrostatic repulsion between membrane surface and negatively charged HA [190]. While the membrane is charged, the free energy (the energy needed to move the counter ions from the bulk to the interface to maintain electroneutrality) has to be overcome by the foulant in order to be deposited on the membrane surface (cathode) [192]. Under electric field, the generation of H_2 and the reduction of oxygen to H_2O_2 microbubbles can also result in an effect of electro-flotation on the membrane surface, creating turbulence and facilitating the foulant detachment and/or preventing the foulant deposition on the membrane surface [58,183,185]. Bubbles produced on the membrane surface can also reduce the temperature polarization effect, achieving a higher driving force and therefore a higher permeate flux [58]. Thus, to utilize the synergetic effect of electrostatic repulsion, the turbulence caused by bubble generation, and electrochemical oxidation for improving the MD performance, enough electric field strength is needed. Nevertheless, an increase of the electric field may not necessarily always lead to intensified MD performance; instead, an optimal range of field intensity should be determined. It is speculated that the turbulence caused by the increased bubble density in higher electric field strength can reduce the electrostatic repulsion between the membrane and the like-charged foulant, increasing the fouling and wetting in MD [58]. It was reported that although an intermittent electric field intensity of 1.0 V/cm resulted in the best antifouling effects while treating a solution composed of NaCl (35 g/L) and HA (20 mg/L), further increasing the applied voltage to 1.5 V/cm led to a reduced flux recovery [183]. The observed inconsistency may be the result of the trade-off between the increasing electrostatic repulsions and the increased bubble density.

Overall, the integrated MD-EAOPs processes have demonstrated several distinct benefits and challenges, such as a compact design without needing an extra electrochemical cell, utilization of the electric field to actively prevent fouling deposition on the membrane surface and simultaneous degradation of organic foulants via electrochemical oxidation. More recent studies highlighted the effectiveness of electrochemical cleaning for MD membranes, demonstrating how a direct current power supply can be used for post-cleaning fouled membranes, whose performance was subsequently evaluated in MD [193,194]. Nevertheless, MD-EAOPs processes still faces several challenges. One challenge is the reduced MD performance while the electrically conductive membrane is used as the anode. While this challenge can be overcome by applying the membrane as a cathode, there would be a complex synergy between electro-flotation, electrostatic repulsion, and electrochemical oxidation. Also, while the cathodic condition would protect the membrane form oxidation and corrosion, it might favour the attachment of positively charged organic wastewater. Therefore, for practical applications, further investigation is needed for maintaining high flux and reduced membrane fouling and wetting.

Table. 2-2.

Summary of electrically conductive membranes utilised for MD reported in literature

MD configuration/ membrane materials	Conductive layer	Incorporation method	Ref
DCMD/PTFE	CNT	layer-by-layer spray coating	[184]
DCMD/PTFE	Graphene	layer-by-layer spray coating	[58]
VMD/PTFE	MWCNTs or a mixture of MWCNTs/graphene	Vacuum filtration	[183]
VMD/PTFE	MWCNTs or a mixture of MWCNTs/graphene	Vacuum filtration	[185]
DCMD/Ceramic substrate	CNT	Chemical vapour Decomposition (CVD)	[189]
VMD/Stainless steel	CNT	CVD	[190]
DCMD/CNT	-	Wet-spinning coupling with fluorination modification	[191]
DCMD/PVDF	Single-wall carbon nanotube (SWCNT)	Filter coating method	[186]
DCMD/PTFE	CNT	Pressure-assisted spray method	[187]
DCMD/PTFE	Reduced graphene oxide (rGO) and CNT	Filter coating method	[188]

2.3 Development of robust MD membranes with fouling- and wetting-resistant properties

Over the years, researchers have introduced various membrane configurations for the MD process, including single-layer, dual-layer, and triple-layer designs. The creation of dual-layer hydrophobic-hydrophilic composites emerged from the need for MD membranes with enhanced flux. Cheng and Wiersma were the first to patent this type of composite membrane [195]. This technique often involves adding a hydrophilic coating over a hydrophobic base, which greatly improves the membrane's antifouling properties [29,30]. Leveraging the strong adhesion properties of polydopamine (PDA) to various substrates, there is increasing interest in applying PDA for surface modification. With its abundance of hydroxyl and amine groups, the PDA coating enhances membrane hydrophilicity, leading to improved MD effectiveness [33,34]. Research suggests that the interaction between PDA and various substrates arises from non-covalent forces, including hydrogen binding [34–36], coordination [33,37], and hydrophobic interactions [34,38]. However, PDA deposition on many material surfaces is often a slow process. To overcome this limitation, oxidants have been explored as a means to speed up dopamine polymerization [30,39–41].

In many MD applications, PDA is often integrated with other materials to enhance specific membrane properties. These membranes have been tested with synthetic salt solutions (10,000 mg/L NaCl), actual seawater, and seawater spiked with surfactants, polyhydric alcohols, and oil emulsions [39,196,197]. For instance, Chen et al. [198] introduced a membrane design inspired by nanofiltration, in which a hydrophobic PVDF base is coated with a PDA/PEI layer functionalized with sodium-functionalized carbon quantum dots (Na^+-CQDs). When tested with a saline oil-in-water emulsion (1 g/L oil, 0.03 g/L SDS, 0.6 M NaCl), this modified membrane demonstrated strong antifouling capabilities. The hydrophilic PDA/PEI layer forms a hydration barrier that prevents oil attachment, creating an energy barrier that minimizes fouling compared to unmodified PVDF. Similarly, combining PDA with silver nanoparticles (AgNPs) has been shown to enhance hydrophilicity and antifouling properties in MD membranes, further improving performance in demanding conditions [39].

PDA-modified MD membranes, known for their hydrophilic properties, show promise in creating membranes resistant to fouling and wetting; however, their use for treating high-strength wastewater with organic content remains underexplored. By extending the use of PDA-modified membranes to complex, industrial conditions, this research provides valuable insights into their performance in demanding environments.

2.4 Salting out effect

An important but often overlooked phenomenon contributing to fouling in high-salinity environments is the salting-out effect. This effect occurs when the solubility of organic compounds decreases in the presence of high salt concentrations, leading to precipitation of the organic matter. Setschenow [45] was the first to formulate an empirical relationship to describe the salting-out effect, known as the Setschenow equation:

$$log({}^{S_0}/_{S}) = K_s C_s \qquad \text{2-1}$$

In this equation, S_0 and S denote the solubilities of the organic compound in deionized water and in the salt solution, respectively. Ks represents the Setschenow constant or salting-out constant, and C_S represents the molar concentration of the salt in the solution. Organic molecules with high molar volumes tend to exhibit larger Ks values, which means that their solubility is more strongly reduced in the presence of salts compared to smaller molecules.

The Hofmeister series provides a framework for understanding how ions influence solute behaviour in aqueous solutions. Originally identified through its impact on protein precipitation, the Hofmeister series categorizes ions by their ability to induce structure within water molecules or disrupt it, often referred to as "kosmotropic" (order-making) and "chaotropic" (disorder-making) effects, respectively. Kosmotropic ions (e.g., SO_4^{2-}) which tend to enhance salting-out, increase water structuring around hydrophobic solutes and promote aggregation, thereby aiding in separation. In contrast, chaotropic ions (e.g., I^-, SCN^-) disrupt water structure and increase solubility, counteracting the salting-out effect [199].

The mechanisms driving salting-out remain complex and are still debated. In simplified terms, anions with high charge density induce salting-out through electronic repulsion and the enhancement of the hydrophobic effect. High charge density anions create repulsive forces at the solute-water interface and further promote the aggregation of nonpolar solutes [199]. This aggregation of organic solutes can exacerbate the formation of fouling layers on the membrane.

While the salting-out effect has been widely studied in other fields, such as liquid-liquid extraction and protein separation, its impact on MD systems has not been fully explored. Quantifying the salting-out effect is essential for optimizing MD applications, particularly in industrial processes where effluents contain high concentrations of electrolytes. In these environments, the presence of salts can significantly alter the behaviour of organic contaminants, leading to increased fouling and reduced membrane performance. Understanding the relationship between salinity, organic solubility, and fouling can provide valuable insights into improving the efficacy of MD systems.

Due to these complexities, advancing MD technology through further research and development is essential to tackle the challenges of high-salinity wastewater treatment. Examining the impact of the salting-out effect on fouling and wetting behaviours in MD systems will be key to enhancing MD's practical use in treating high-strength wastewater.

2.5 Conclusions

In conclusion, this review has focused on coupling MD with reactions, particularly oxidation processes, which are widely studied in the literature, along with recent advancements in membrane design and the salting-out effect.

Reactive processes were identified and classified into “*hybrid*” and “*integrated*” processes where the reactive materials were loaded into the feed tank and incorporated into/onto the membrane, respectively. Our evaluation of both hybrid and integrated processes showed that the oxidation of organics plays a crucial role in intensifying the MD performance. However, its application has primarily been limited to scenarios with low salinity and organic concentrations. Despite these advances, significant gaps remain in the effectiveness of reactive MD for treating high-strength wastewater.

The development of robust MD membranes with fouling- and wetting-resistant properties has shown promise in addressing key challenges in MD applications. Dual-layer hydrophobic-hydrophilic composites, modified with PDA, enhance antifouling and hydrophilicity, leading to improved MD performance. However, the application of PDA-modified membranes in high-salinity, high-strength wastewater remains underexplored. Furthermore, understanding the salting-out effect, a phenomenon where high salinity reduces the solubility of organic compounds and leads to fouling, offers valuable insights for optimizing MD systems in industrial applications.

To better understand reactive MD processes in high salinity environments, several aspects need further study. First, the efficiency of reactive MD in highly concentrated streams needs investigation. Additionally, it is important to consider the role of membrane surface hydrophobicity and hydrophilicity to understand how fouling and wetting are impacted in modified membranes. Lastly, studying the interactions among ions, solvents, and nonelectrolytes, specifically the solubility effects of organics in high-salt solutions (the salting-out effect, a phenomenon that is well-studied in areas outside of MD literature) is crucial.

Therefore, to bridge these gaps and enhance the practicality of reactive MD, this review identifies several critical areas for this research:

- Extending the application of reactive MD for treatment of concentrated organic wastewater, with the salinity of over 80 g/L which is the limit of RO process [200] compared to low salinity wastewater containing low organic content;
- Investigating the impact of membrane surface hydrophobicity/hydrophilicity on the fouling tendencies in concentrated organic wastewaters, considering that the inherent hydrophobic nature of MD membranes increases their susceptibility to fouling.
- Studying the complex interactions between high salinity and the solubility of organic compounds to better understand how these factors affect MD performance, as organics can behave differently in electrolyte solutions.

Accordingly, this research aims to explore the capabilities of both reactive (specifically, the hybrid process) and modified MD processes in treating high-strength wastewater. This study will delve deeper into understanding the complex effects of high salinity and high organic concentrations on MD performance, with a particular focus on how salinity influences the solubility and behaviour of organic compounds within the MD system.

Chapter 3

Materials and methods

3.1 Materials and chemicals

Commercial hydrophobic PVDF membranes with an average pore size of 0.2 µm and 0.45 µm, specifically Immobilon® membranes, were obtained from Merck-Millipore (Germany). PTFE flat-sheet membranes with a nominal pore size of 0.5 µm were obtained from Ningbo Chanqi (China). Additionally, Oleophobic/hydrophobic Versapor membranes with an average pore size of 0.2 µm were acquired from Pall Corp. The chemicals used included methylene blue (≥82.0%), Orange G (≥80.0%), Oxone, dopamine hydrochloride (>98%), and sodium periodate (≥99.8%), which were purchased from Sigma-Aldrich (St. Louis, USA).

Methylene blue (MB) is a heterocyclic aromatic compound with the molecular formula $C_{16}H_{18}N_3SCl$ and a molecular weight of 319.85 g/mol. As a cationic dye, MB contains a central thiazine ring, and its chemical structure is shown in Figure 3.1. All chemicals, including MB, were used as received without further purification. All chemicals, including MB, were used as received without further purification.

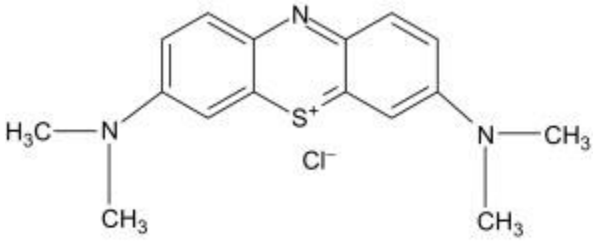

Figure. 3-1 MB chemical structure

3.2 Direct contact membrane distillation (DCMD) tests

3.2.1 Setup and equipment

The DCMD tests were performed as described elsewhere [201]. The experimental setup for MD involved the use of a self-made module in two sizes: Module A (156.25 cm^2) and Module B (11.2 cm^2), as shown in Figure 3-2. Both the feed and permeate solutions were recirculated through the DCMD module in a counter current mode. To minimize heat loss, insulation was applied to the membrane module and tubing. Throughout the experiments, the inlet feed temperature was maintained at a constant temperature of 60 °C, while the permeate temperature remained at 20 °C. In some of the performed tests, a check valve was introduced on the outlet of the feed side to maintain a consistent back pressure of 30-

40 kPa (gauge). This was performed to improve the consistency of the wetting observation (ensures slight pressure to cause liquid phase flow of feed to permeate), and align with full scale MD modules which experience these orders of pressure drop across the feed channel.

The solution preparation was conducted at room temperature. The feed solution consisted of a fixed initial concentration of MB (3750 mg/L) mixed with varying NaCl concentrations ranging from 3.5 to 100 g/L. The mixing process was performed using an overhead mixer overnight in a water bath at the desired temperature of 60 °C. After thorough mixing and heating, the feed solution was recirculated using a peristaltic pump at the desired flow rate.

Concurrently, deionized water cooled to 20°C using a chiller was recirculated in a co-current manner on the permeate side of the module, also using the same peristaltic pump at the same flow rate. The feed inlet and outlet temperatures were continuously monitored online through Pico data logger unit. Additionally, the permeate quality was monitored using an electrical conductivity meter and data recorder (microCHEM conductivity transmitters). The permeate flux was calculated by dividing the collected permeate, measured at set time intervals using an analytical balance, by the effective membrane area.

The MD experiments were conducted at least three times, with each trial utilizing a fresh membrane and solution. A representative result was selected for presentation, analysis, and further discussion.

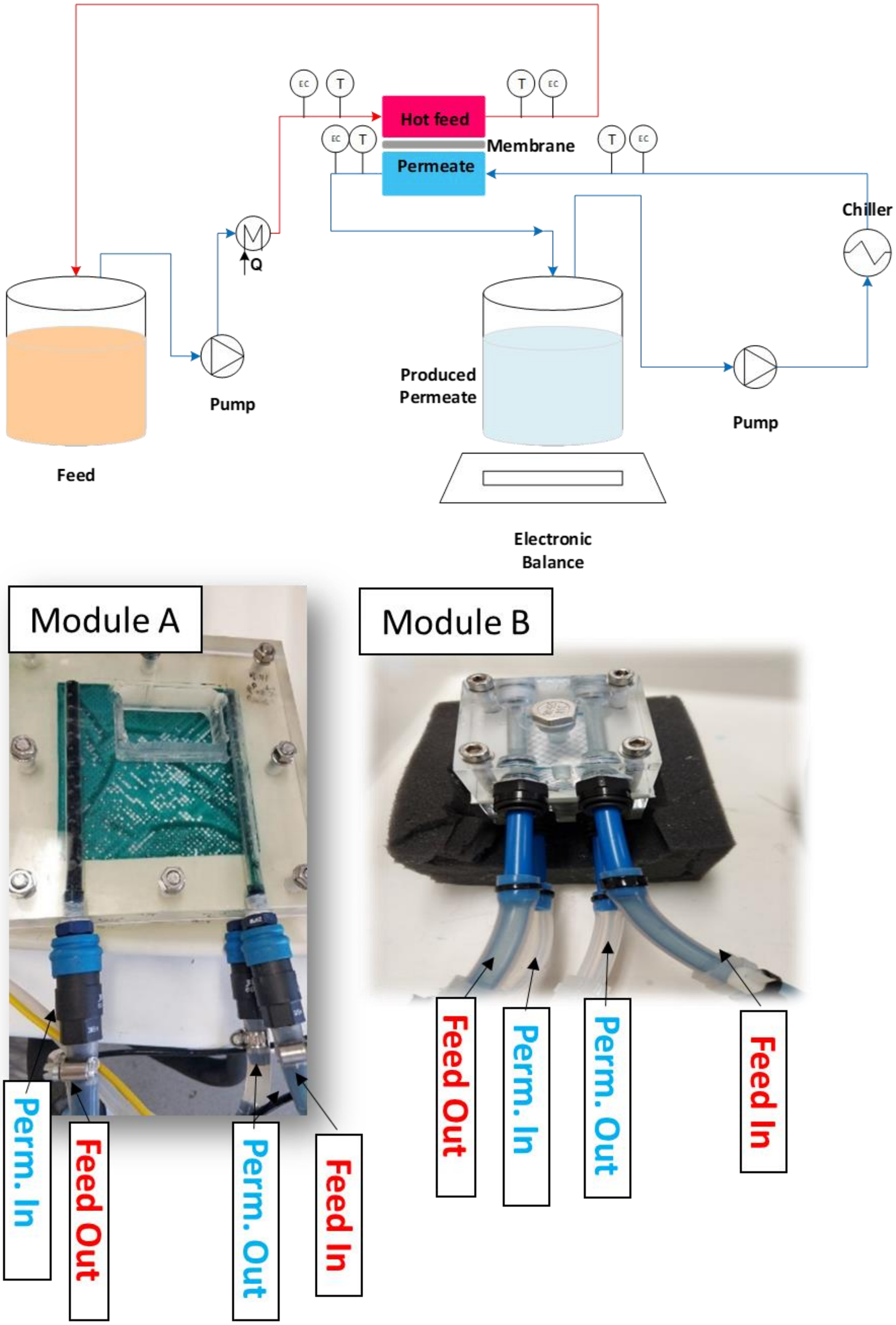

Figure.3-2 MD setup used to conduct experiments in this work. (Module A (A = 156.25 cm^2) ,Module B (A = 11.2 cm^2))

3.2.2 Calculation of cumulative specific permeate volume

To quantify the performance of the MD process, the volumetric flow of the permeate in each hour was normalized based on the effect membrane surface area. The specific permeate volume was calculated using the following formula:

$$Specific\ permeate\ volume\ (L/m^2) = \frac{P(t) - P(0)}{A} \qquad 3\text{-}1$$

Where:

- P (t) represents the permeate produced at a given time.
- P (0) is the permeate volume at the initial time t = 0, serving as the baseline for subsequent measurements.
- A denotes the surface area of the membrane, which is 156.25 cm^2 for Module A and 11.2 cm^2 for Module B.

3.2.3 Real-time permeate NaCl concentration

To evaluate the MD performance in terms of wetting, it is important to determine the NaCl concentration in the permeate. This involves an approach that includes measuring permeate electrical conductivity (EC), translating this EC into an equivalent NaCl concentration, and then quantifying the total salt content in the permeate. The procedure is outlined below and detailed in **Equations 3-2 and 3-3**:

- EC measurement: Initially, the EC of the produced permeate is measured to obtain an indirect indication of its ionic content.
- EC to NaCl conversion: The measured EC value is then converted into an approximate NaCl concentration by multiplying the EC by a fixed parameter of 0.55 [202,203], providing a direct measure of the NaCl content in the permeate.
- Total salt quantification: The NaCl concentration is multiplied by the permeate volume to calculate the total salt content (**Equation 3-3**).
- Salt increase calculation: The change in salt content is determined by comparing the total salt in the permeate at two consecutive time points, t and t+1.
- Permeate flow calculation: The total flow of the permeate is calculated by noting the difference in the volume of permeate collected between two time points, t and t+1.

- True NaCl concentration: The actual NaCl concentration in the permeate is calculated by dividing the increase in salt content by the total flow of the permeate.

The formula for calculating the real-time NaCl concentration in the permeate is given by:

$$Realtime\ permeate\ flow\ NaCl\ Conc\ (ppm) = \frac{(total\ salt)(t+1) - (total\ salt)(t)}{(produced\ permeate)(t+1) - (produced\ permeate)(t)} \tag{3-2}$$

$$Total\ salt(mg) = Permeate\ NaCl\ concetration\ * \ total\ permeate\ volume \tag{3-3}$$

3.3 Oxidation experimental conditions

The introduction of oxidation to MD focuses on assessing the impact of Oxone on membrane resistance to wetting and fouling. Oxone, a triple salt, once introduced into a solution, can lead to a decrease in the solution pH. Therefore, three different conditions were considered:

- The use of Oxone without any pH adjustments;
- The use of Oxone along with pH adjustments to raise the solution pH to approximately 6.7; and
- Evaluating the sole effect of pH adjustment, achieved by using hydrochloric acid (HCl), to understand its influence on membrane fouling and wetting.

The experimental data presented below encompasses these conditions, including fixed initial MB concentration and varying NaCl concentration, alongside the presence or absence of Oxone in the feed solution, and different pH levels to elucidate the individual effects on membrane performance.

Table. 3-1. Concentrations of MB, NaCl, Oxone, and pH levels in MD assisted SR-AOPs

Solution #	**1**	**2**	**3**	**4**	**5**	**6**
MB (mg/L)	3750	3750	3750	3750	3750	3750
NaCl (g/L)	85	85	85	100	100	100

Oxone (mg/L)	500	-	500	500	-	500
pH	3.2	3.2 (HCl)	6.7	3.2	3.2 (HCl)	6.7

3.3.1 Effect of Oxone on solution pH

Oxone, a triple salt with the formula of $2KHSO_5.KHSO_4.K_2SO_4$, once introduced into a solution at a concentration of 500 mg/L, led to a decrease in the solution pH to 3.2. To quantify this change, a series of calculations were performed.

Upon dissolution, Oxone releases hydrogen sulphate ions (HSO_4^-) and peroxymonosulfate ions (HSO_5^-), which can further dissociate into hydrogen ions (H^+). For simplicity in calculating the pH, only HSO_4^- was considered here. The concentration of HSO_4^- for 500 mg/L of Oxone can be calculated as follows:

$$[HSO_4^-]=500\,\frac{mg}{L}\,Oxone * \frac{1\,g}{1000\,mg}\,Oxone * \frac{1\,mol}{614.8\,g}\,Oxone * \frac{1\,mol\,HSO_4}{1\,mol\;Oxone} = 8.1 * 10^{-4}\,mol/L$$

HSO_4^- dissociates into H^+ and sulphate ions (SO_4^-) as represented by below reaction, altering the solution pH. From the molar concentration of HSO_4^-, the concentration of H^+ can be deduced using the dissociation constant (Ka) from reaction below. Consequently, the pH is calculated to be 3.1, which aligns closely with the experimentally observed value (Table 3-1).

$$KHSO_4 \rightarrow H^+ + SO_4^- \qquad K_a = 1.2 * 10^{-2}$$

3.4 Preparation of PDA modified membrane

To modify the PVDF membrane surface, this study uses the modification procedure described by Chew et al. [30]. Firstly, the pristine PVDF membrane with a mean pore size of 0.2 µm was placed inside a lab-made module for partial pre-wetting. The membrane was securely fixed within the module to ensure that only one side (the feed side) undergoes modification. **Figure 3-3** shows the membrane fixed inside the module before and after modification. The specific steps for PVDF membrane modification with PDA are as follows:

1. Prior to modification, the pristine PVDF membrane was partially pre-wetted by exposing it to a predetermined concentration of isopropyl alcohol (IPA) for approximately 1 hour. The concentration used was 15 wt% of IPA.
2. An aqueous solution was prepared by dissolving dopamine (DA) at a concentration of 2 g/L in a sodium acetate buffer with a concentration of 50 mM. Sodium periodate (SP) was then added to the solution as the oxidant, with a concentration of 20 mM. The pH of the solution was adjusted to pH 5 using 2 M hydrochloric acid (HCl).
3. The prepared solution from the previous step was poured onto the surface of the PVDF membrane held in a membrane holder. The membrane holder was subjected to shaking at a rate of 30 rpm for a specific reaction time of 2 hours, under ambient conditions.
4. After the designated reaction time, the modified membrane was rinsed with distilled water for 3 minutes to remove any residual unbound PDA.
5. Finally, the modified membrane was dried before further use or analysis.

Figure 3-3 PVDF membrane module before and after PDA modification

3.5 Characterization

3.5.1 Attenuated total reflectance fourier transform infrared spectroscopy (ATR-FTIR)

The ATR-FTIR measurements of the modified membranes were conducted using a Perkin Elmer ATR-FTIR spectrometer (Perkin Elmer, Germany). These measurements were taken across a wavenumber range of 600-4000 cm^{-1}, with the data for each specimen averaged over 16 scans.

3.5.2 Contact-angle experiments

Contact angle experiments to indicate surface hydrophilicity/hydrophobicity were carried out using a drop shape analyser (DSA25E, Krüss, Germany). For in-air water contact angle experiments, each sample was tested at least 5 times at different spots to ensure accuracy and reliability.

3.5.3 Scanning electron microscopy (SEM)

SEM was performed using a Phenom II scanning electron microscope (ThermoScientific, USA). The SEM images were acquired at magnifications ranging from 1000 to 20,000x. Prior to image acquisition, the samples were gold-sputtered using a sputter coater.

3.5.4 Total organic carbon (TOC) analysis

TOC of MB solutions was determined by a Shimadzu TOC-V CSH analyser. TOC analyser was calibrated prior to measurements using a series of prepared standards, including potassium hydrogen phthalate (KHP) as the calibration standard. Calibration involved establishing a zero baseline with DI water and generating a calibration curve through the analysis of KHP solutions with known TOC concentrations.

Chapter 4

Limitations of MD in high-salinity dye solutions

This chapter identifies the operational limits and key factors influencing the performance of MD systems, which sets the groundwork for further detailed investigations in the rest of the chapters. Here, the focus is on understanding the fouling and wetting behaviour of PVDF and PTFE membranes under various experimental conditions, using solutions containing MB, Orange G (OG), and NaCl. By conducting tests with a range of NaCl concentrations from 3.5 g/L to 100 g/L, MB concentrations from 20 mg/L to 3750 mg/L, and OG concentration of 100 mg/L, this chapter aims to establish a performance baseline. The PVDF with mean pore sizes of 0.2 μm and 0.45 μm and PTFE membrane with mean pore size of 0.5 μm, are evaluated to determine their wetting behaviour and fouling potential under these conditions.

The findings from this chapter are essential in understanding the operational boundaries and challenges associated with MD, providing a solid foundation for improving and optimizing MD systems.

4.1 Experimental conditions of the performed trials

The experimental study examined the performance of PVDF and PTFE membranes in MD, utilizing two modules, Module A and Module B, as introduced in Chapter 3, Figure 3-1. The objective was to identify the performance baseline for the wetting behaviour of commercially available membrane types at different stages, involving varying feed solutions and experimental conditions.

The summarized MD trials assessing wetting behaviour under diverse conditions are listed in **Table 4-1**. This table provides an essential overview of the trials, detailing key parameters such as membrane pore size, feed composition, and the resulting wetting behaviour. The structured comparison across different membrane types, pore sizes, and feed conditions offers valuable insights into how these factors interact to affect wetting and fouling tendencies. These insights became particularly important when inconsistencies were observed during the initial tests, which will be discussed in section 4.2.

Table. 4-1. Overview of MD trials assessing wetting behaviour under diverse feed solutions and experimental conditions. For each experiment, Qf and Qp = 70 mL/min; Tf = 60 °C, Tp= 20 °C)

No	Membrane (pore size in µm)	Feed solution	Module	Wetting
1	PTFE (0.5)	35 g/L NaCl	Module A	No
2	PTFE (0.5)	35 g/L NaCl + 50 mg/L Orange G (OG)	Module A	Yes, from beginning
3	PTFE (0.5)	35 g/L NaCl +100 mg/L OG	Module A	Yes, from beginning
4	PTFE (0.5)	35 g/L NaCl +100 mg/L OG	Module A	Yes, from beginning
5	PTFE (0.5)	35 g/L NaCl +100 mg/L OG	Module A	Yes, from beginning
6	PTFE (0.5)	35 g/L NaCl +100 mg/L OG + 100 mg/L MB	Module A	Yes, from beginning
7	PTFE (0.5)	35 g/L NaCl +100 mg/L OG + 100 mg/L MB	Module A	Yes, from beginning
8	PTFE (0.5)	DI water	Module A	-
9	PTFE (0.5)	DI water	Module A	-
10	PTFE (0.5)	35 g/L NaCl +100 mg/L MB	Module A	Yes, from beginning
11	PTFE (0.5)	35 g/L NaCl	Module A	Yes, from beginning
12	PTFE (0.5)	35 g/L NaCl +100 mg/L MB	Module A	Yes, from beginning
13	PTFE (0.5)	35 g/L NaCl	Module A	Yes, from beginning
New tests after washing and changing the tubing				
14	PTFE (0.5)	35 g/L NaCl	Module A	Yes, from beginning
15	PTFE (0.5)	35 g/L NaCl	Module A	Yes, from beginning
16	PTFE (0.5)	35 g/L NaCl	Module A	Yes, from beginning
17	PTFE (0.5)	35 g/L NaCl +100 mg/L MB	Module A	Yes, from beginning

New module (all tubing and coils were changed as well)				
18	PVDF Immobilon (0.2)	35 g/L NaCl	Module B	Yes, after 300 min
19	PVDF Immobilon (0.2)	90 g/L NaCl	Module B	Yes, after 300 min
20	PVDF Immobilon (0.2)	3.5 g/L NaCl	Module B	Yes, after 460 min
21	PVDF immobilon (0.45)	3.5 g/L NaCl	Module B	Yes, from beginning
22	PVDF Immobilon (0.2)	3.5 g/L NaCl + 0.9 g/L Oxone	Module B	No
Removing Feed EC				
23	PVDF Immobilon (0.2)	3.5 g/L NaCl	Module B	No
24	PVDF Immobilon (0.2)	3.5 g/L NaCl	Module B	No
25	PVDF Immobilon (0.2)	3.5 g/L NaCl + 20 mg/L MB reacted with Oxone	Module B	No
With original coils				
26	PVDF Immobilon (0.2)	DI water	Module B	-
27	PTFE	DI water	Module B	-
With removing coil and feed EC				
28	PVDF immobilon (0.2)	DI water	Module B	No
29	PVDF immobilon (0.2)	3.5 g/L NaCl	Module B	No
30	PVDF immobilon (0.45)	3.5 g/L NaCl	Module B	No
31	PVDF immobilon (0.2)	3.5 g/L NaCl	Module B	No
32	PVDF immobilon (0.2)	3.5 g/L NaCl + 20 mg/L MB reacted with Oxone	Module B	No
33	PVDF immobilon (0.45)	3.5 g/L NaCl + 20 mg/L MB reacted with Oxone	Module B	No

4.2 MD testing on moderate to high salinity wastewater containing dye

Trials began with a larger-sized membrane module (referred to as Module A in **Figure 3-1**), which was already available in the lab. A PTFE membrane was utilized for the initial MD tests, with the intention of designing a smaller module (Module B in **Figure 3-1**) and expanding the experiments to include the PVDF membrane.

During these initial MD tests, an inconsistency in the wetting behaviour was noticed when using Module A and the PTFE membrane, even when using a 35 g/L NaCl solution, which is typically manageable in MD [204]. This concentration was selected to replicate the feed for high pressure RO similar to seawater salinity, which is around 3.5% (or 35 g/L), making it a practical benchmark as a feed for ambient pressure MD processes. To understand the reasons behind this inconsistency, modifications to the experimental conditions at each stage were made. Two main factors contributing to the observed inconsistency were identified:

1. The sealing of the PTFE membrane inside Module A presented a challenge due to the uneven surface of the membrane. As a result, the EC started to rise from the beginning in most cases where the PTFE membrane was employed; and
2. The second factor considered was the potential contamination from previous usage of the heating coils. To investigate this, the coils were completely removed from the system.

By implementing these modifications reflected in Table 4-1, the goal was to mitigate any factors that could potentially contribute to the inconsistent wetting behaviour during MD. This stage of the study aimed to enhance the understanding of the factors influencing wetting inconsistency in MD and to develop a reliable and consistent condition for future testing.

In the next stage of the work, the impact of wastewater with moderate and high salinity (3.5 g/L starting NaCl concentration) was investigated on membrane fouling and wetting. While **Table 4-1** provides a concise summary of the experimental conditions and overall outcomes, the detailed membrane performance, particularly flux and permeate EC over time, is captured in **Figures 4-1 to 4-9**.

Figures 4-1 to 4-3 display the flux and permeate EC results for the model solutions (3.5 g/L NaCl + 20-1000 mg/L MB) over the experimental period. The results indicated that the PVDF membrane did not experience any fouling or wetting in the tested solutions, as shown in **Figures 4-1 to 4-3.**

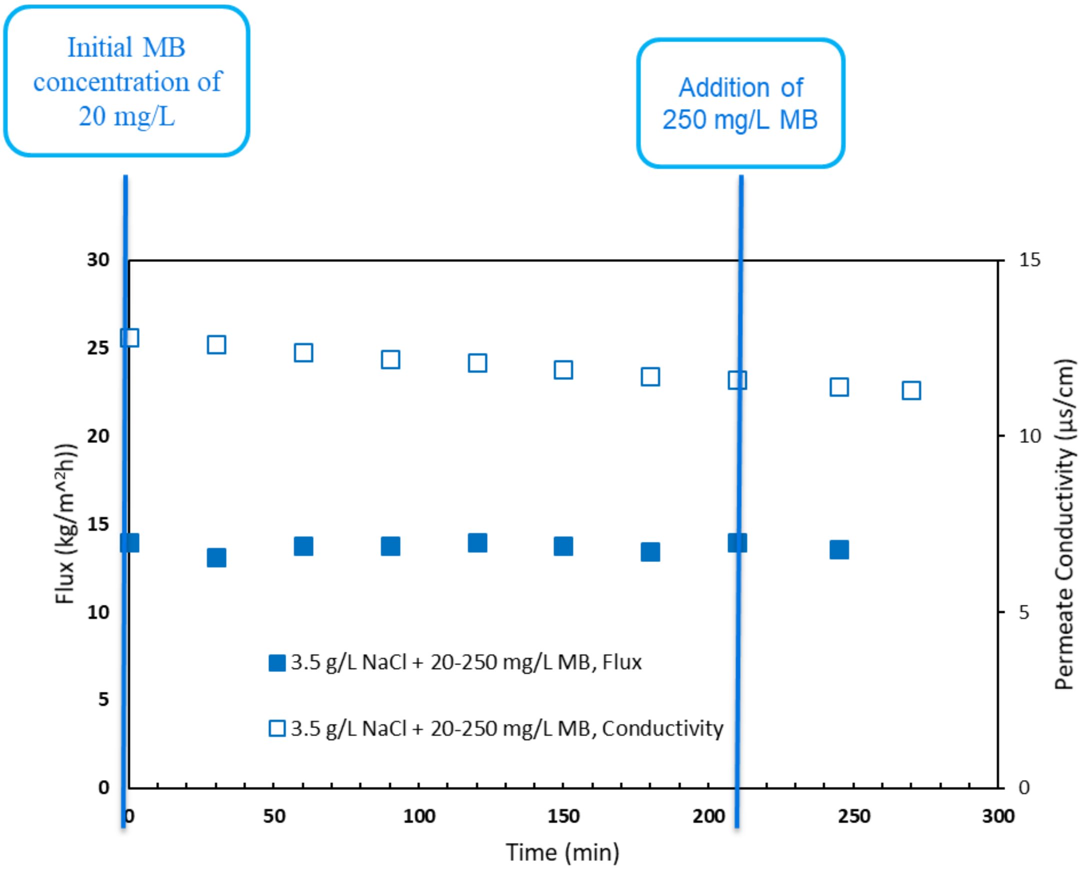

Figure. 4-1. DCMD performance of the commercial PVDF membrane (mean pore size=0.2 μm) in treatment of solutions starting with 3.5 g/L NaCl and initial MB concentration of 20 mg/L and subsequent addition of 250 mg/L MB at the time of 0 and 210 min. (For each experiment, 1L of feed solution was used, Qf and Qp = 70 mL/min; Tf = 60 °C, Tp= 20 °C)

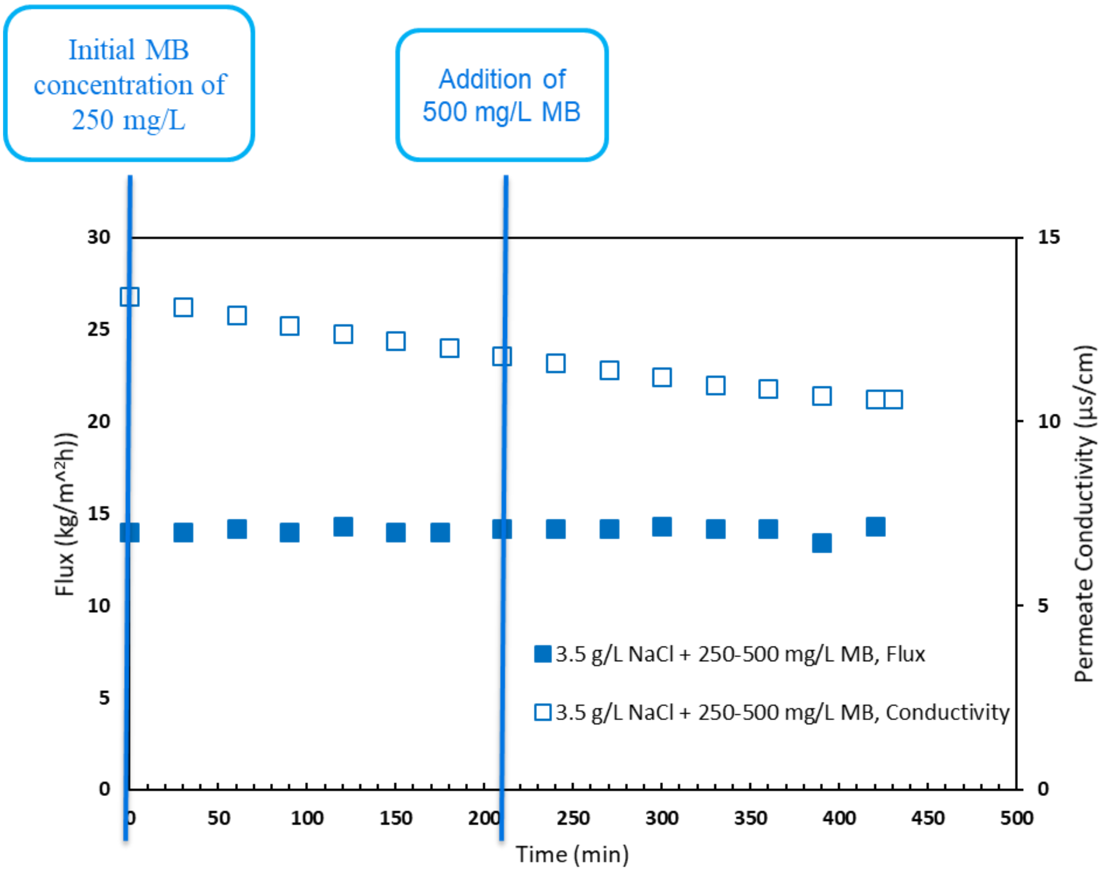

Figure. 4-2. DCMD performance of the commercial PVDF membrane (mean pore size=0.2 μm) in treatment of solutions starting with 3.5 g/L NaCl and initial MB concentration of 250 mg/L and subsequent addition of 500 mg/L MB at the time of 0 and 210 min. For each experiment, 1L of feed solution was used, Qf and Qp = 70 mL/min; Tf = 60 °C, Tp= 20 °C)

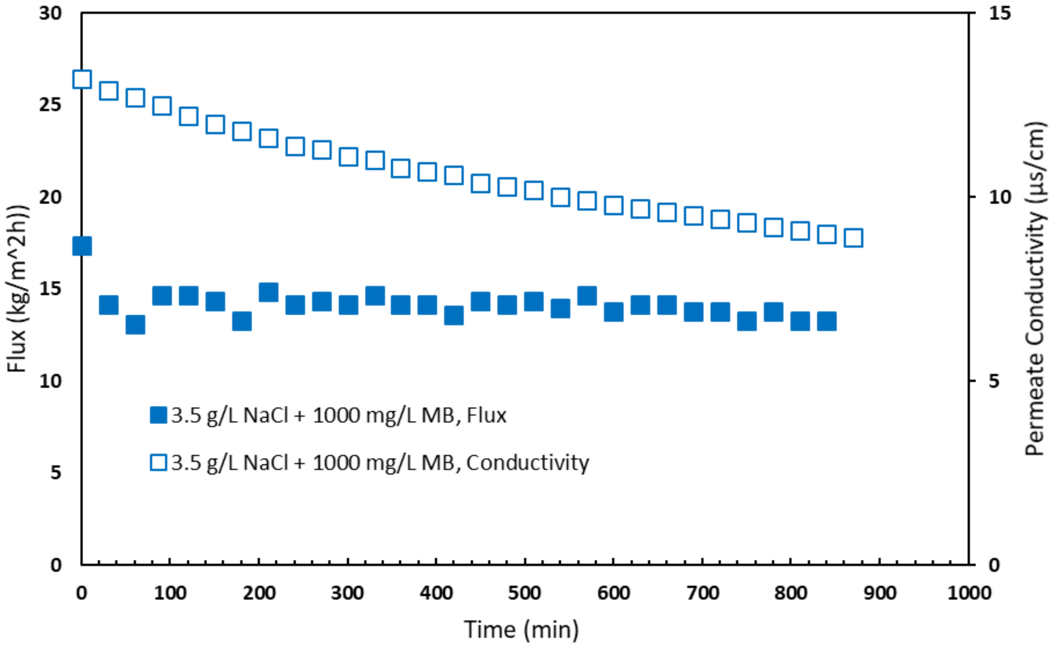

Figure. 4-3. DCMD performance of the commercial PVDF membrane (mean pore size=0.2 μm) in treatment of solutions starting with 3.5 g/L NaCl and starting MB concentration of 1000 mg/L. For each experiment, 1L of feed solution was used, Qf and Qp = 70 mL/min; Tf = 60 °C, Tp= 20 °C)

In the next stage of testing, a check valve was introduced on the outlet of the feed side as described in chapter 3. The same range concentration of MB to investigate flux and wetting behaviour. **Figures 4-4 to 4-6** illustrate the flux and permeate EC for the treatment of model solutions of 3.5 g/L NaCl + 50-1000 mg/L MB over the experimental period. The results displayed in **Figures 4-4 to 4-6** indicated no fouling or wetting for the tested solutions.

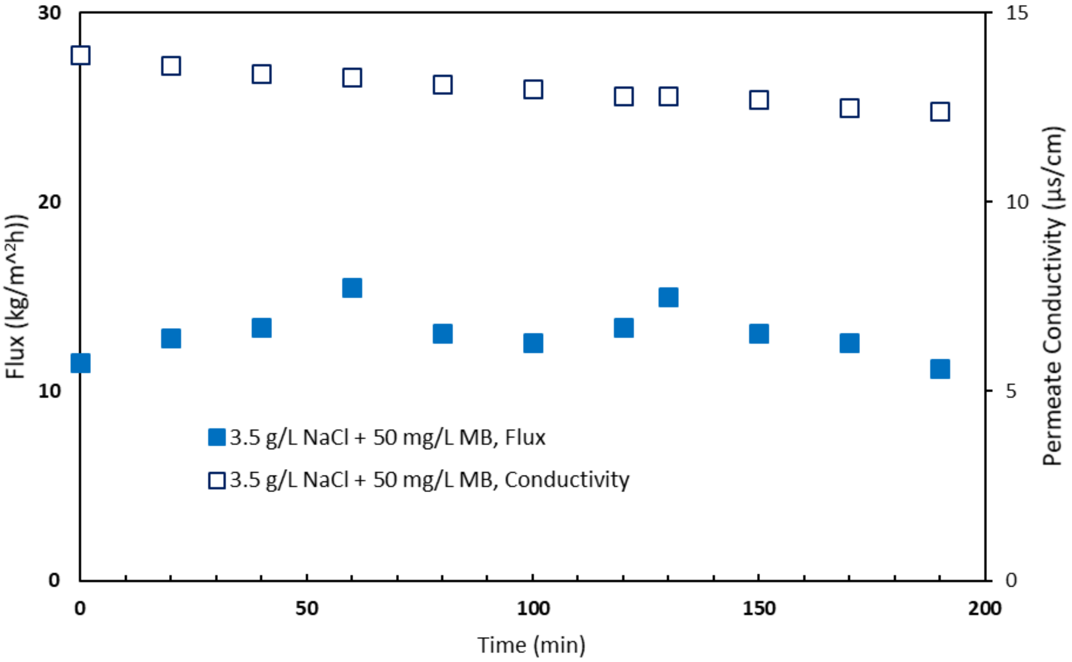

Figure. 4-4. DCMD performance of the commercial PVDF membrane (mean pore size=0.2 μm) in treatment of solutions starting with 3.5 g/L NaCl and starting MB concentration of 50 mg/L. (For each experiment, 1L of feed solution was used, For each experiment, 1L of feed solution was used, Qf and Qp = 70 mL/min; Tf = 60 °C, Tp= 20 °C, Pback=35-40 kPa(g))

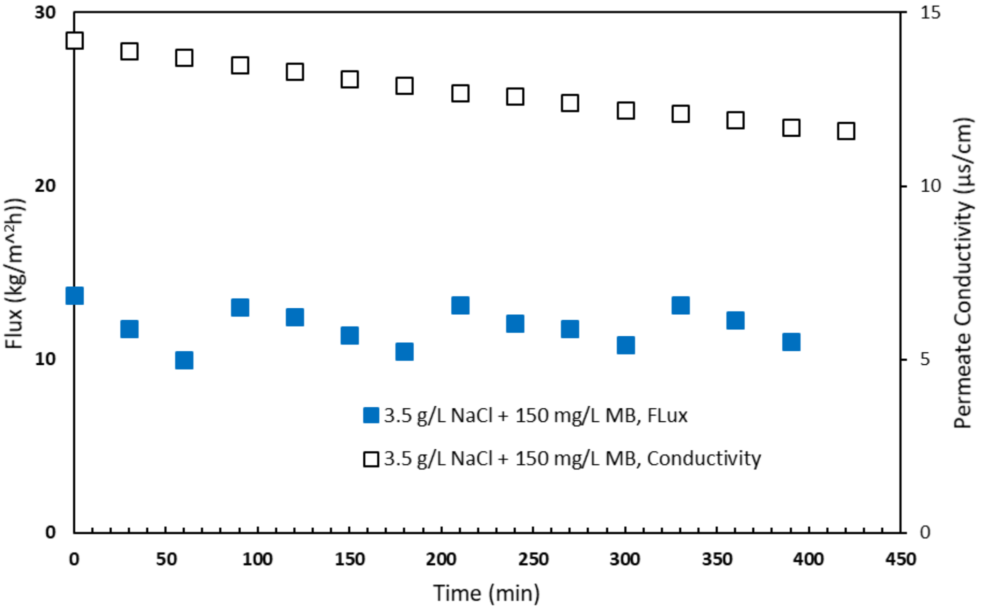

Figure. 4-5. DCMD performance of the commercial PVDF membrane (mean pore size=0.2 μm) in treatment of solutions starting with 3.5 g/L NaCl and starting MB concentration of 150 mg/L. For each experiment, 1L of feed solution was used, Qf and Qp = 70 mL/min; Tf = 60 °C, Tp= 20 °C, Pback=35-40 kPa(g))

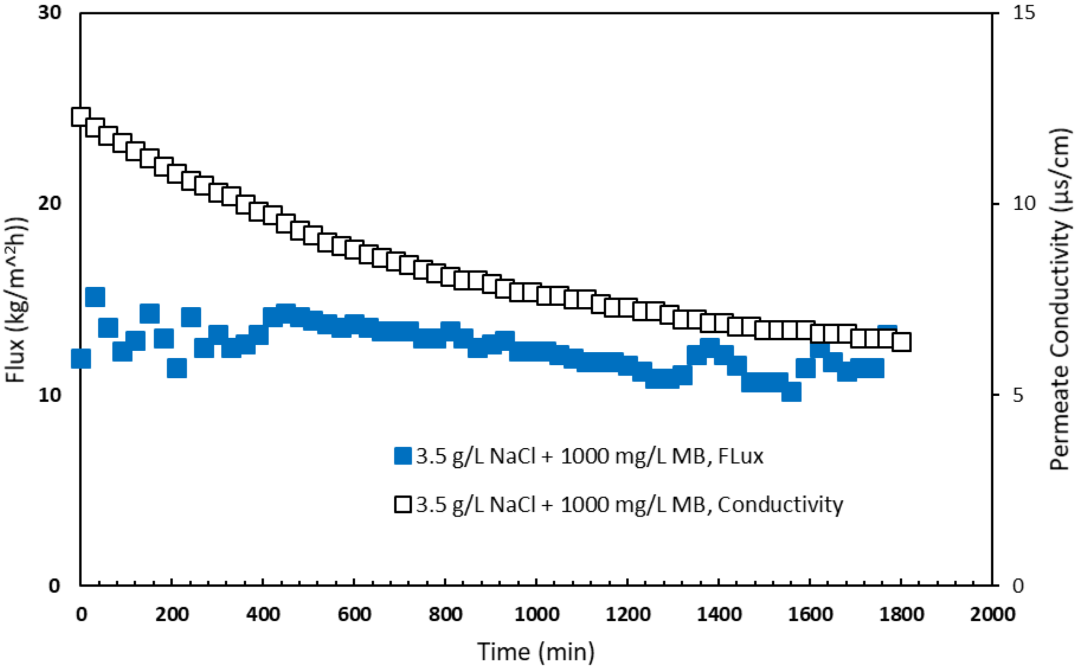

Figure. 4-6. DCMD performance of the commercial PVDF membrane (mean pore size=0.2 μm) in treatment of solutions starting with 3.5 g/L NaCl and starting MB concentration of 1000 mg/L. For each experiment, 1L of feed solution was used, Qf and Qp = 70 mL/min; Tf = 60 °C, Tp= 20 °C, Pback=35-40 kPa(g))

When the initial salt concentration was increased from 3.5 g/L to 50 g/L, along with an increase in the dye concentration (3000 mg/L MB), the PVDF membranes showed considerable fouling and wetting as depicted in **Figure 4-7.** This experiment was conducted multiple times, and the same trend for flux and EC was observed. However, upon replacing the MB source with a new source from the supplier, the EC breakthrough did not occur. This suggests that variability in the lab stock of MB, potentially caused by differences between batches or changes over time due to aging or storage conditions, may have contributed to the observed fouling and wetting behaviour. **Figure 4-8** displays the flux and EC outcomes of the PVDF membrane utilizing the new MB source solution, indicating no fouling or wetting.

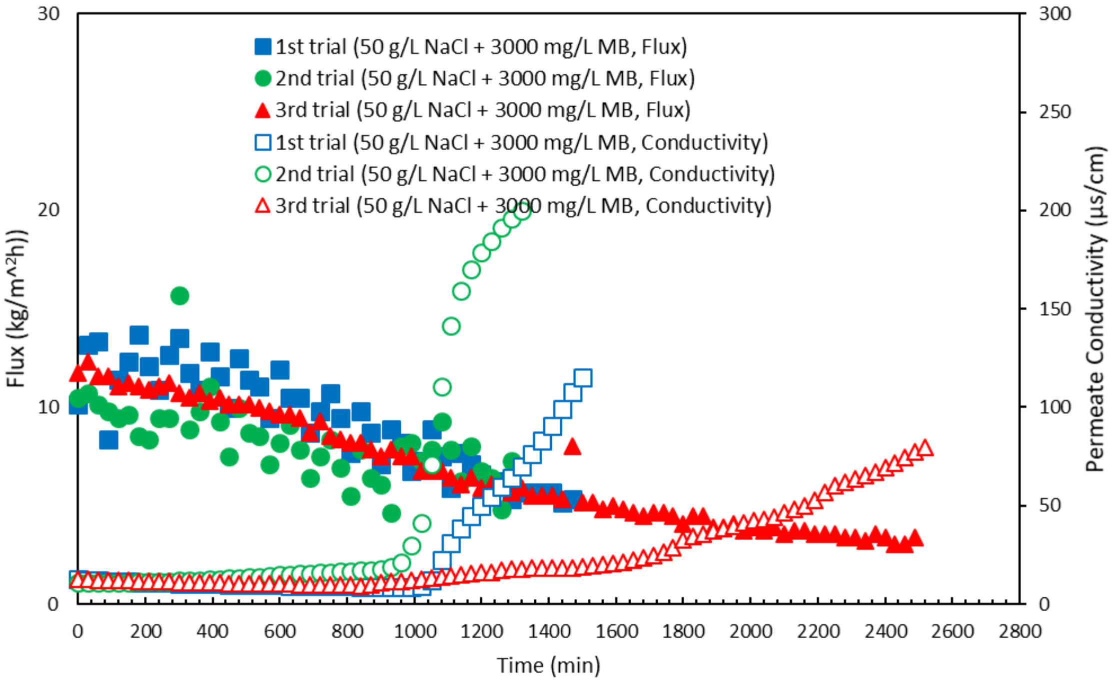

Figure. 4-7. DCMD performance of the commercial PVDF membrane (mean pore size=0.2 μm) in treatment of solutions starting with 50 g/L NaCl and starting MB concentration of 3000 mg/L. For each experiment, 1L of feed solution was used, Qf and Qp = 70 mL/min; Tf = 60 °C, Tp= 20 °C, Pback=35-40 kPa(g))

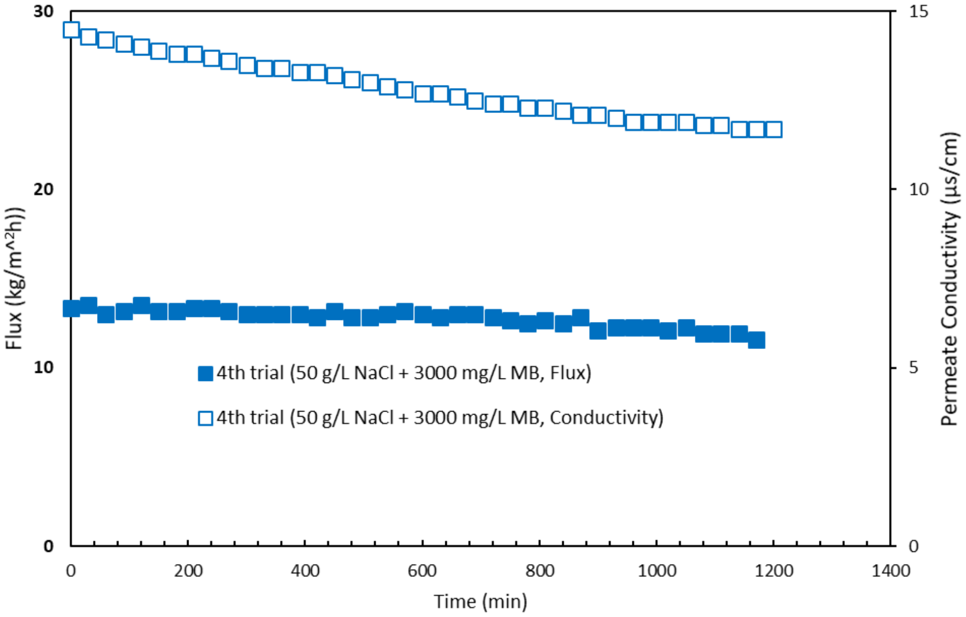

Figure. 4-8. DCMD performance of the commercial PVDF membrane (mean pore size=0.2 μm) in treatment of solutions starting with 50 g/L NaCl and starting MB concentration of 3000 mg/L. For each experiment, 1L of feed solution was used, Qf and Qp = 70 mL/min; Tf = 60 °C, Tp= 20 °C, Pback=35-40 kPa(g))

After validating the test setup and source chemicals, MD testing revealed that, in most cases, there was no flux decline or EC increase (**Figure 4-9**), indicating an absence of fouling and wetting. However, a flux decline and EC increase was observed in the case of 100 g/L NaCl + 3750 mg/L MB, suggesting fouling and wetting potential of this solution. The behaviour and stability of foulants are significantly influenced by their surface charge and hydrophobicity, as these properties, combined with solution conditions [75,84–86], affect foulant aggregation, which can block membrane pores [67].

The fouling behaviour of dyes in MD systems is well-documented in the literature. For example, Banat et al. [205] explored vacuum membrane distillation (VMD) for removing MB in solutions with NaCl concentrations ranging from 0.05 to 1 M, showing that VMD effectively concentrated dye on the feed side. However, some decline in permeate flux was observed over time due to membrane fouling. Criscuoli et al. [17] tested VMD with various dyes, including reactive black and acid dyes, and reported flux decay in all cases due to fouling. Similarly, Fang Li et al. [206] investigated DCMD using PTFE and PVDF membranes for treating industrial and synthetic dyeing wastewater with COD levels ranging from 149 mg/L to 2300 mg/L. This study highlighted the impact of suspended solids and dispersed dyes in promoting fouling and wetting, which negatively affected long-term operation. Building on these findings, Laqbaqbi et al. [86] examined DCMD with PVDF membranes, showing that cationic dyes, such as Maxilon Blue and Drimarene Yellow, caused significant fouling due to electrostatic and hydrophobic interactions, with increased feed salinity further intensifying these effects.

In this study, flux decline was likely due to the predominance of cationic MB (MB^+) at unadjusted pH [207,208], which increased the attraction of MB to the negatively charged PVDF membrane surface, thus intensifying membrane interactions. Additionally, MB molecules may adhere to the membrane through hydrophobic interactions, further contributing to fouling [16,21].

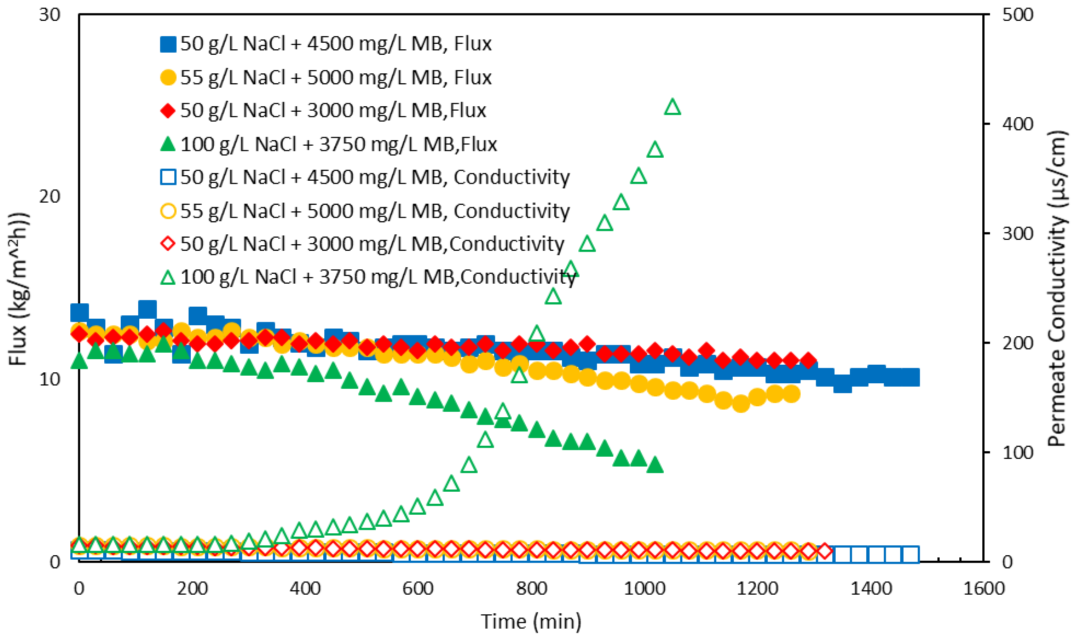

Figure. 4-9. DCMD performance of the commercial PVDF membrane (mean pore size=0.2 μm) in treatment of solutions starting with 50-100 g/L NaCl and starting MB concentration of 3000-5000 mg/L. (For each experiment, 1L of feed solution was used except for the 100g/L NaCl test when 700 ml was used, Qf and Qp = 70 mL/min; Tf = 60 °C, Tp= 20 °C, Pback=35-40 kPa(g))

4.3 Conclusions

This chapter identified critical sensitivities related to the MD setup and the chemicals used, which initially interfered with conducting valid tests. The tests involved PVDF membranes (mean pore size: 0.2 µm and 0.45 µm) and PTFE membrane (mean pore size: 0.5 µm) with NaCl concentrations from 3.5 g/L to 100 g/L, MB concentrations from 20 mg/L to 3750 mg/L, and OG concentration of 100 mg/L. The main issues identified were:

Inconsistencies:

- Inconsistencies in wetting behaviour due to the issues with the sealing of the PTFE membrane in the module
- Potential contamination from the residue left from previous usage of heating coils
- Variability in the lab stock of MB, which may have been affected by differences between batches or changes over time due to aging or storage conditions

These findings highlight the importance of considering variability in MB properties, which may significantly influence MD performance.

Performance limitations:

By addressing these factors, consistent experimental conditions were achieved, allowing successful testing of the PVDF membrane with various salt and dye concentrations. Performance limits were observed under high salinity conditions for the PVDF membrane. Specifically, the PVDF membranes showed fouling and wetting when exposed to a mixture with NaCl concentrations of 100 g/L and MB concentration of 3750 mg/L. These findings not only highlight the critical factors affecting MD performance but also provide a comprehensive understanding of the operational challenges and limitations. By establishing baseline limitations in Chapter 4, the conditions are now defined for the following investigations to the need for strategies to mitigate wetting and fouling in high-strength solutions, potentially broadening the operational range of MD in high-strength wastewater applications. Recognising these limits, Chapter 5 builds on this work by exploring the potential of sulphate radical-based advanced oxidation processes (SR-AOPs), specifically using Oxone, as a strategy to overcome the observed performance barriers.

Chapter 5

Advanced oxidation assisted MD for wetting mitigation during treatment of high salinity dye solutions

5.1 Introduction

In this chapter, the integration of MD with sulphate radical-based advanced oxidation processes (SR-AOPs) was explored as a strategy to reduce wetting as potential challenges to MD. The SR-AOPs is an emerging concept, in which the activation of PS or PMS can be achieved by introducing heat. Some studies have investigated thermal activation of PS at various temperatures (20-100 °C) depending on the target pollutant [126,209]. It has been reported that the activation of PS or PMS was sufficiently achieved for organic degradation via the waste heat discharged from many industries including textile [126]. Thus, given the spontaneous advantage of readily available heat sources in MD, the development of an integrated system (MD and SR-AOPs (MD/SR-AOPs)) for simultaneous water recovery and pollutant degradation seems to be an attractive solution.

As discussed in Chapter 4, the treatment of high salinity MB solutions exhibited wetting behaviour when the salt concentration was high (100 g/L). This finding emphasizes the need for additional strategies to prevent wetting and improve MD performance under challenging conditions. Therefore, this chapter focuses on evaluating whether the addition of Oxone, a potent oxidizing agent, can improve the MD performance. The investigation specifically targeted at high-strength wastewater containing MB and high NaCl concentrations to assess improvements in fouling and wetting resistance of MD membranes. It is also important to note that each MD experiment was conducted at least three times, with a fresh membrane and solution used for every trial. A representative result was selected for presentation, analysis, and further discussion.

The effects of Oxone were studied under varying conditions, including with and without pH adjustment of the feed solution, to determine its impact on the MD process. This approach aimed to determine whether partial oxidation could transform hydrophobic pollutants into less fouling-prone forms and whether these changes could reduce the wetting and fouling tendencies of the MD membranes. Previous research [23] reported that, compared to MD only, where severe wetting happened in 130 min at 0.3 mM SDS, the hybrid MD/electro-assisted oxidation process (EAOP) achieved stable flux over 240 minutes operation even at SDS concentration of 0.5 mM as semi-volatile organics and SDS were degraded by sulphate radicals. This improvement in wetting resistance was attributed to SDS's structural change due to oxidation, specifically the loss of its amphiphilic properties [155,156].

Therefore, the use of low concentrations of Oxone, more representative of practical environmental settings, aimed to provide insights into the feasibility and limitations of integrating SR-AOPs with MD for treating high-strength saline wastewater.

5.2 Results and discussion

5.2.1 Membrane performance in DCMD tests

5.2.1.1 Effect of saline feeds with MB

DCMD experiments were conducted using a pristine PVDF membrane with feed solutions containing 3750 mg/L MB and NaCl concentrations of 35 g/L to 100 g/L. The performance of these solutions in DCMD is depicted in **Figures 5-1**.

The data presented in **Figure 5-1** show a significant flux reduction for the solution with 100 g/L NaCl, which experienced a 42% decline after 21 hours of operation. This contrasts with a smaller decrease in flux observed for the 85 g/L and 70 g/L NaCl solutions, and a relatively constant flux for the 35 g/L NaCl solution. Wetting intensity was also more pronounced at higher NaCl concentrations, following the order: 100 g/L NaCl > 85 g/L NaCl > 70 g/L NaCl > 35 g/L NaCl, all containing an initial MB concentration of 3750 mg/L.

The properties of foulants, such as surface charge and hydrophobicity, play a significant role in their stability aggregation behaviour in solution [75,84–86]. For instance, the tendency of foulants to aggregate, which depends on both the inherent characteristics of the contaminants and the solution environment, often leads to pore blockage in the membrane [68]. Laqbaqbi et al. [86] reported that aggregates can form from dye molecules containing both positively and negatively charged groups, causing pore blockage and resulting in a decline in flux.

In this study, the observed overall decline in flux can be attributed to the predominance of the cationic form of MB (MB^+) at neutral pH [207,208]. The attraction of MB ions to surfaces of opposite charge, in this case negatively charged PVDF membrane, exacerbates the interaction between positively charged MB ions and the membrane [210]. Additionally, MB molecules may adhere to the membrane through hydrophobic interactions, leading to increased fouling [16,21]. In contrast, negatively charged dyes (e.g., Acid Red 18 (AR 18), Acid Yellow 36 (AY 36)) have shown a lower fouling tendency on negatively charged membranes due to electrostatic repulsion, which reduces the likelihood of pore blockage and preserves flux [92,93].

Moreover, the decline in MD flux and accelerated wetting may also be linked to reduced solubility of MB at higher salt concentrations, a phenomenon known as salting-out. This effect, which involves the precipitation of dyes as salt concentrations increase, also enhances the hydrophobicity of the dyes, thereby destabilizing dye molecules and promotes membrane fouling [44,211]. The salting-out effect is harnessed for practical benefit in industrial processes where large quantities of inorganic salts are used to precipitate dyes from solutions [48,211]. These findings further support the potentially significant role of salting out in influencing fouling and wetting behaviours in MD during the treatment of high-salinity streams. The impact of the salting-out phenomenon on MD flux decline and wetting will be explored in greater detail in **Chapter 7**.

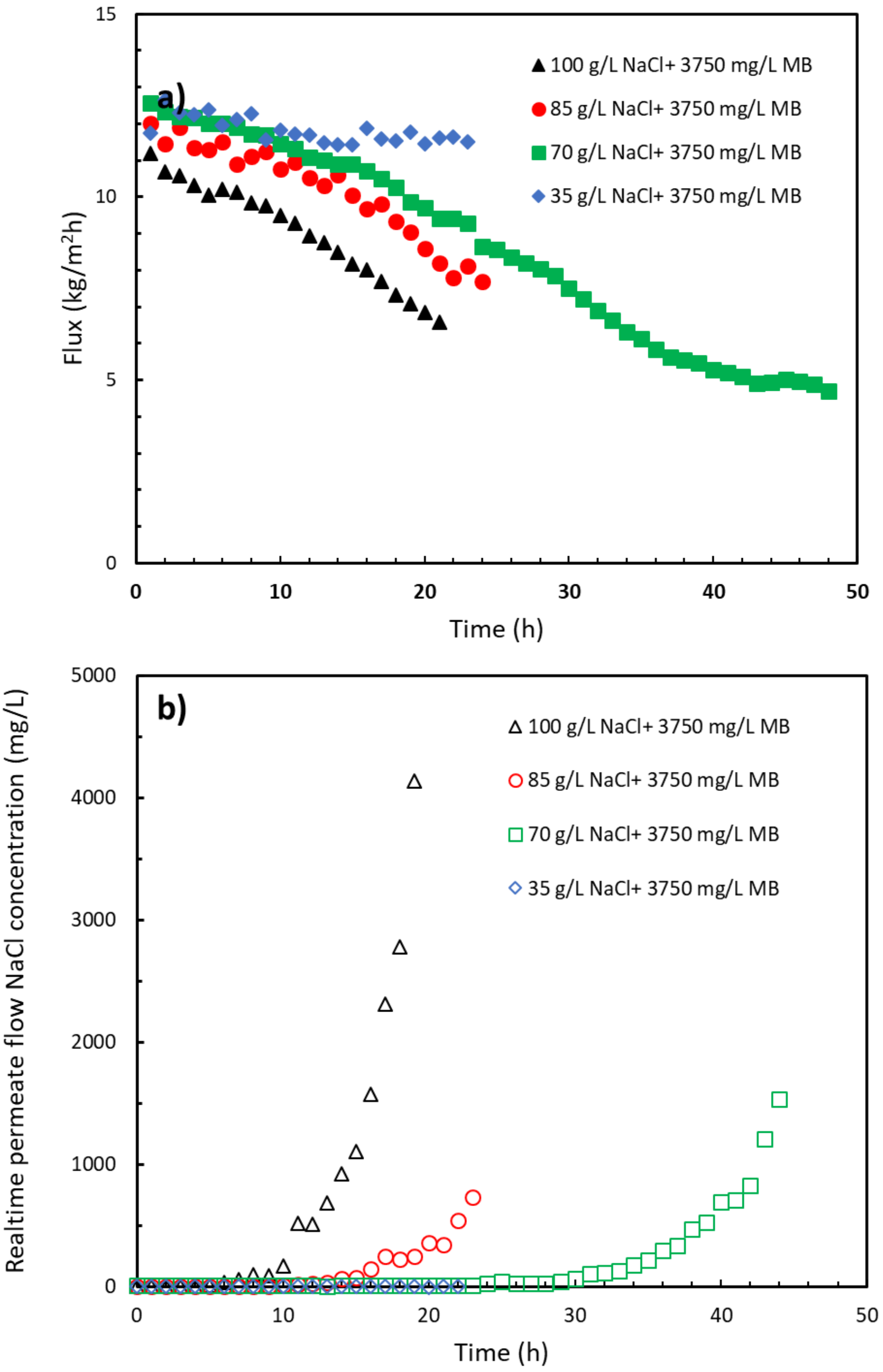

Figure. 5-1. DCMD performance in terms of a) Flux vs time and b) real-time permeate flow NaCl concentration vs time of the commercial PVDF membrane (mean pore size=0.2 μm) in treatment of solutions starting with 35-100 g/L NaCl and starting MB concentration of 3750 mg/L. (For each

experiment, 1L of feed solution was used, Qf and Qp = 70 mL/min; Tf = 60 °C, Tp= 20 °C, Pback=35-40 kPa(g))

5.2.1.2 Effect of Oxone and pH adjustment

To assess the impact of Oxone on MD efficiency, experiments utilized a commercial PVDF membrane to treat two high-salinity solutions (100g/L and 85g/L NaCl). The specific impact of pH on MD efficiency was studied without the presence of Oxone by adding HCl to the same feed solution. To determine the influence of pH adjustments on Oxone's ability to mitigate fouling and wetting in MD, NaOH was applied to neutralize the pH after Oxone initially reduced the feed pH to 3.2. Additionally, the effect of an acidic environment alone was studied by adding HCl to the MB and salt solution to reduce the pH to 3.2. The data acquired on the flux and real-time permeate flow NaCl concentration were plotted over time in **Figures 5-2 and 5-3**.

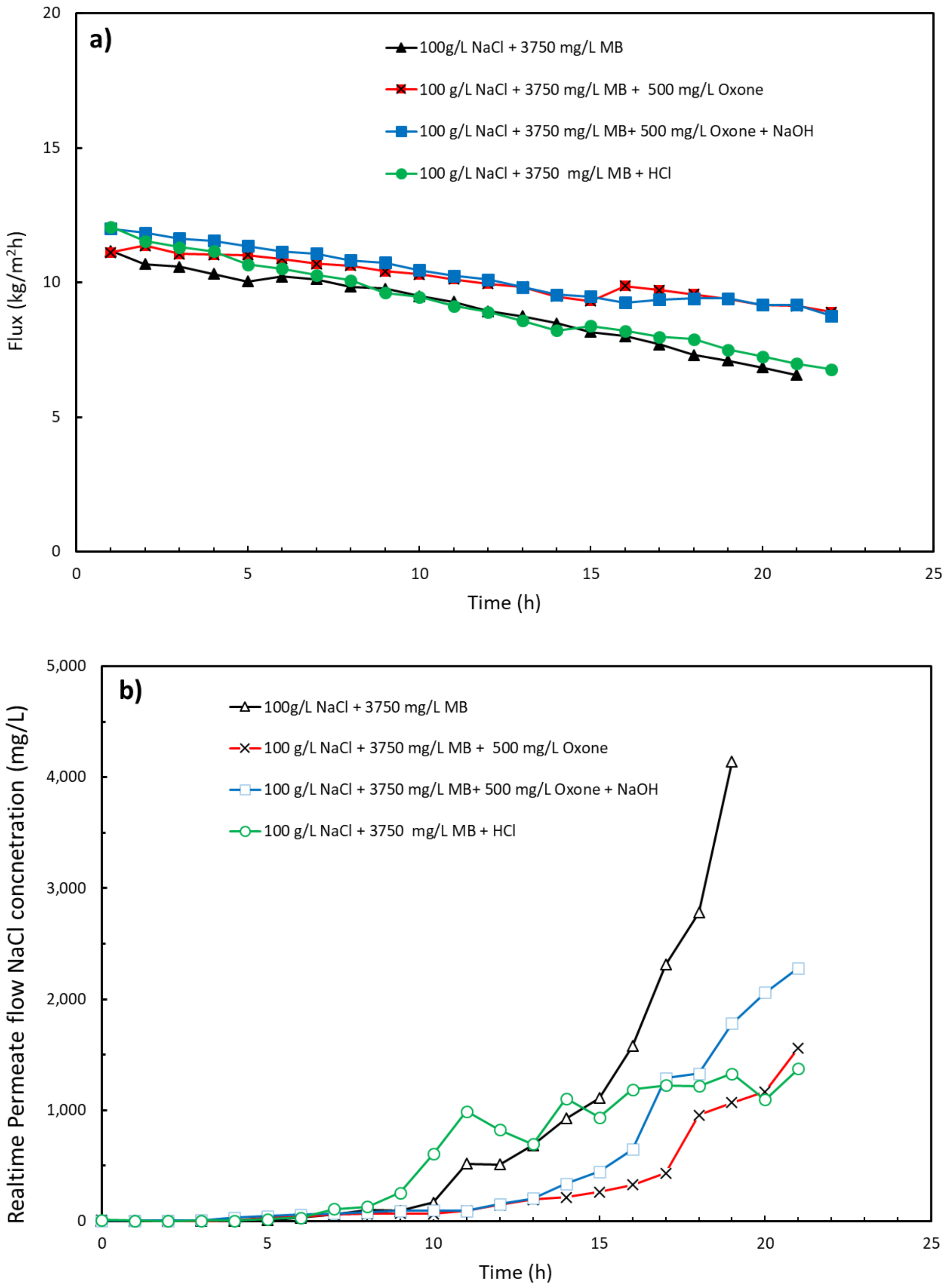

Figure. 5-2. DCMD performance in terms of Flux and Real-time permeate flow NaCl concentration vs time of the commercial PVDF membrane (mean pore size=0.2 μm) in treatment of solutions starting with 100 g/L NaCl and starting MB concentration of 3750 mg/L. The graph compares the baseline performance with the effects of adding 500 mg/L Oxone and the combined effects of 500 mg/L Oxone with NaOH, and HCl

only. (For each experiment, 1L of feed solution was used, Qf and Qp = 70 mL/min; Tf = 60 °C, Tp= 20 °C, Pback=35-40 kPa(g))

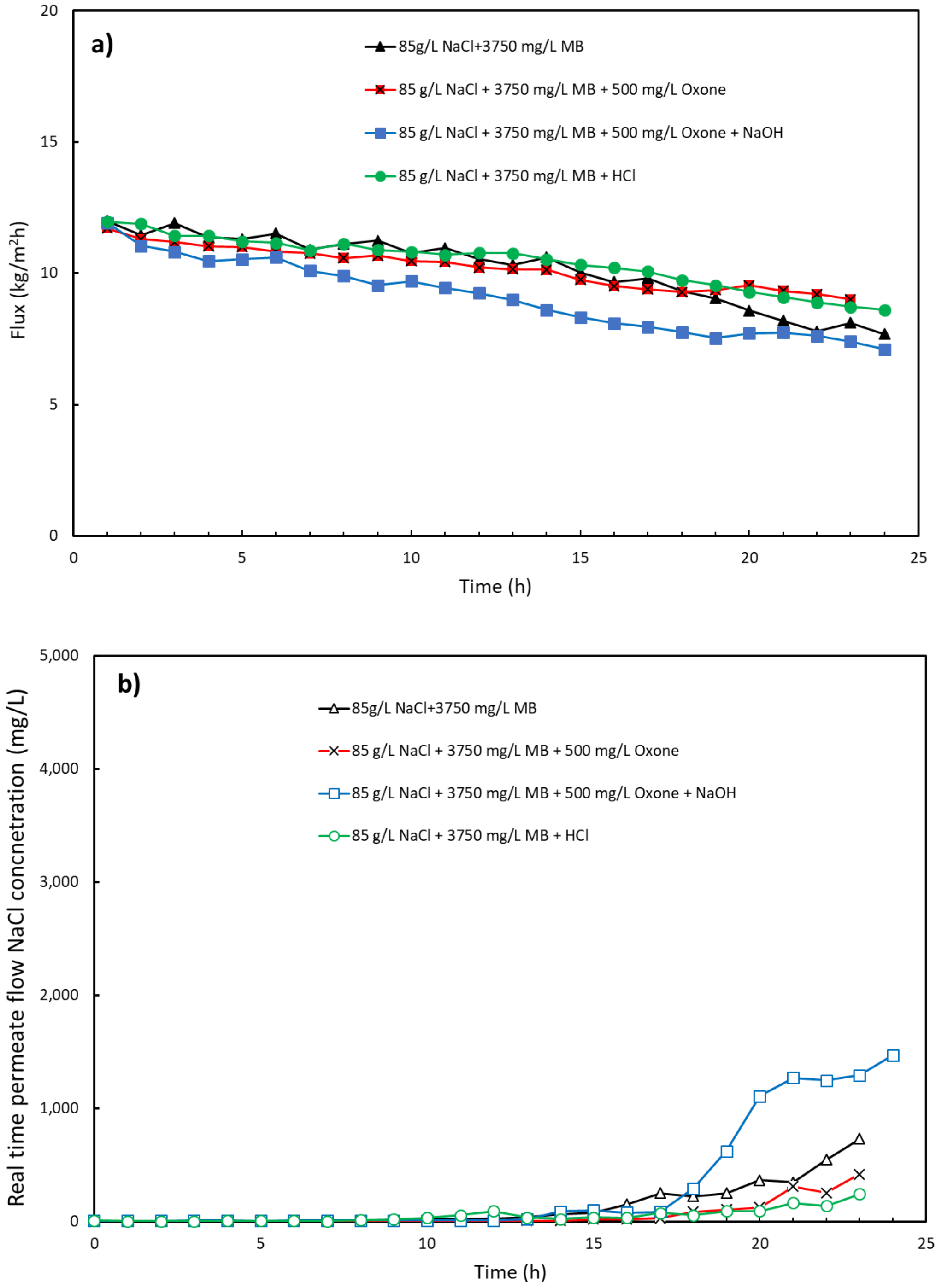

Figure. 5-3. DCMD performance in terms of Flux and Real-time permeate flow NaCl concentration vs time of the commercial PVDF membrane (mean pore size=0.2 μm) in treatment of solutions starting with 85 g/L NaCl and starting MB concentration of 3750 mg/L. The graph compares the baseline performance with the effects of adding 500 mg/L Oxone and the combined effects of 500 mg/L Oxone with NaOH, and HCl only. (For each experiment, 1L of feed solution was used, Qf and Qp = 70 mL/min; Tf = 60 °C, Tp= 20 °C, Pback=35-40 kPa(g))

In **Figures 5-2** and **5-3**, the behaviour of the PVDF membrane was evaluated during the treatment of solutions containing 3750 mg/L MB at salinity concentrations of 85 g/L and 100 g/L. The results suggest that the addition of Oxone to the MD system does not significantly improve the process in terms of flux, although it may slightly delay and reduce the rate of wetting. It also appears that adjusting the pH to neutral after adding Oxone doesn't substantially enhance flux performance, although it may delay the onset of wetting. In addition, the acidic environment alone did not offer a significant improvement in terms of flux and wetting compared to the use of Oxone without pH adjustment. Several factors contribute to these behaviours:

Firstly, the Oxone concentration in the solution is relatively low compared to the MB concentration, i.e., MB is present at more than seven times the concentration of Oxone. This significant difference likely limits the ability of Oxone to effectively degrade or transform MB. Although literature suggests that SO4^{o} generated by Oxone have a strong capability to oxidize organic pollutants, their application typically focuses on low concentrations of organics where the oxidant and pollutant concentrations are comparable [14,212–214]. For example, Pan et al. [215] found that when the PMS concentration was approximately four times higher than that of Rhodamine B (on mass basis), the removal efficiency was significantly enhanced. In another study, the PMS concentration was nine times higher the MB concentration on mass basis [216]. In this study's context, the findings imply that an increased Oxone concentration or reduced organic content might be required to achieve a meaningful impact on MB degradation and to enhance MD process efficiency. However, the potential benefits of partial oxidation should not be overlooked. Partial oxidation can sometimes enhance MD performance by transforming the pollutants into less hydrophobic compounds. Oxidation can lead to the loss of hydrophobicity or the amphiphilic nature of low surface tension contaminants, reducing their tendency to accumulate on the membrane surface due to hydrophobic-hydrophobic interactions [23]. Yet, in this study, a low Oxone dosage and hence a partial oxidation did not yield significant improvements in flux or wetting behaviour in MD. Nonetheless, in practical environmental settings, the feasibility of using high levels of oxidants is often restricted due to the detrimental effects they may pose to aquatic life [217].

Secondly, the decrease in performance may be linked to the 'salting out' effect as discussed previously, which refers to the decreased solubility and subsequent precipitation of organics in high-salt solutions. Wherein increased salinity raises the mass of MB aggregates, thus reducing MD flux and leading to membrane wetting.

Additionally, pH variation significantly influences foulant-membrane interactions. As the concentration of H^+ ions increases (lowering the pH), both the surface charge of the membrane and the foulant become more positive, altering the interaction dynamics. For instance, one study demonstrated that lowering the pH of coal gasification wastewater to 3.5 to reject ammonium nitrogen (NH_4^+-N) through MD accelerated fouling. This was attributed to reduced electrostatic repulsion between humic acids (HA) with a negative charge and the membrane surface, which carried a slight negative charge at low pH levels [68].

In the present study, lowering the pH to 3.2 using either Oxone or HCl may have contributed to the limited fouling mitigation observed. In aqueous solutions, MB exists in two forms: as the cationic species (MB^+) and as undissociated molecules (MB°). At pH 3, approximately 86% of MB is undissociated (MB°) [207,208]. When the pH approaches the pKa of 3.8, MB is equally split between MB^+ and MB°. At pH levels above 6, MB is found almost exclusively in its cationic form (MB^+) [207,208]. Theoretically, the net interaction between particles or particles and a surface is composed of Van der Waals forces, acid-base interactions, and electrostatic double-layer interactions. Particles with a charge opposite to that of the membrane surface will be attracted to it [210]. At the acidic pH induced by either Oxone or HCl, the PVDF membrane surface remains negatively charged [30,218], facilitating electrostatic attraction with any cationic MB in the system. Moreover, MB°, which are predominant at this pH, can deposit on the membrane surface through hydrophobic interactions. In the neutral pH scenario which was achieved through NaOH addition enhances the PVDF membrane's negative charge, thereby intensifying the interaction between the positively charged MB ions. Additionally, MB molecules can adhere to the membrane via hydrophobic interactions, contributing to the fouling.

In general, it is important to note that the obtained results do not show a significant difference to identify any beneficial effects of the addition of Oxone to the feed solution within the tested conditions. As observed from the MD test results (**Figures 5-2 and 5-3**), in both acidic and neutral pH cases, the membrane eventually fails, indicating that the interplay between electrostatic and hydrophobic interactions leads to wetting under both conditions.

5.3 Conclusions

This chapter systematically explored the integration of MD with SR-AOPs, specifically using Oxone, to address fouling and wetting issues in high-strength saline wastewater. The integration of oxidation processes in MD, particularly for high-strength wastewater, remains underexplored, as most previous studies have focused on low concentrations of organics with little or no salinity, which presents fewer challenges for MD systems. As discussed in Chapter 2, treating high-strength saline wastewater is a significant challenge for MD.

The use of oxidation processes has typically targeted scenarios when oxidant and pollutant concentrations are comparable (close to stoichiometric ratios). However, in practical environmental settings, high oxidant concentrations are often impractical due to potential harmful effects on aquatic life. Therefore, this study focused on the impact of using low oxidant dosages in treating high-strength dye wastewater, which is more representative of real-world conditions.

The investigation revealed that low concentration of Oxone (500 mg/L) relative to the pollutant, MB (3750 mg/L) in our case had no effect on the occurrence of wetting. However, the presence of Oxone delayed the onset of membrane wetting in the tested solutions. It was hypothesized that the pH change due to the presence of Oxone may have influenced the surface properties of the membrane as well as the charge of MB molecules, leading to the adhesion of MB to the membrane. To test this hypothesis, pH was adjusted using NaOH and HCl in different sets of experiments. When the pH was adjusted to neutral with NaOH, the enhancement in MD performance was marginal. Therefore, higher oxidant to pollutant ratios are needed for significant degradation efficiency, a balance that was not met in the current experimental setups. Adjustments of the solution pH with HCl to study the isolated effects of pH did not also yield substantial improvements, indicating that other factors beyond pH play a critical role in MD performance. The salting-out phenomenon could possibly have a significant impact on MD process, where decreased MB solubility led to a decline in flux and increased wetting.

Although the results showed that adding Oxone did not significantly improve flux or prevent membrane wetting, several important contributions emerged from this work:

- **Targeting niche applications of reactive MD systems:** Extending reactive MD to treat concentrated organic wastewater with salinity levels above 80 g/L (beyond the limits of reverse osmosis) is crucial. Additionally, The effects of ionic species on inorganic-organic interactions and foulant-membrane interactions are complex and have not been fully addressed in the existing MD literature.
- **Impact of pH adjustment on MD performance:** pH adjustment, whether to acidic or unadjusted, did not significantly enhance flux or prevent wetting, indicating that factors beyond pH such as foulant-membrane interactions and foulant-foulant are critical.
- **Limits of SR-AOP integration in MD:** The study identified the limitations of SR-AOP integration under high-strength dye solutions, providing a baseline for optimizing oxidant concentration and exploring the practical applicability of reactive MD systems.
- **Effectiveness of partial oxidation:** While literature suggests that even incomplete oxidation can transform organic pollutants into more hydrophilic fractions, thereby reducing their fouling tendency, the experiments suggested that partial oxidation of organics did not yield significant improvements at low oxidant dosages, underscoring the challenges in reducing fouling with insufficient oxidant levels.

In summary, while the integration of SR-AOPs with MD did not significantly enhance performance under the tested conditions, this study provides valuable insights into the limitations and challenges of reactive MD in high-strength dye solutions. Further work is needed to characterise the membranes to understand the antifouling behaviour of selected materials showing promise. These findings guide future research in optimizing MD processes and integrating alternative strategies, such as membrane surface modifications, to mitigate fouling and wetting, which is the topic of next chapter.

Chapter 6

Surface modification to prevent wetting during MD with high salinity dye solutions

6.1 Introduction

The advancement of MD membrane technology involves enhancing the membrane resistance to fouling and wetting. This method includes the engineering of a hydrophilic coating on top of a hydrophobic substrate. Such a design significantly boosts the antifouling properties of the membrane. The strategic placement of a thin hydrophilic film over the hydrophobic membrane is known to promote the development of a hydration layer. This layer plays a crucial role in reducing the adhesion of foulants to the membrane surface, thereby elevating its operational efficiency [29,30]. Research suggests that this configuration can effectively reduce the membrane fouling issues, leading to sustained membrane performance [30–32].

Inspired by the strong binding affinity of polydopamine (PDA) toward substrates with different properties, there has been an increasing interest in implementation of PDA for surface modification [33,34]. It is reported that the interaction between PDA and different substrates is originated from non-covalent interactions such as hydrogen binding [34–36], coordination [33,37], and hydrophobic interactions [34,38]. However, the PDA deposition on most material surfaces has been reported to be a time-consuming process [30,33]. To address this problem, the use of oxidants [30,39–41] was considered to accelerate the dopamine polymerization.

In MD applications, PDA is often combined with other materials to enhance specific membrane properties. For instance, PDA/PEI (polyethylenimine) coatings create Janus membranes with a hydrophilic side and a hydrophobic nanofiber layer, which improves anti-wettability and permeate flux [197,219]. These membranes have been tested with various pollutants, including synthetic salt solutions (10,000 mg/L NaCl), actual seawater, and seawater spiked with surfactants, polyhydric alcohols, and oil emulsions [39,196,197]. The novelty of this study lies in applying PDA-modified membranes in the context of high-salinity dye wastewater treatment, an area that has not been explored in previous research. High-salinity environments with high organic loads present a greater challenge in terms of both fouling and wetting. By targeting these more complex conditions, this study aims to assess whether the hydrophilic properties imparted by PDA can enhance MD membrane performance in situations that are more representative of industrial wastewater. This research extends the application of PDA-modified membranes beyond the previously studied scenarios, offering new insights into their effectiveness under more demanding conditions.

Therefore, in this chapter to assess the performance of PDA-modified membranes, bench-scale MD experiments were conducted with a synthetic solution containing MB, serving as a standard pollutant to observe fouling and wetting behaviour. The outcomes were then compared to those from MD processes using unmodified commercial PVDF membranes to benchmark the effectiveness of the PDA modification. Prior to MD testing, the membranes were characterized to confirm the success of the PDA coating.

6.2 Results and discussion

6.2.1 ATR-FTIR characterisation

Figure 6-1 shows the FTIR spectra for both the unmodified and the PDA-modified PVDF membrane. These spectra reveal evidence of PDA deposition on the surface of the PVDF membrane, highlighted by two distinct absorption peaks at 1507 cm^{-1} and 1600 cm^{-1}. These peaks correspond to the N-H bending and the C=C aromatic stretching within the PDA structure, respectively[30,220]. Furthermore, the appearance of an absorption peak at 1708 cm^{-1} in the spectrum of the PDA-modified PVDF membrane points to the presence of carbonyl/carboxyl groups [30,40,220]. This indicates the successful addition of carboxyl-functional groups during the PDA deposition process, which is facilitated by the sodium periodate (SP) in a mildly acidic environment.

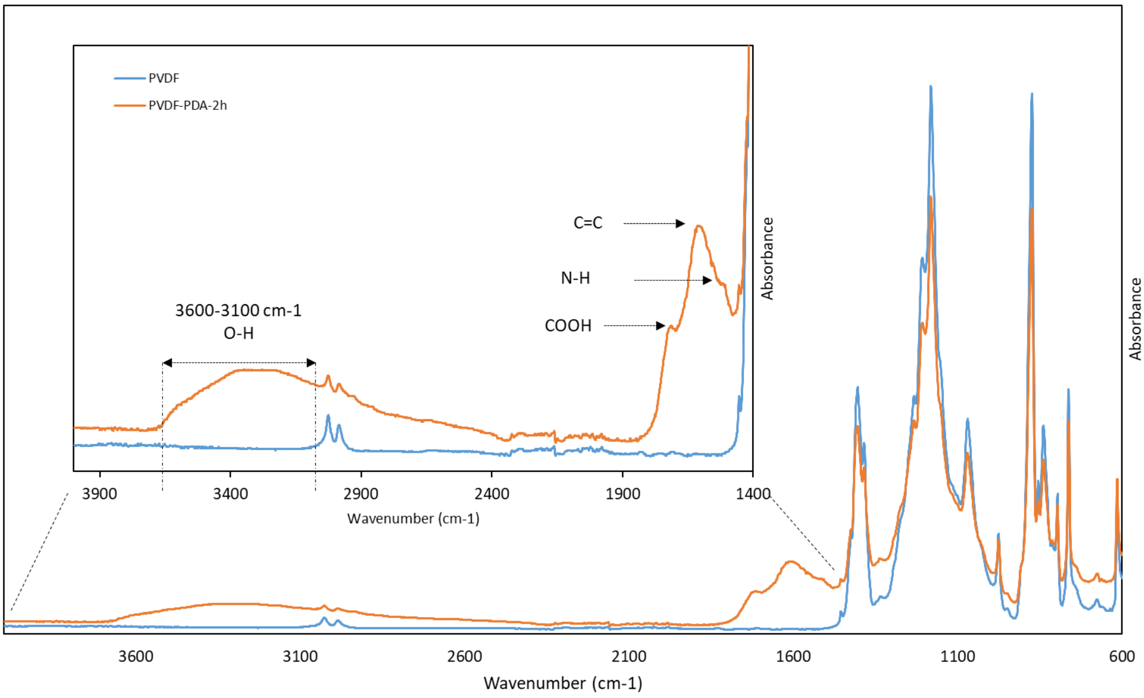

Figure. 6-1 FTIR spectra of the pristine and PDA modified PVDF membrane

6.2.2 Water contact angle results

Based on the water contact angle data presented in **Figure 6-2**, the pristine PVDF membrane was intrinsically hydrophobic, presenting an in-air water contact angle value of 125.5 ± 0.65°. Conversely, the PDA-modified PVDF membrane showed a significantly lower in-air water contact angle of 50.9 +1.8°, indicating addition of a hydrophilic surface property. However, the bottom surface of the modified membrane retained its hydrophobicity, with a water contact angle of approximately 129.8 +1.5°. This increase in hydrophilicity for the PDA-modified PVDF membrane can be attributed to the presence of polar functional groups such as amine, hydroxyl, and carboxyl onto the membrane surface after the modification process [30]. Similar results were also observed in other studies. Chew et al. [30] reported a reduction in water contact angle by modifying the PVDF membrane surface with PDA deposition, reducing the water contact angle from 109.5 ± 1.2° for the pristine PVDF to 13.2 ± 2.4° for PDA-modified PVDF after 6 hours of modification. In another study, a PDA-modified PVDF membrane employing the same modification method exhibited excellent superhydrophilicity with an initial contact angle of 19° [220].

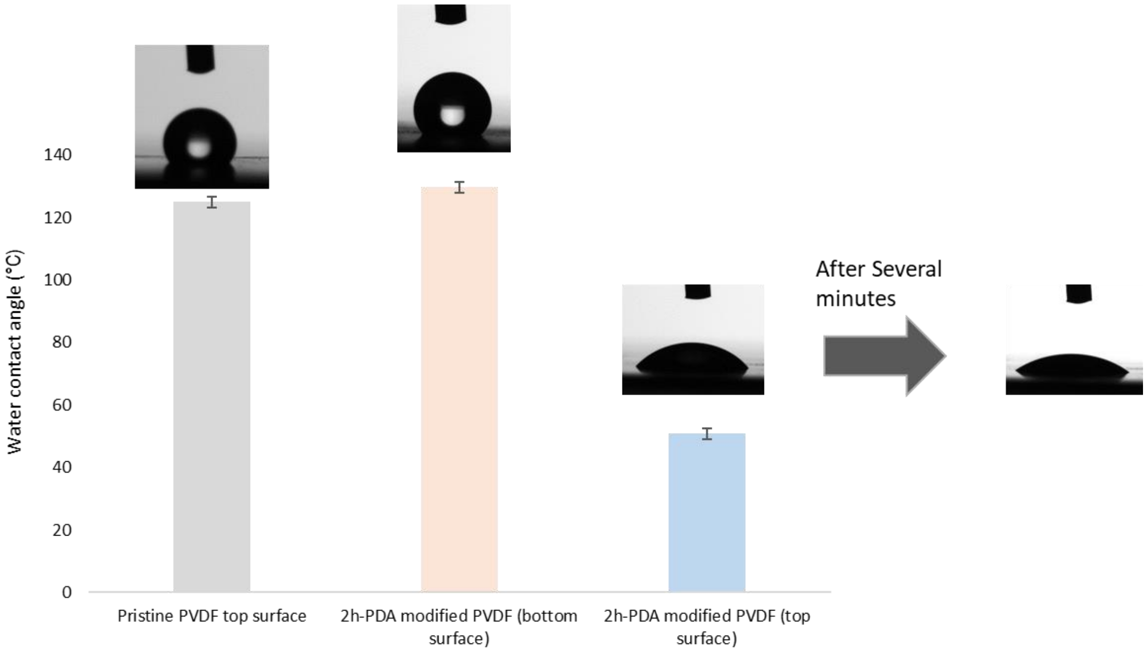

Figure. 6-2. Water contact angle in air of the pristine PVDF membrane, and PDA modified PVDF membrane

6.2.3 DCMD tests

To assess the MD capabilities of the PDA modified PVDF membrane, initial tests were carried out with a 100g/L NaCl solution as the feed. The data concerning the permeate flux and conductivity of the PDA-modified membrane (which was modified on the outer surface only) over a 25-hour period are depicted in **Figure 6-3**. Initial tests for the commercial PVDF membrane were conducted within the first hour to ensure reliable baseline data before testing the PDA-modified membrane.

The results indicate that both membranes initially exhibited similar flux levels, suggesting that the PDA modification did not introduce additional resistance to vapour transport, and there was no incidence of salt penetration. It was observed that the modified membrane maintained consistent flux and conductivity levels during its operation.

It can be hypothesized that the consistent or slightly improved flux of the PDA modified PVDF membrane is due to the presence of hydrophilic functional groups like carboxyl-, amine-, and hydroxyl-functional groups on the outer surface of the PDA modified PVDF membrane. These groups promote favourable polar-polar interactions with vapour molecules, enhancing their adsorption. Consequently, the hydrophobic PVDF substrate effectively repels both water and non-volatile NaCl solute, ensuring the collection of high-quality distillate [30,221,222].

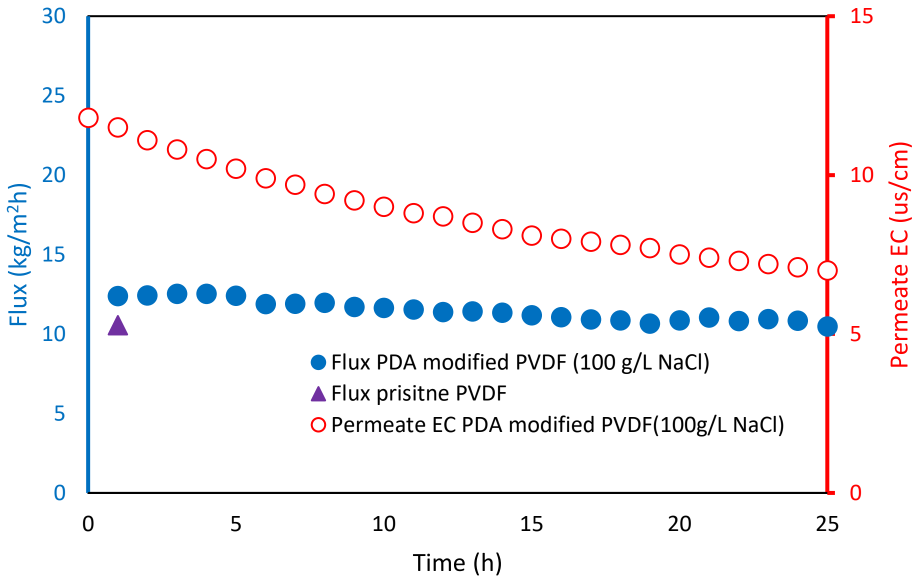

Figure. 6-3. DCMD performance in terms of Flux and permeate EC vs time of the PDA modified PVDF membrane in treatment of solution of 100 g/L NaCl (For the experiment, 1L of feed solution was used, Qf and Qp = 70 mL/min; Tf = 60 °C, Tp= 20 °C, Pback=35-40 kPa(g))

To further explore the performance of modified PVDF membranes in MD, tests were conducted using a high salinity solution of 100g/L NaCl, with an initial MB concentration of 3750 mg/L. The permeate flux and conductivity of the PDA-modified PVDF membrane were monitored over the experiment period and compared with pristine PVDF membrane, as illustrated in **Figure 6-4**. The results showed that the flux decline pattern of the modified membrane followed the same pattern of the commercial PVDF membrane. While wetting was still observed in the modified membrane, its onset was delayed compared to the pristine membrane. This delay in wetting is likely due to differences in surface chemistry and wetting properties between the two membranes.

The pristine PVDF membrane, being inherently hydrophobic, exhibited stronger hydrophobic interactions with MB molecules, leading to adsorption on the membrane surface. This adsorption contributed to pore blockage and accelerated pore wetting. In contrast, the PDA-modified PVDF membrane, with its hydrophilic surface, demonstrated slightly improved resistance to wetting, though the improvement was not substantial.

It is important to note that the results do not indicate a significant difference in wetting behaviour that would suggest any major advantage of PDA modification in this context. As discussed in Chapter 5, wetting phenomena in high-salinity conditions may be attributed to the salting-out effect, which will be further investigated in Chapter 7.

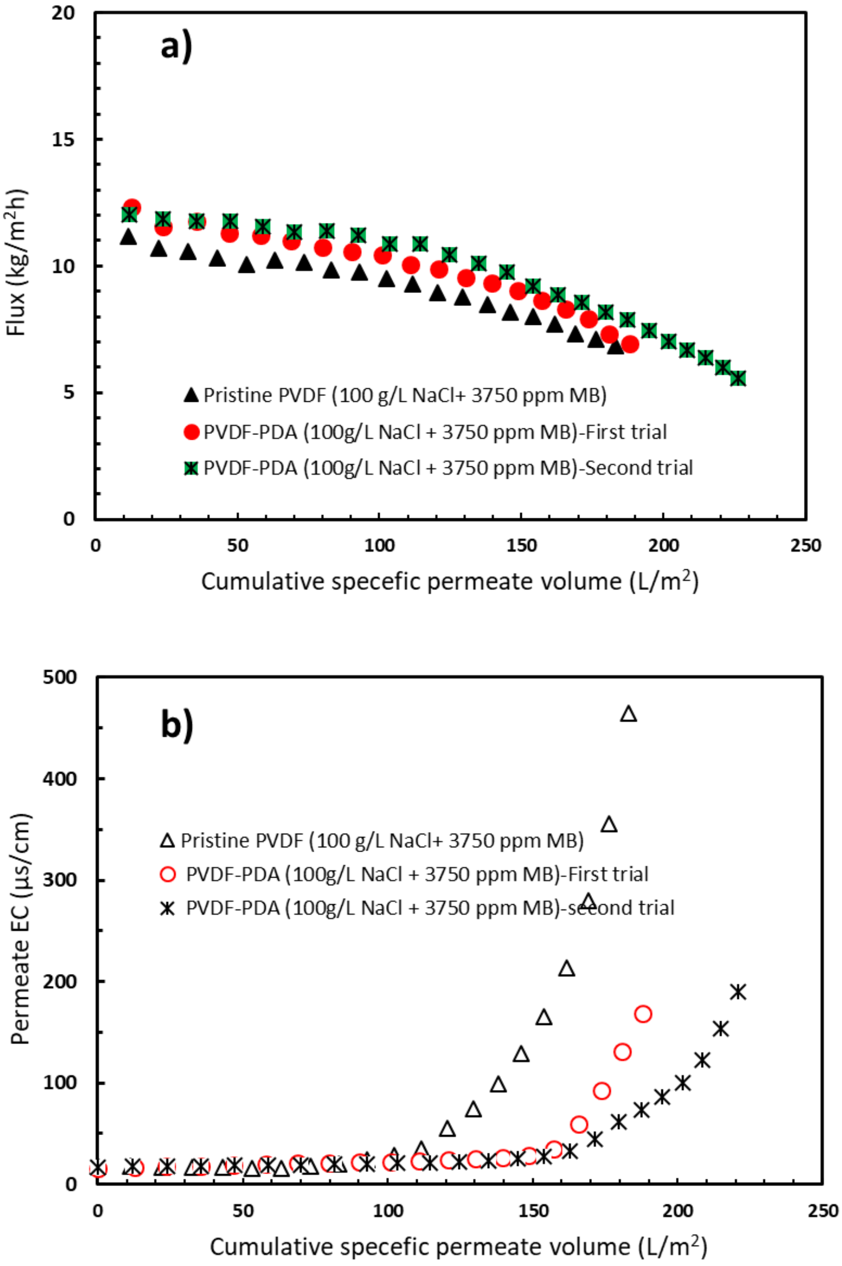

Figure. 6-4. DCMD performance in terms of a) Flux vs Cumulative specific permeate volume and b) permeate EC vs Cumulative specific permeate volume of the pristine and PDA modified PVDF membrane in treatment of solution of 100 g/L NaCl and starting MB concentration of 3750 mg/L (For the experiment, 1L of feed solution was used, Qf and Qp = 70 mL/min; Tf = 60 °C, Tp= 20 °C, Pback=35-40 kPa(g))

6.3 Conclusions

This chapter explored the performance of PDA-modified PVDF membranes in MD applications, particularly focusing on their resistance to wetting when exposed to high salinity dye solutions, a topic that has not been previously studied in MD literature.

The characterization of the modified membranes through FTIR spectroscopy and water contact angle measurements confirmed the successful deposition of PDA, which introduced hydrophilic functional groups such as carboxyl, amine, and hydroxyl onto the membrane surface. These modifications significantly enhanced the hydrophilicity of the membrane while maintaining the hydrophobicity of the underlying PVDF substrate.

Initial DCMD tests with a 100 g/L NaCl solution demonstrated that the PDA-modified membrane maintained consistent flux and conductivity levels. Further experiments with a high salinity solution (85 and 100 g/L NaCl) containing 3750 mg/L MB revealed that while the flux decline pattern of the PDA-modified membrane was similar to that of the pristine PVDF membrane, the onset of wetting was delayed.

These findings demonstrate that while surface modification with PDA enhances membrane hydrophilicity and delays wetting, it is not sufficient to fully prevent wetting when treating feeds with simultaneously high salinity and high organic pollutant. This study provides new insights into the limitations of surface modifications and highlights the importance of considering salting-out effects in MD processes which is going to be the topic of next chapter.

Chapter 7

Salting-out effect during MD for treating high salinity dye solution

7.1 Introduction

High-strength dye solutions containing also high salt concentration can adversely affect the performance of MD in terms of fouling and wetting. As shown in Chapters 5 and 6, neither partial oxidation in a hybrid process or hydrophilic surface modification with PDA used often by researchers to improve MD membrane resilience could resolve wetting issues at the limits identified in Chapter 4. The work indicated that the salting out effect is potentially overarching the simple interaction between dyes and membrane that researchers usually target to improve MD, and must be better understood in further attempts to develop sustainable MD processes.

The salting-out effect occurs when the solubility of an organic phase decreases and precipitates in an aqueous solution with high ionic strength [45,199]. Although this effect has not been explored in MD research, it is widely utilised in applications such as homogeneous liquid-liquid extraction, protein separation, and the isolation of reactive dyes [46–48]. Moreover, membranes utilized in these contexts, such as those for separating proteins or dyes, have shown a decrease in membrane flux or rejection rates. It has been observed that high-concentration organics/colloids/foulants (e.g., proteins, dyes) or those with lower solubility (e.g., minerals like calcium ions (Ca^{2+})) may push a foulant beyond its solubility limit due to concentration polarization, leading to the formation of scale or gel layers that progressively impair membrane flux [43,44].

The influence of adding salts to nonelectrolytes introduces considerable complexity due to the diverse interactions among ions, solvents, and nonelectrolytes. Various theories have been put forth to elucidate the mechanisms underlying these processes, though they remain subjects of ongoing debate. Figure 7-1 illustrates a basic mechanism for salting out, as proposed by Hyde et al. [199], highlighting the roles of electrostatic repulsion and the hydrophobic effect. These interactions collectively promote the aggregation of organic solutes.

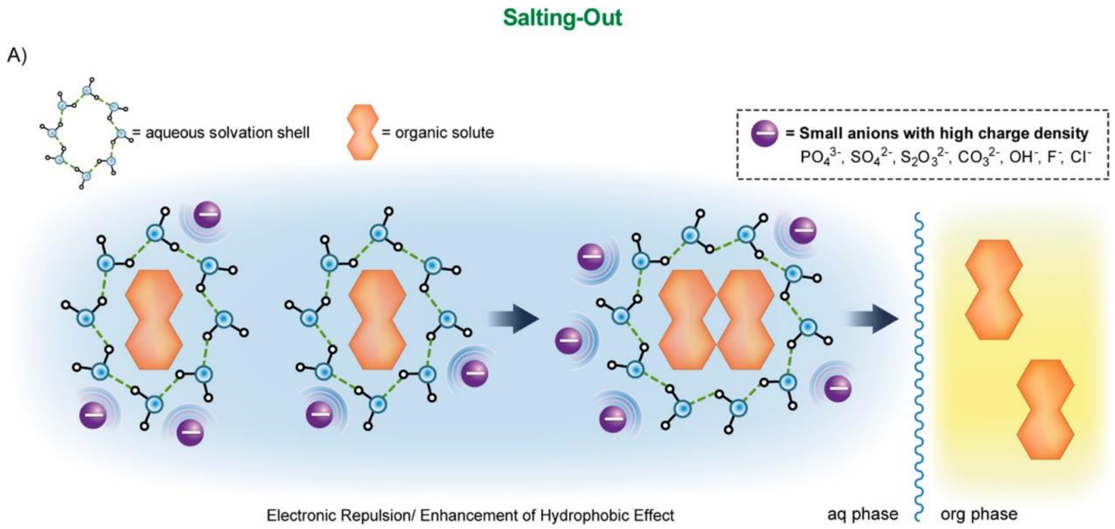

Figure 7-1. Molecular interactions that determine the solubility of organic compounds [199].

Quantifying the salting-out effect is important as industrial processes produce effluents with a high concentration of electrolytes, which can impact the treatment processes as organics exhibit different behaviour in electrolyte solutions. Therefore, to broaden the capability of MD membranes in ZLD for treating highly concentrated solutions, it is important to understand the relationship between MD flux and colloidal particle accumulation that contribution to the fouling effect.

The measurement of the Setschenow constant is a key step in quantifying the salting-out effect, as it provides valuable insights into the solubility behaviour of organic foulants in high-salinity environments. The solubility and mass aggregation of foulants during MD operation are calculated to enhance understanding of how these factors contribute to membrane fouling and wetting. This directly aligns with the primary objective of the thesis- addressing the critical challenges in MD, particularly those related to the treatment of high-strength wastewater streams. Specifically, this chapter expands on the investigation of how high-salinity conditions impact MD performance, as outlined in the thesis objectives, focusing on the phenomena of salting-out and its implications for flux decline and membrane wetting.

Therefore, this chapter is dedicated to examining the effect of salting-out on the fouling and wetting behaviour in MD for the treatment of high salinity waste streams. The step by step objectives of the work presented in this chapter are:

a. Measuring the Setschenow/salting-out constant for the selected MD foulant;

b. Using this measurement to calculate the solubility and mass aggregate of the selected foulant during MD operation; and
c. Analysing the fouling and wetting behaviours of MD during batch and continuous operation.

For this purpose, a model organic foulant, MB, was employed, and a range of solutions with a fixed initial MB concentration of 3750 mg/L and different concentrations of NaCl salt (35, 70, 80, 100 g/L) were prepared, as also described in **Chapter 3**.

7.2 Experimental and theoretical procedures of Setschenow /salting out constant determination

7.2.1 Experimental measurement of solubility using TOC

To determine the Setschenow constant of MB in NaCl solution, the solubility of MB first needs to be measured at different NaCl concentrations. The procedure for preparing MB-saturated solutions to measure MB solubility began with dissolving a fixed excess amount of MB (5 g/L) in deionized water. The solution was then stirred using a magnetic stirrer for 3 hours at the desired temperature. Various quantities of NaCl (ranging from 35 to 125 g/L NaCl) were then added to the prepared MB solutions, followed by an additional hour of mixing. The resulting saturated solutions were transferred to a shaker and left overnight at a mixing speed of 100 rpm and the desired temperature. Subsequently, the solutions were allowed to equilibrate at the same temperature for a specific period without any further shaking to ensure equilibrium is reached. Samples were collected using a syringe and filtered through a PVDF syringe filter with a pore size of 0.2 µm to separate any undissolved MB particles. The collected samples were then diluted volumetrically in deionized water, and the solubility of MB was determined using a TOC. After measuring the solubility of MB, a plot of MB solubility versus NaCl molar concentration was created, and the Setschenow/salting out constant was obtained from the slope of the plot. This allowed the salting out constant of MB in NaCl solution to be calculated based on its solubility behaviour.

There are two approaches for establishing the solubility of MB: solubility ratio analysis and direct logarithmic analysis. Solubility ratio analysis, detailed in Appendix A, utilizes the Arrhenius equation to determine solubility in pure water. However, due to the need for additional calculations or reliance on external data, the direct logarithmic analysis method described below is chosen for its straightforward approach. Once the solubility is established using the direct logarithmic analysis, this data is then utilized to calculate the aggregate mass of MB.

Solubility measurement: direct logarithmic analysis

The impact of NaCl on the solubility of MB from 35°C down to 20°C can be examined using direct logarithmic analysis [223], as outlined in **Equation 7-1**. This process involved plotting $Log(S)$ versus the molar concentration of NaCl according to the Setschenow equation to assess the solubility of MB. In this approach, S_0 is deduced from the intercept, indicating the solubility of MB in deionized water.

$$Log(S) = Log(S_0) - K_s C_s \tag{7-1}$$

Here, S_0 and S represent the solubilities of MB in deionized water and NaCl solution, respectively, K_S represents the salting-out constant, and Cs is the molar concentration of the NaCl solution.

Figure 7-2 illustrates the relationship between MB solubility (expressed as *Log(s)* and NaCl concentration over the temperature range of 35 °C to 20 °C. The observations from **Figure 7-2** suggest that temperature influences the Setschenow constant and, consequently, solubility. Although there is limited research on the temperature effect on the salting-out constant, a study by May et al. [224], indicate temperature independence of Setschenow constant, while Gold et al. [225], demonstrate a pronounced temperature dependency. In this study, measuring the Setschenow constant at 60 °C was not experimentally feasible due to uncertainties in sample collection at high temperatures (e.g., cooling effects in the syringe). Instead, the slope and intercept from the solubility ratio plots was utilized to estimate solubility at elevated temperatures, specifically at 60 °C, which is relevant to the feed temperature in MD operations.

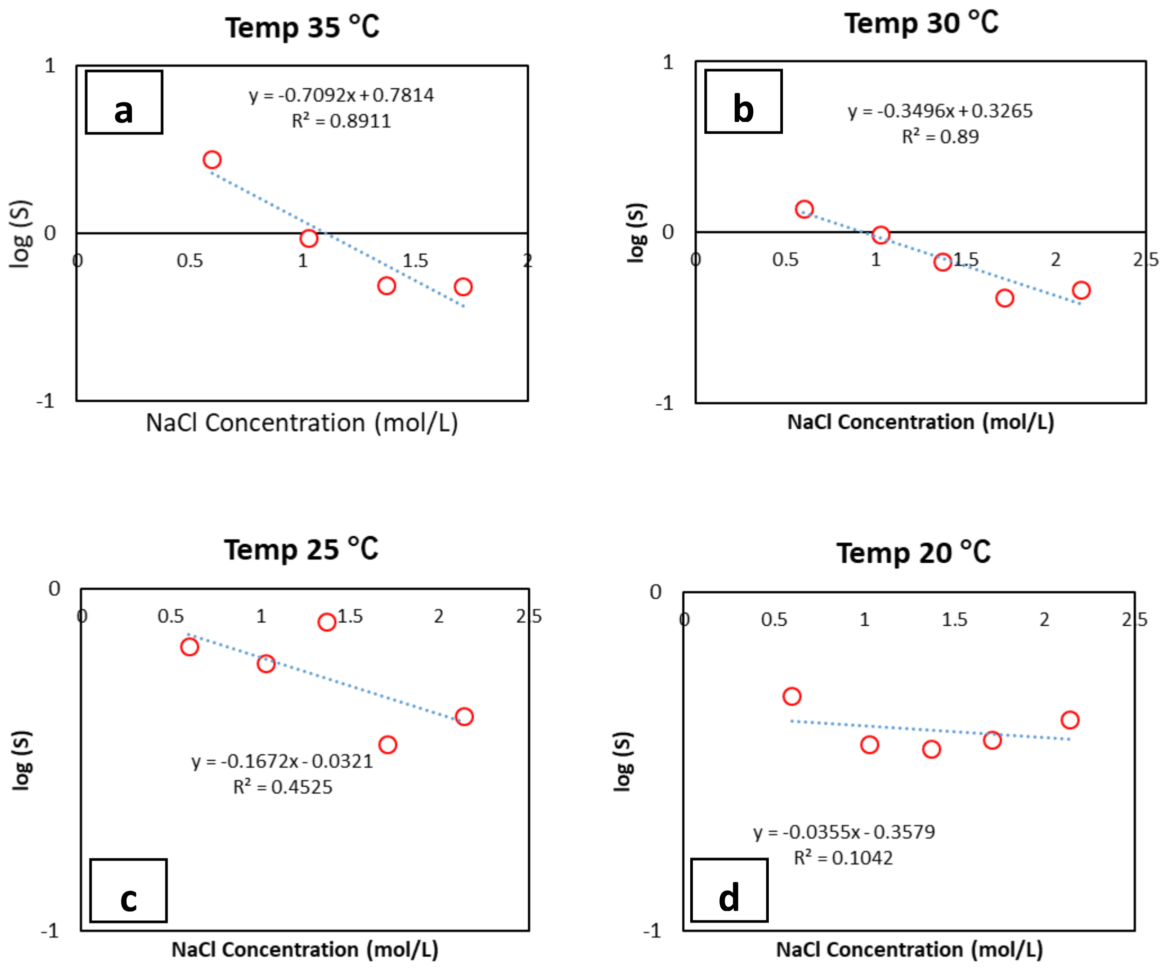

Figure. 7-2 Solubility of MB (expressed as Log (S), where S is MB solubility in salt solution) versus NaCl concentrations at temperatures of 35 ° to 20 °C.

Figure 7-3 displays the correlation between the slope, intercept, and temperature in solubility assessments. Utilizing the fitted data, the solubility for specific temperatures and NaCl concentrations was determined using **Equation 7-2**:

$$log(S) = -(0.044 * T - 12.85)C_s + (0.075 * T - 22.53) \tag{7-2}$$

Where Cs the molar concentration of NaCl is solution, and *T* (k) refers to the temperature. At 60 °C, **Equation 7-2** simplifies to:

$$log(S) = -1.7C_s + 2.62 \tag{7-3}$$

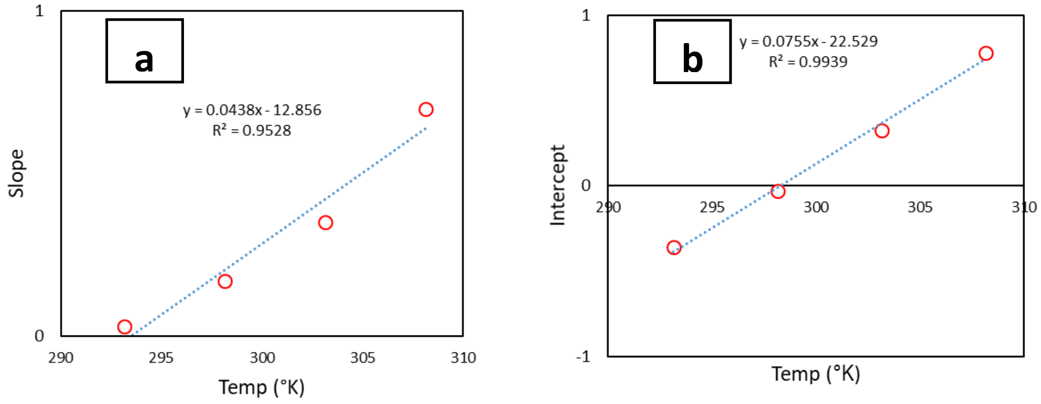

Figure. 7-3 Correlation between Slope, intercept, and temperature for solubility measurements

7.2.2 Experimental measurement of aggregate

To calculate the mass of MB aggregates, it is crucial to determine the difference between the total MB concentration and its solubility in the solution. During MD treatment, the feed solution becomes concentrated, leading to reduced solubility and increased total MB concentration. It should be noted that the aggregate mass is measured in the bulk solution, rather than near the membrane surface. Although it is understood that concentration polarization may exacerbate the salting-out effect near the membrane surface, quantifying this effect would require in-situ analysis, which is challenging to perform in highly turbid MB solutions.

Figure 7-4 illustrates this, specifically the difference between the solubility of MB and the total MB concentration over time for a representative solution (70 g/L NaCl + 3750 mg/L MB). This difference is used to calculate the mass of MB aggregates at any given time.

$$M_{MB}(t) = (C_{MB}(t) - S_{MB}(t)) * V_F(t) \qquad 7\text{-}4$$

Where $M_{MB}(t)$ is the mass of MB aggregate at each time, $C_{MB}(t)$ is the total concentration of MB at each time, $S_{MB}(t)$ is solubility of MB in salt solution at each time, and $V_F(t)$ is the volume of feed at each time.

Thus, **Equation 7-4** can be applied across various salinity levels to determine the MB concentration at different stages of the MD process.

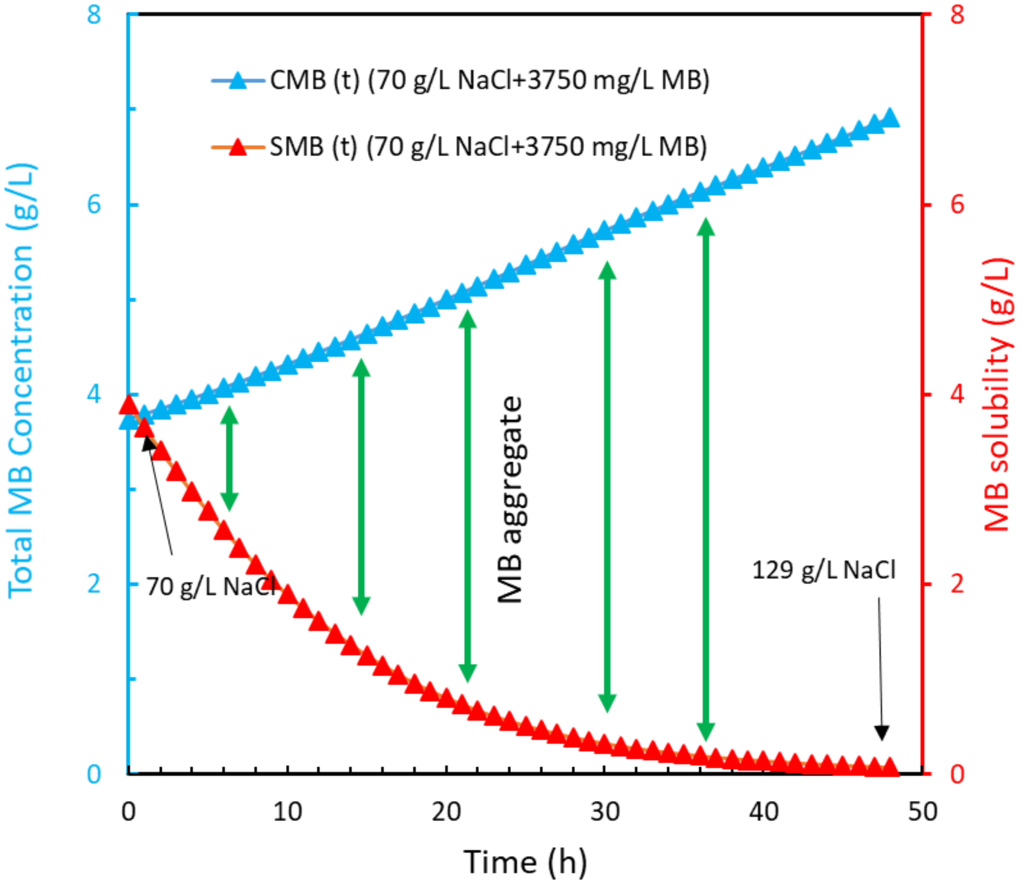

Figure. 7-4. Total MB concentration (C_{MB}(t)) and MB solubility (S_{MB}(t)) over time for the representative solution (70 g/L NaCl + 3750 mg/L MB)

7.2.3 Theoretical measurement of solubility

The solubility of MB in NaCl solutions was theoretically modelled using the Setschenow equation, an empirical formula that quantitatively describes the effect of salt on the solubility of organic compounds [45]. This equation is given by:

$$log({}^{S_0}/_{S}) = K_s C_s \qquad 7\text{-}5$$

Here, S_0 and S denote the solubilities of the organic compound (in this case, MB) in deionized water and in the salt solution, respectively. Ks represents the salting-out constant, and C_S is the molar concentration of the NaCl solution.

The salting-out constant (Ks) is crucial for predicting how the presence of salt influences the solubility of organic compounds. A traditional approach to estimate K_S involves using the partial molar volume V_H (cm^3/mol) of the solute in solution, The relationship is given by:

$$K_s = V_H \emptyset \tag{7-6}$$

In this context, $\emptyset$ is a coefficient with a reported value of 0.0025, as noted by Yuen et al. [226]. The partial molar volume V_H is derived from the molecular weight and density of the solute. For MB, V_H is calculated to be 319.85 cm^3/mol. Therefore, Ks is calculated to be 0.8.

With Ks established, the solubility of MB in the NaCl solution can be calculated using the Setschenow equation:

$$log\left({}^{S_0}/{}_{S}\right) = 0.8C_s \tag{7-7}$$

This theoretical approach is applicable for measuring the solubility patterns of MB in NaCl solutions. Although there may be differences between the experimental findings and the theoretical estimations concerning the parameters of the Setschenow equation, the values obtained provide valuable qualitative insights. These insights help in understanding the trends related to flux behaviour and membrane wetting, which will be elaborated on in the following sections.

7.2.4 Theoretical measurement of aggregate

To estimate the mass of MB aggregates, as it is already discussed in **Section 7.2.2.**, the next step is to determine the difference between the total MB concentration and its solubility in the salt solution. This difference represents the portion of MB that precipitates out or forms aggregates due to exceeding the solubility limit. The aggregate mass at any given time can be calculated by:

$$M_{MB}(t) = (C_{MB}(t) - S_{MB}(t)) * V_F(t) \tag{7-8}$$

Where $M_{MB}(t)$ is the mass of MB aggregate at each time, $C_{MB}(t)$ is the total concentration of MB at each time, $S_{MB}(t)$ is solubility of MB in salt solution at each time, and $V_F(t)$ is the volume of feed at each time.

7.3 Results and discussion

7.3.1 Membrane surface characterization

The SEM images in **Figure 7-5** depict the outer surface morphologies of the pristine PVDF and Versapor membranes. Abundant pores are distinctly visible on both the PVDF and Versapor membranes.

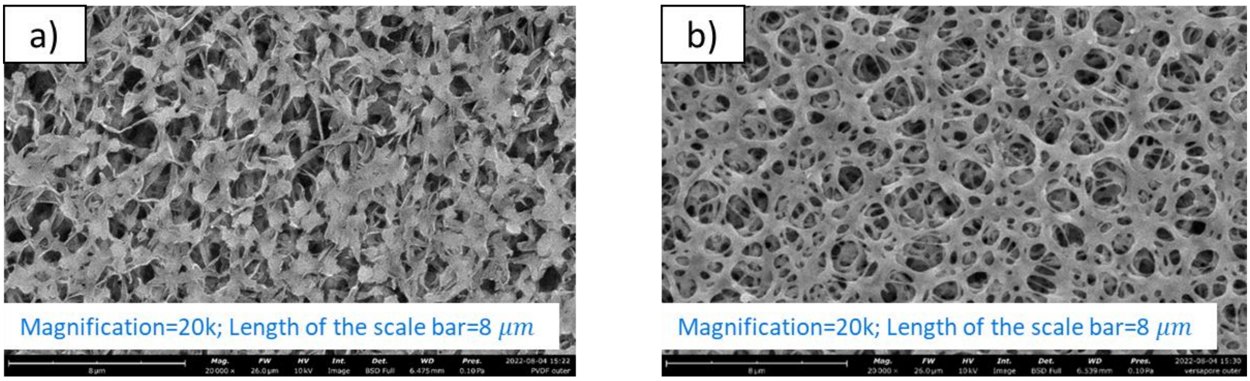

Figure. 7-5 SEM images of the commercial PVDF and Versapor membrane

Water contact-angle tests were performed to analyse the surface properties of the modified and pristine membranes. The results showed that the water contact angles for the commercial PVDF membrane was 125 ± 1°, while the Versapor membrane exhibited a slightly higher contact angle of 132 ± 3°. These data indicate that both the commercial PVDF and Versapor membranes exhibit significant hydrophobicity.

7.3.2 Effect of salting out on MD performance

7.3.2.1 Flux-EC versus cumulative specific permeate volume

In the batch mode evaluation of the MD performance, the primary focus was on monitoring how salinity impacts MD performance, particularly through changes in MD flux and EC as a function of cumulative specific permeate volume (L/m²). This analysis was conducted using commercial PVDF and Versapor membranes. **Figures 7-6 and 7-7** illustrate these effects, utilizing commercial PVDF and Versapor membranes.

Figures 7-6 and 7-7 indicate that both flux reduction and wetting tended to occur at lower cumulative specific permeate volumes. With the PVDF membrane, a noticeable drop in flux was recorded at a permeate volume of 190 L/m² for the solution containing 100 g/L NaCl, showing a significant flux reduction of 53%. This decrease in flux was not as pronounced at lower salinity levels, since the flux remained relatively stable throughout the MD operation of 35 g/L NaCl +3750 mg/L MB. When using the Versapor membrane, the pattern was similar. The flux for the 100 g/L NaCl solution declined rapidly, by 63%, after 95 L/m² of permeate was collected, compared to a lesser decline in flux at the lower salinity of 50 g/L NaCl.

There was also a rise in the permeate EC across most of the solutions tested, indicating membrane wetting. This was not the case for the lower salinity solution (35 g/L NaCl) while using PVDF membrane, where the EC remained constant. The onset of wetting as visually observed when EC rise started to appear, seemed to occur at lower permeate volumes with the salinity level from 35 to 100 g/L NaCl, with all solutions containing an initial 3750 mg/L MB.

The higher flux decline observed at increased salinity for both PVDF and Versapor membranes can largely be attributed to the decreased solubility of MB. As the MD process concentrates the solution, MB's solubility decreases while its overall concentration in the feed increases, as previously shown in **Figure 7-4**. Additionally, studies using in-situ 3D fouling visualization through Optical Coherence Tomography (OCT) have provided insights into fouling on MD membranes [227,228]. Wong et al. [228] demonstrated that differences in fouling layer growth were influenced by surface energy and hydrophilic/hydrophobic interactions between dye molecules and membrane surfaces. For example, the commercial PTFE membrane exhibited better antifouling performance than PVDF due to its relatively low surface energy.

In this study, flux decline can also be linked to the predominance of the cationic form of MB (MB^+) at neutral pH [207,208]. The strong attraction between positively charged MB ions and the negatively charged PVDF membrane intensifies fouling, as MB ions interact readily with the membrane surface [210]. Additionally, MB molecules may adhere to the membrane through hydrophobic interactions, further increasing fouling [16,21].

To identify the main factors influencing flux behavior and permeate EC rise, the following sections present flux and real-time permeate EC data in relation to MB solubility and aggregate mass. Constant concentration tests were also conducted to allow for prolonged exposure of the membrane to MB, enabling us to assess any effects of MB-PVDF interactions over time.

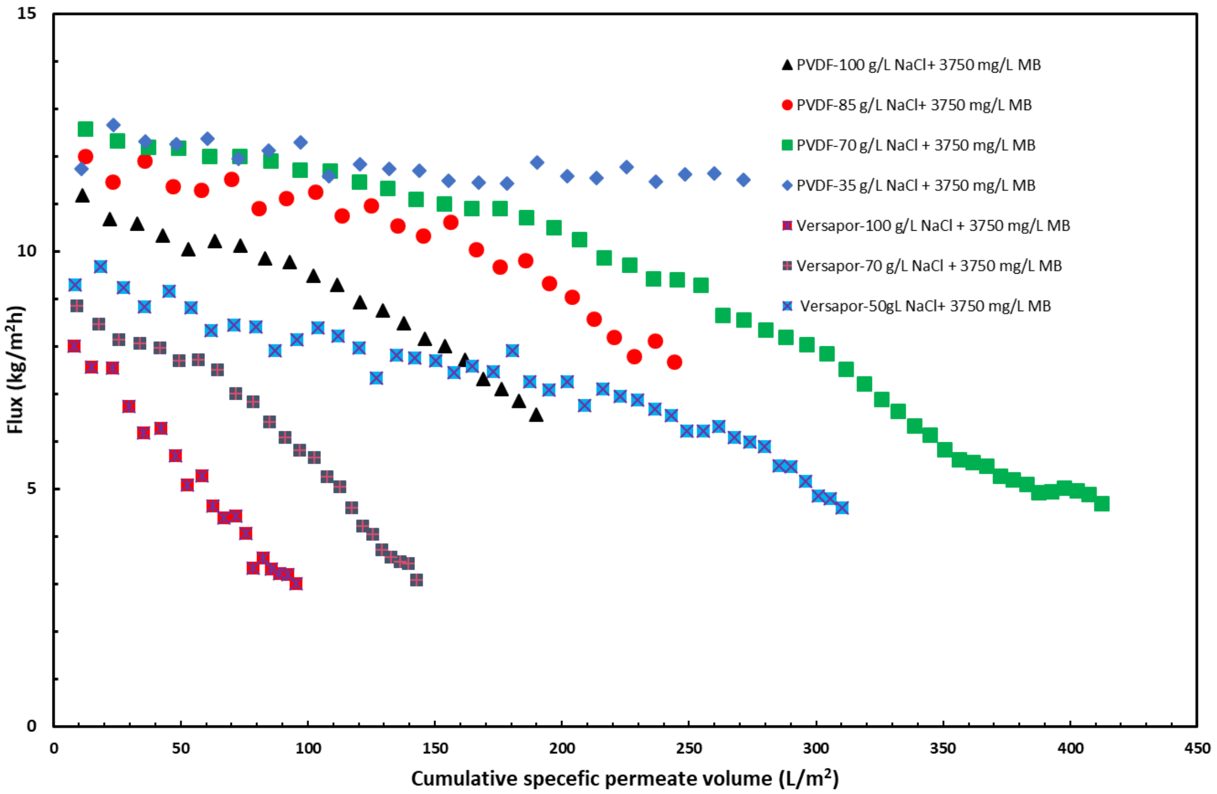

Figure. 7-6. DCMD performance in terms of Flux of the commercial PVDF and Versapor membranes (mean pore size=0.2 μm) in treatment of solutions starting with 35-100 g/L NaCl and starting MB concentration of 3750 mg/L. (For each experiment, 1L of feed solution was used, Qf and Qp = 70 mL/min; Tf = 60 °C, Pback = 35-40 kPa(g))

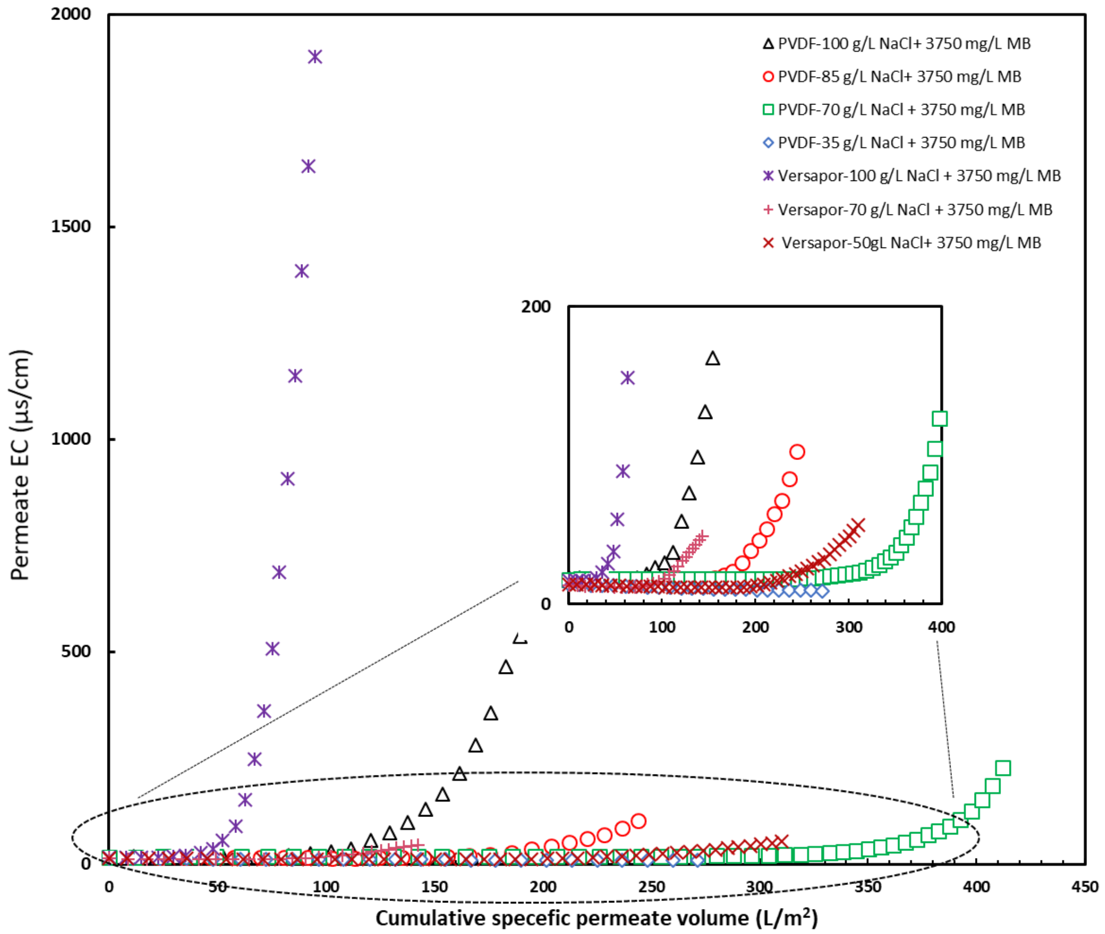

Figure. 7-7. DCMD performance in terms of permeate EC of the commercial PVDF and Versapor membranes (mean pore size=0.2 μm) in treatment of solutions starting with 50-100 g/L NaCl and starting MB concentration of 3750 mg/L. (For each experiment, 1L of feed solution was used, Qf and Qp = 70 mL/min; Tf = 60 °C, Pback = 35-40 kPa(g))

7.3.2.2 Flux versus theoretical and experimental solubility

To further investigate the effects of salting out on MD performance, flux data from MD experiments conducted with PVDF, Versapor, and PDA-modified PVDF membranes, as discussed in Chapter 6, were plotted against the solubility of MB. The solubility was determined through both experimental and theoretical calculations.

In **Figures 7-8 and 7-9**, the flux behaviour of PVDF membrane in treating a 3750 mg/L MB solution across a range of salinities (from 35 g/L to 100 g/L) is presented, alongside the MB solubility determined during the MD process. The solubility of MB over time was assessed using both experimental measurements (from **Equation 7-3)** and theoretical values derived from the Setschenow equation (from **Equation 7-7).**

Figures 7-8 and 7-9 show that the solubility of MB significantly influences the efficiency of the MD process in the tested solutions. Moreover, the PDA-modified PVDF membrane data (represented in yellow in Figures 7-8 and 7-9) shows the membrane exhibited similar flux behaviour as the unmodified PVDF membrane under high salinity (100 g/L NaCl). The flux trends suggest that the salting-out effect still dominates MD performance at elevated salinities and concentrations of organic foulants such as MB.

Although flux trends were seen to correlate with solubility, the time the membrane is exposed to MB is also important in determining MD performance. The time exposed refers to the duration for which the membrane was exposed to operational conditions to achieve a given solubility level. Therefore, the possibility that the wetting would occur eventually if the concentrations were held constant needs to be ruled out. For example, for a solution containing 100 g/L NaCl and 3750 mg/L MB, the initial solubility of MB, as calculated using the Setschenow equation (**Equation 7-7**), was approximately 1.87 g/L. In contrast, for a solution with 35 g/L NaCl, the initial solubility was around 14 g/L, indicating that reaching equivalent solubility levels in solutions of different salinities required varying durations.

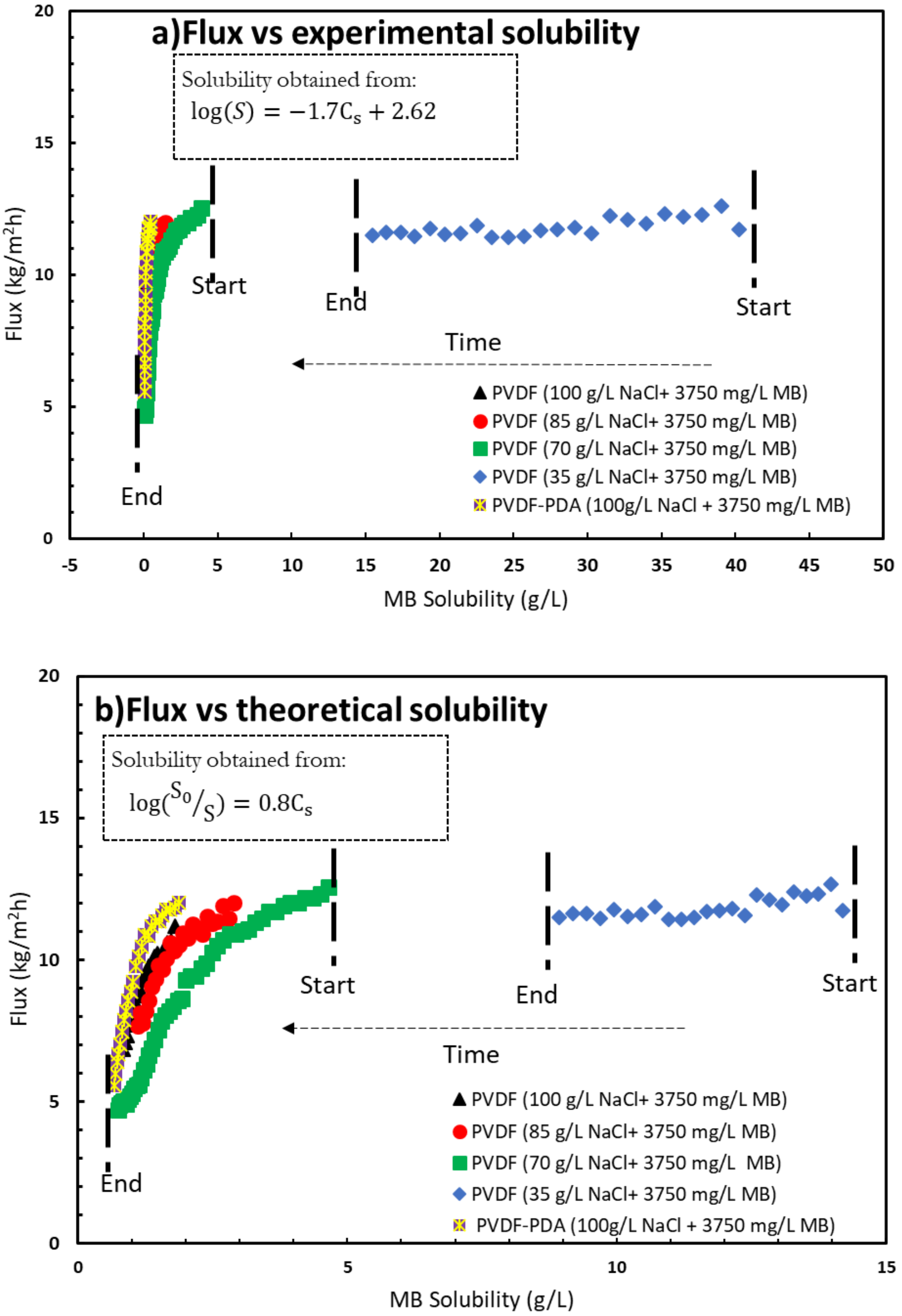

Figure. 7-8. DCMD performance in terms of a) Flux vs experimental solubility and b) Flux vs theoretical solubility of the commercial PVDF membrane (mean pore size=0.2 μm) and PDA-modified PVDF membrane in treatment of solutions starting with 35-100 g/L NaCl and starting MB concentration of 3750 mg/L. (For each experiment, 1L of feed solution was used, Qf and Qp = 70 mL/min; Tf = 60 °C, Pback = 35-40 kPa(g))

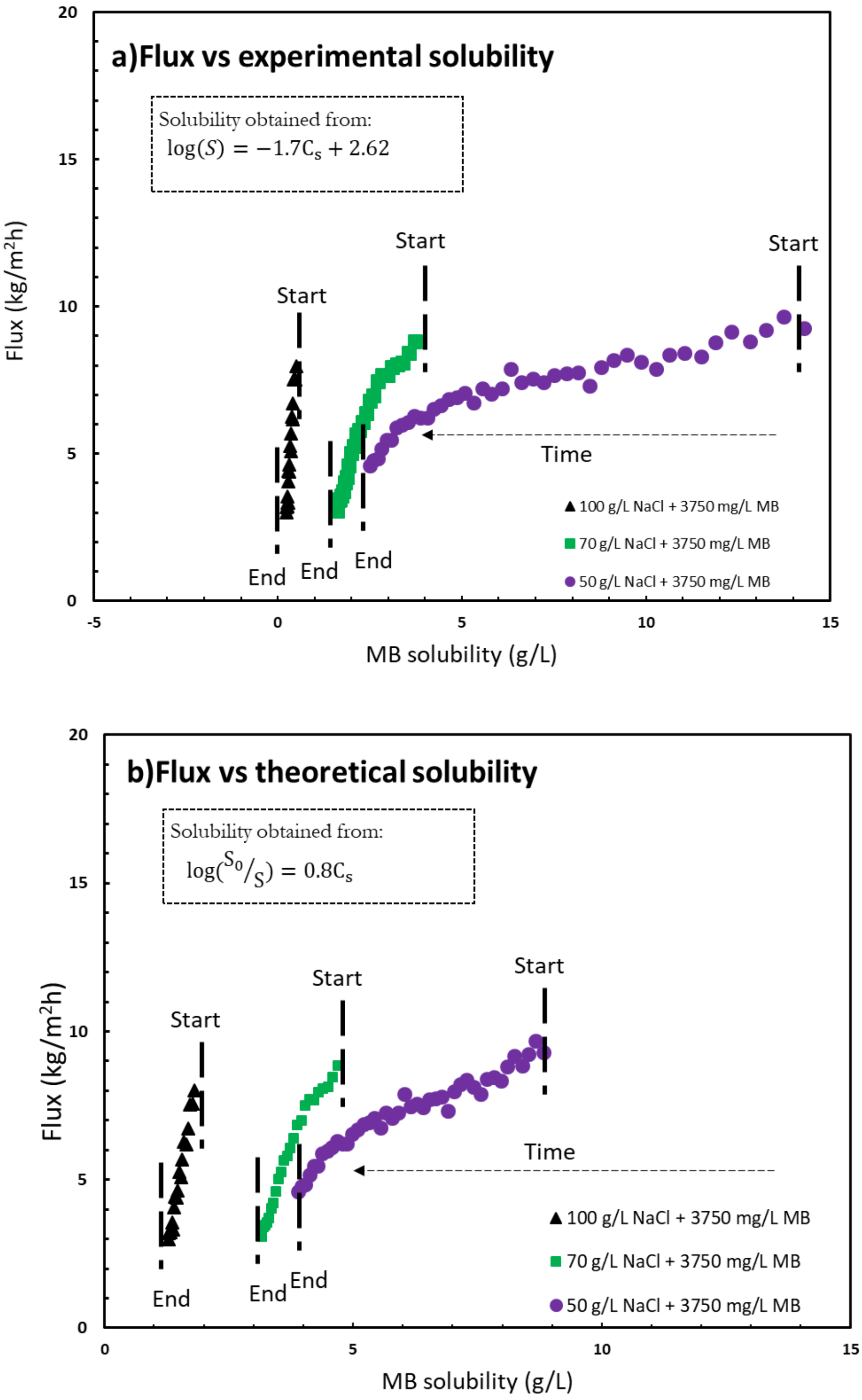

Figure. 7-9. DCMD performance in terms of a) Flux vs experimental solubility and b) Flux vs theoretical solubility of the commercial Versapor membrane (mean pore size=0.2 μm) in treatment of solutions starting with 35-100 g/L NaCl and starting MB concentration of 3750 mg/L. (For each experiment, 1L of feed solution was used, Qf and Qp = 70 mL/min; Tf = 60 °C, Pback = 35-40 kPa(g))

To further study the effect of time, two salinity levels, 100 g/L NaCl and 70 g/L NaCl, were chosen for continuous operations where the concentration levels remain stable, unlike in batch mode where they change dynamically as the system concentrates. **Figures 7-10 and 7-11** show the results, suggesting that continuous mode operations exhibit a more stable flux over time for both salinity levels. The continuous mode also maintains low EC levels for the 70 g/L NaCl solution, indicating effective salt rejection. However, the 100 g/L NaCl solution shows a gradual increase in EC, suggesting the impact of MB solubility. Nonetheless, the increase in EC for the 100 g/L NaCl solution is much more gradual compared to the sharp rise seen in batch mode, where the solution is concentrating.

The flux consistency depends on the MB solubility or aggregate mass present in the solution. If the feed solution already has an aggregate mass near the threshold, then wetting and fouling are likely to occur, regardless of the operation mode. In contrast, when the solution aggregate mass is below the threshold, wetting and fouling do not occur in a system with constant concentration of MB even through an extended duration of the process, thus ruling out time as being a factor in the salting out analysis.

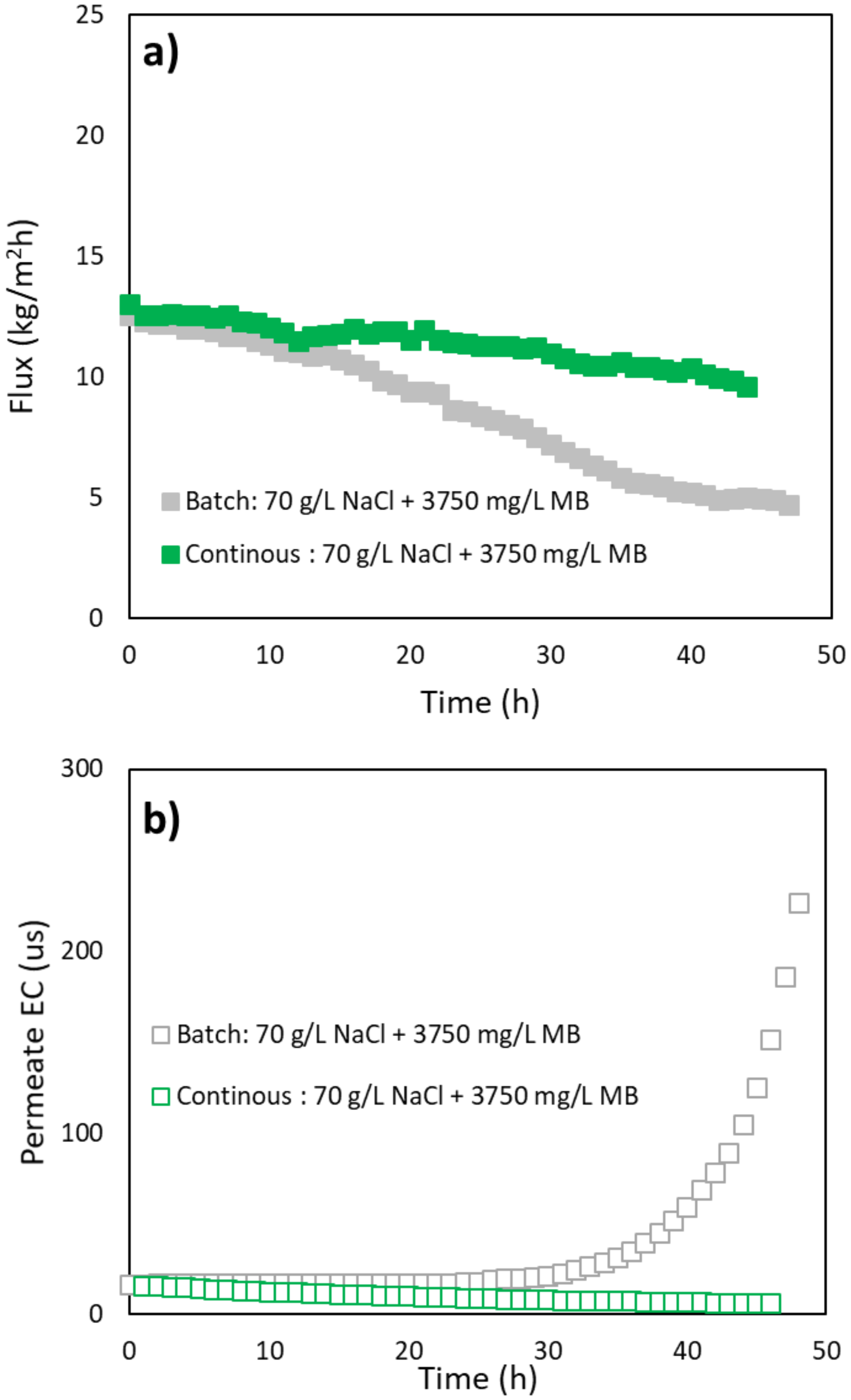

Figure. 7-10. DCMD performance in terms of a) Flux vs time and b) permeate EC vs time of the commercial PVDF membrane (mean pore size=0.2 μm) in treatment of 70 g/L NaCl and starting MB concentration of 3750 mg/L. (For the experiment, 1L of feed solution was used, Qf and Qp = 70 mL/min; Tf = 60 °C, Pback = 35-40 kPa(g))

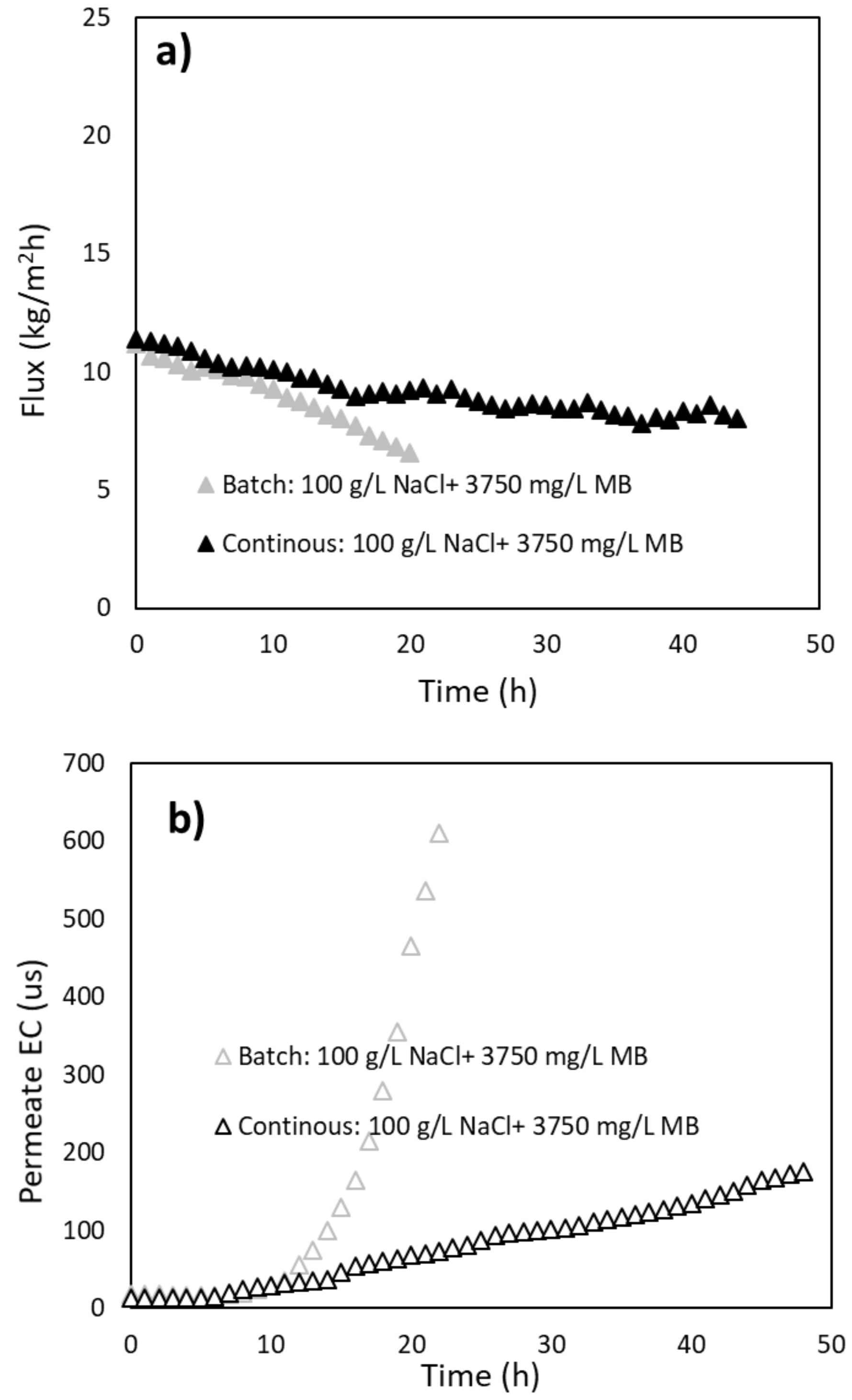

Figure. 7-11. DCMD performance in terms of a) Flux vs time and b) permeate EC vs time of the commercial PVDF membrane (mean pore size=0.2 μm) in treatment of 100 g/L NaCl and starting MB concentration of 3750 mg/L. (For the experiment, 1L of feed solution was used, Qf and Qp = 70 mL/min; Tf = 60 °C, Pback = 35-40 kPa(g))

7.3.2.3 Real-time permeate flow NaCl concentration versus theoretical and experimental solubility

Figures 7-12 and 7-13 illustrate the real-time permeate NaCl concentration in MD experiments against the solubility of MB using PVDF, Versapor membrane, and PDA-PVDF membrane. These Figures indicate a solubility threshold, beyond which breakthrough were observed across all tested solutions. The point where the real-time permeate flow NaCl concentration sharply increases was considered as the threshold.

The PDA-modified PVDF membrane (represented in yellow in Figure 7-12) showed slightly better resistance to wetting, but the breakthrough still occurred. While the PDA modification provided some resistance, wetting was ultimately triggered as the solubility threshold was exceeded, similar to what was observed with the unmodified PVDF membrane.

It is crucial to acknowledge that the exact solubility value at which this breakthrough occurs might differ based on the solubility measurement approach being either theoretical or experimental. Taking the PVDF membrane as an example, the breakthrough was noted at a solubility level of nearly zero based on experimental measurements, whereas it was nearly 2 g/L based on theoretical measurement for the same solution. Despite these variations in specific solubility values, the underlying principle remains consistent. The key finding is that the existence of a solubility threshold triggers wetting in the MD process for the cases studied.

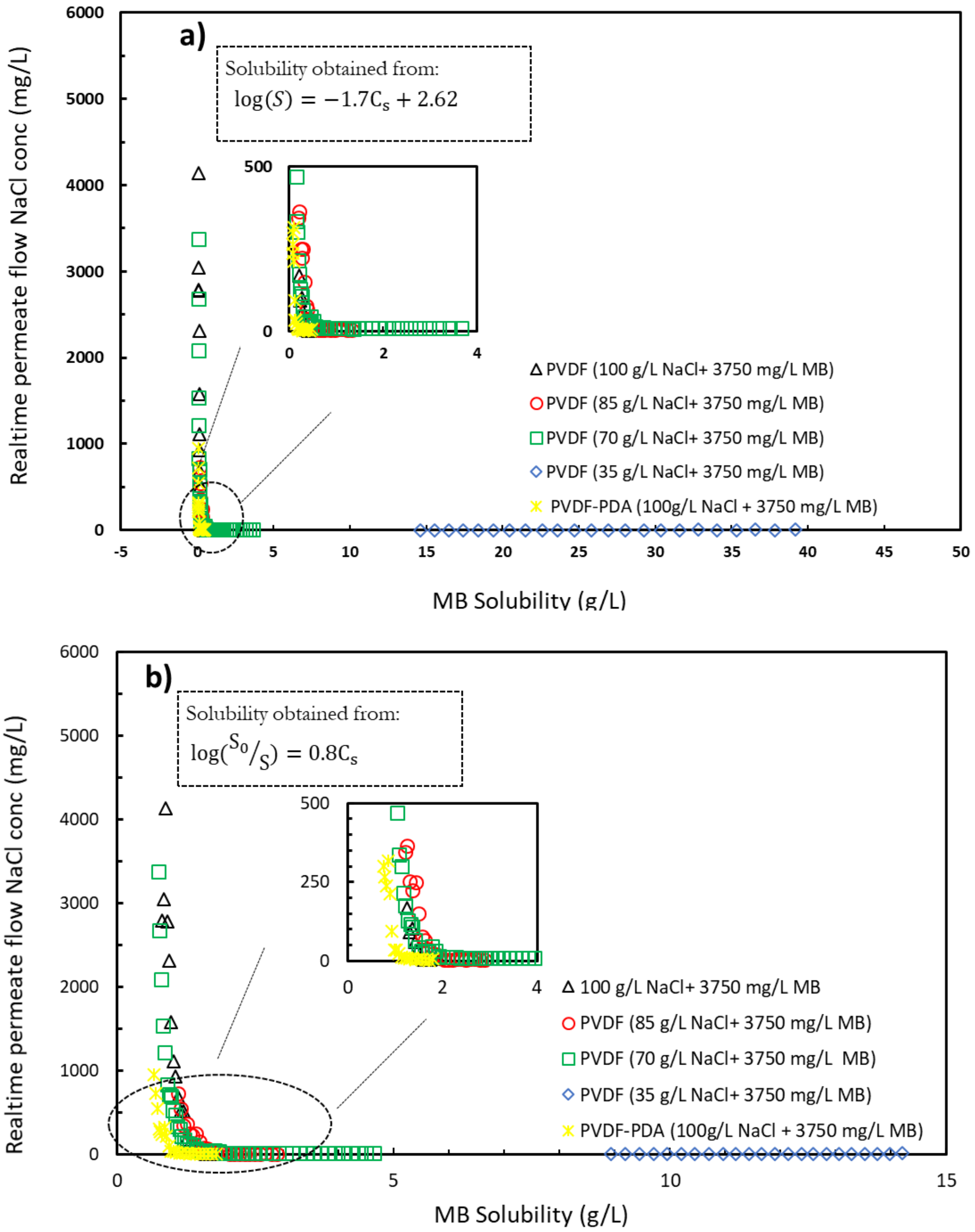

Figure. 7-12. DCMD performance in terms of a) Real-time permeate flow NaCl concentration vs experimental solubility and b) Real-time permeate flow NaCl concentration vs theoretical solubility of the commercial PVDF membrane (mean pore size=0.2 μm) and PDA-modified PVDF membrane in treatment of solutions starting with 35-100 g/L NaCl and starting MB concentration of 3750 mg/L. (For each experiment, 1L of feed solution was used, Qf and Qp = 70 mL/min; Tf = 60 °C, Pback = 35-40 kPa(g))

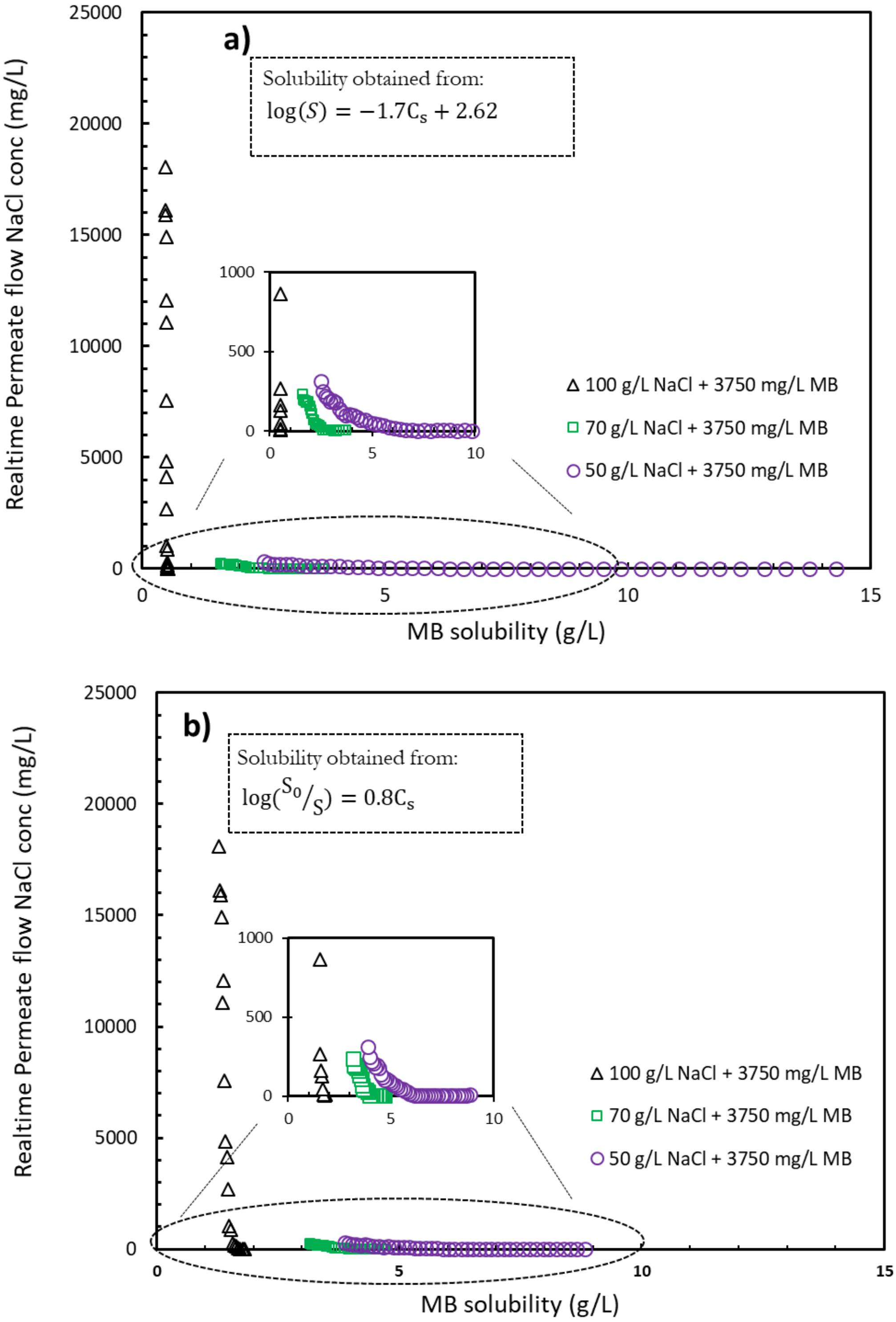

Figure. 7-13. DCMD performance in terms of a) Real-time permeate flow NaCl concentration vs experimental solubility and b) Real-time permeate flow NaCl concentration vs theoretical solubility of the commercial Versapor membrane (mean pore size=0.2 μm) in treatment of solutions starting with 35-100 g/L NaCl and starting MB concentration of 3750 mg/L. (For each experiment, 1L of feed solution was used, Qf and Qp = 70 mL/min; Tf = 60 °C, Pback = 35-40 kPa(g))

7.3.2.4 Flux and real-time permeate flow NaCl concentration versus MB aggregate

While solubility does play a significant role in initiating the wetting threshold or similar flux decline behaviour observed in **Figures 7-8 and 7-9 and Figures 7-12 and 7-13,** the primary factor influencing MD performance is the mass of MB aggregates. This aggregate mass as previously discussed is determined by the difference between solubility (both experimental and theoretical) and the total MB concentration. With prolonged MD operation, the aggregate mass increases, attributed to the widening gap between the total MB concentration and its solubility, a trend illustrated in **Figure 7-4.**

Consequently, the flux and real-time permeate flow NaCl concentration were plotted against the mass of MB aggregates for both PVDF and Versapor membranes. It is important to note that the MB aggregate values shown in these graphs are calculated based on solubility using both experimental and theoretical calculations**. Figures 7-14 to 7-17** show the relationship between the flux and real-time permeate flow NaCl concentration for both PVDF and Versapor membranes during MD treatment of a 3750 mg/L MB solution, with salinity levels ranging from 35 g/L to 100 g/L, and the corresponding mass of MB aggregates. The analysis suggests that there is a correlation between the MB aggregate mass and the flux and wetting of MD. **Figures 7-14 to 7-17** show the presence of a threshold for wetting (2-4 g) based on the MB aggregate calculated from the salting-out theory for each theoretical or experimental calculations on each membrane, including the PDA-modified PVDF membrane (represented in yellow). The PDA-modified membrane exhibited a slightly delayed onset of wetting, but as the MB aggregate mass increased, wetting occurred, similar to the unmodified membranes. MB aggregate mass is affected by solubility and salinity, and as it increases, it leads to a decline in the MD flux. This observation signifies the effect of salting-out on fouling and wetting in MD applied in the treatment of model solutions studied.

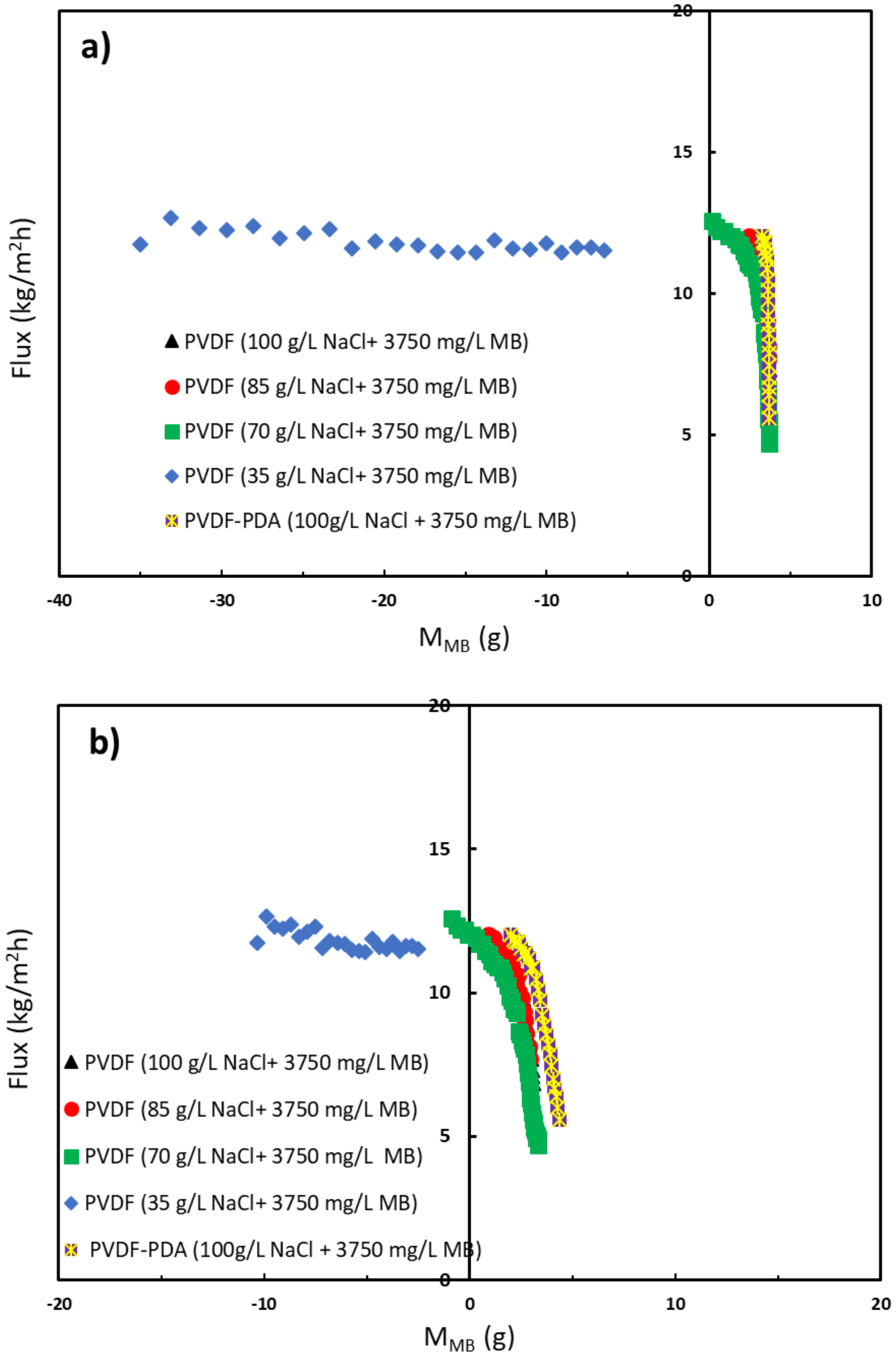

Figure. 7-14. DCMD performance in terms of a) Flux vs experimental MB aggregate mass and b) Flux vs theoretical MB aggregate mass of the commercial PVDF membrane (mean pore size=0.2 μm) and PDA-modified PVDF membrane in treatment of solutions starting with 35-100 g/L NaCl and starting MB concentration of 3750 mg/L. (For each experiment, 1L of feed solution was used, Qf and Qp = 70 mL/min; Tf = 60 °C, Pback = 35-40 kPa(g))

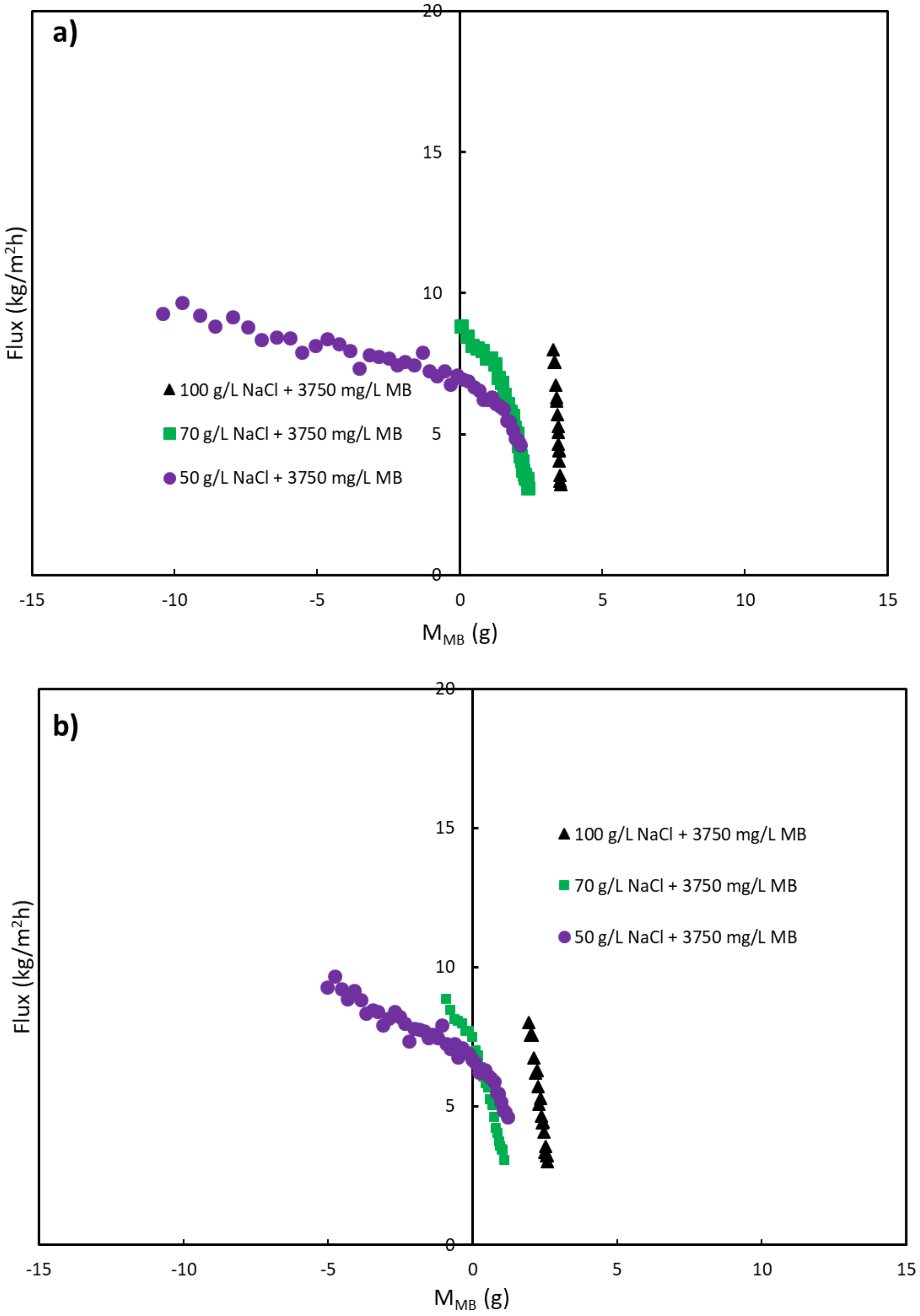

Figure. 7-15. DCMD performance in terms of a) Flux vs experimental MB aggregate mass and b) Flux vs theoretical MB aggregate mass of the commercial Versapor membrane (mean pore size=0.2 μm) in treatment of solutions starting with 35-100 g/L NaCl and starting MB concentration of 3750 mg/L. (For each experiment, 1L of feed solution was used, Qf and Qp = 70 mL/min; Tf = 60 °C, Pback = 35-40 kPa(g))

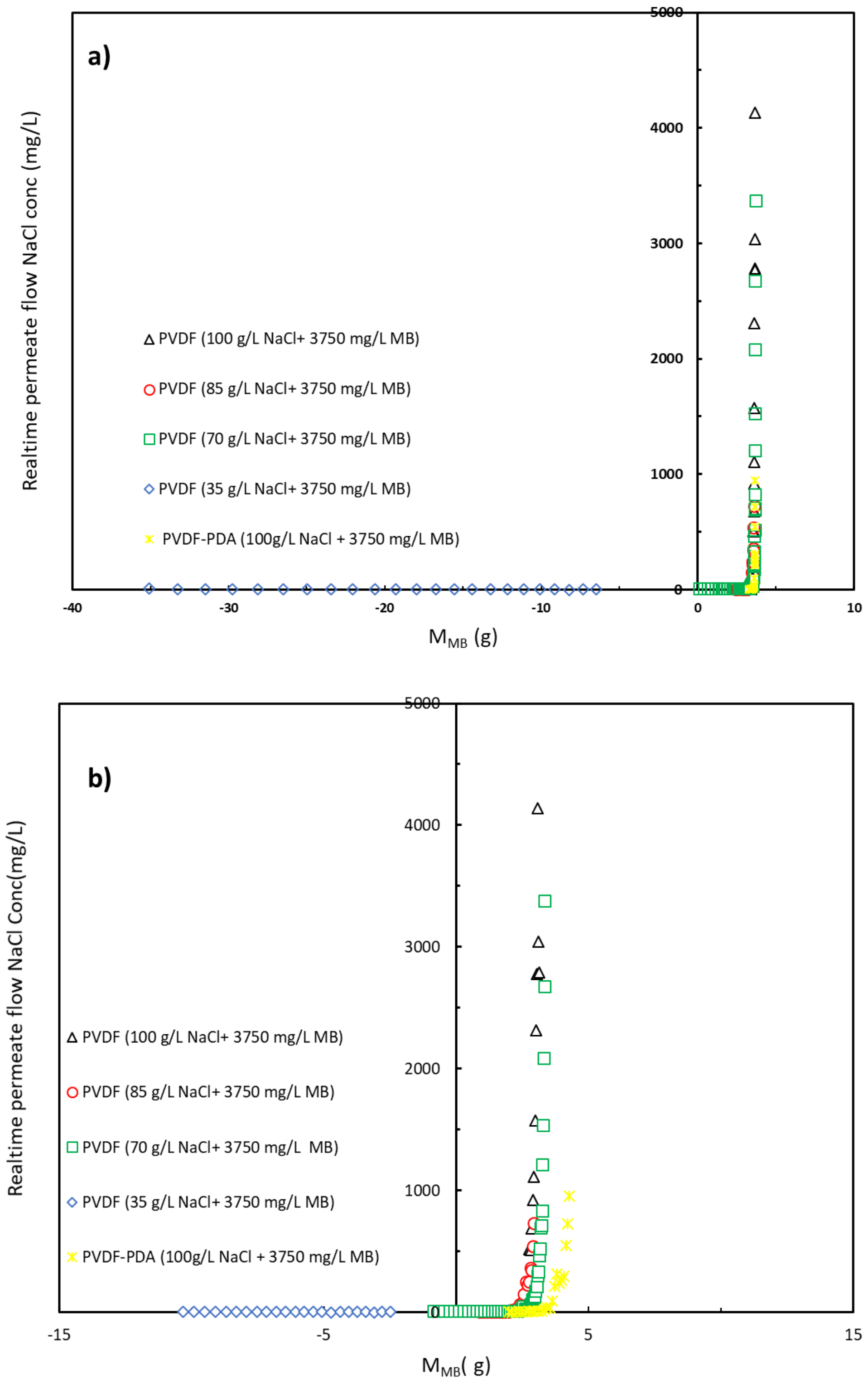

Figure. 7-16. DCMD performance in terms of a) Real-time permeate flow NaCl concentration vs experimental MB aggregate mass and b) Real-time permeate flow NaCl concentration vs theoretical MB aggregate mass of the commercial PVDF membrane (mean pore size=0.2 μm) and PDA-modified PVDF membrane in treatment of solutions starting with 35-100 g/L NaCl and starting MB concentration of 3750 mg/L. (For each experiment, 1L of feed solution was used, Qf and Qp = 70 mL/min; Tf = 60 °C, Pback = 35-40 kPa(g))

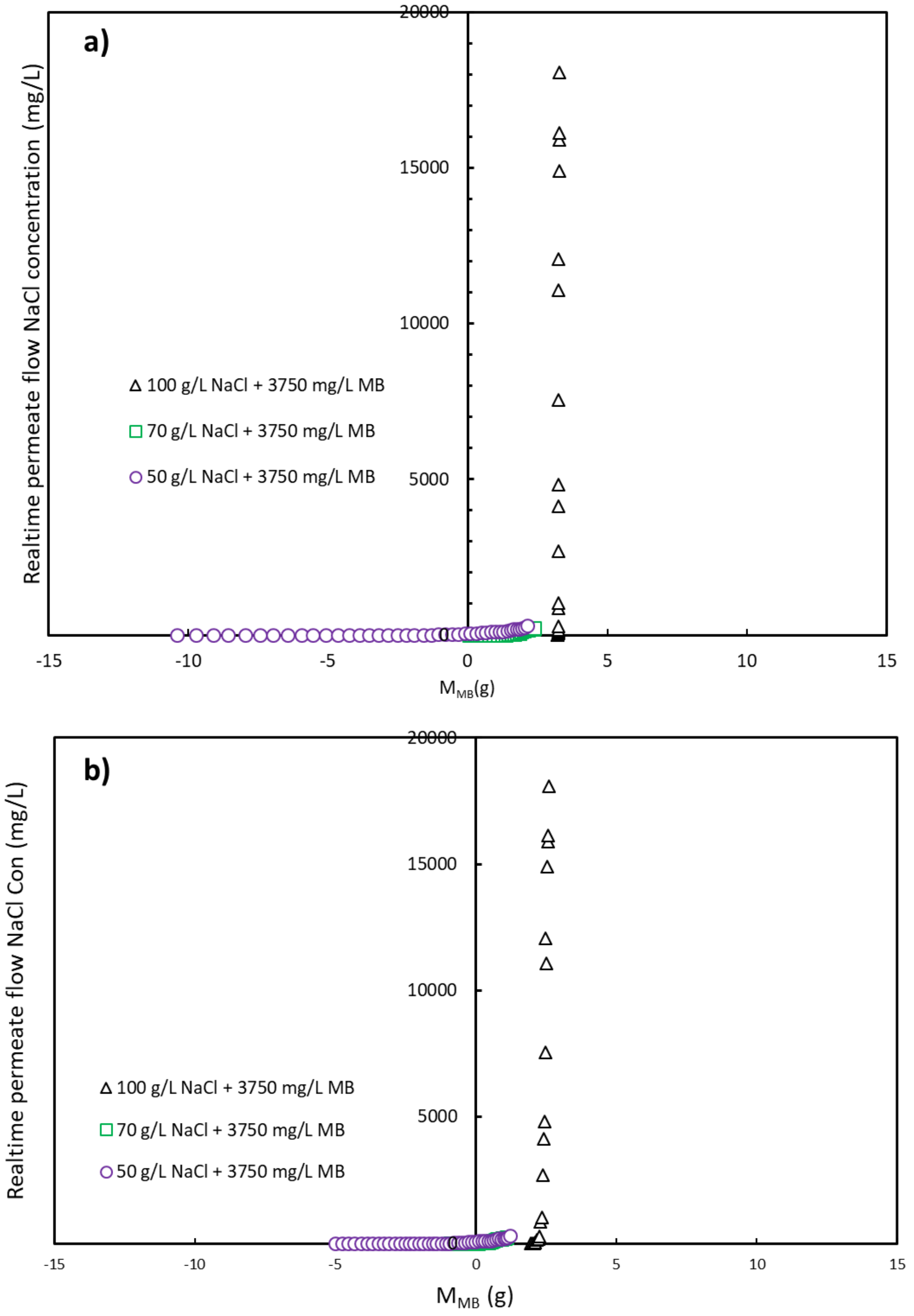

Figure. 7-17. DCMD performance in terms of a) Real-time permeate flow NaCl concentration vs experimental MB aggregate mass and b) Real-time permeate flow NaCl concentration vs theoretical MB aggregate mass of the commercial Versapor membrane (mean pore size=0.2 μm) in treatment of solutions starting with 35-100 g/L NaCl and starting MB concentration of 3750 mg/L. (For each experiment, 1L of feed solution was used, Qf and Qp = 70 mL/min; Tf = 60 °C, Pback = 35-40 kPa(g))

7.4 Conclusions

In conclusion, the phenomenon of salting-out were found to significantly influence MD performance across a range of initial NaCl concentrations (35 to 100 g/L) and an initial MB concentration of 3750 mg/L on three membrane types with different surface chemistries (oleophobic/hydrophobic for the Versapor, hydrophobic for the PVDF, and hydrophilic for the PDA modified PVDF membrane). The Setschenow constant, which characterizes the salting-out effect, proved to be a useful tool for determining the solubility as a function of salt concentration. In addition, both solubility and MB aggregate mass emerged as the primary governing factors, with their influence on MD performance evident through comparable flux decline and wetting patterns across the tested solutions. Existence of a critical threshold for MB aggregate mass (2-4 g) and solubility was identified, beyond which breakthrough and membrane wetting occurred in all cases. Moreover, while the influence of process time on fouling and wetting behaviours is mitigated when NaCl and MB concentrations remain stable, in continuous operations, the initial mass of MB aggregates present plays a critical role. If the initial aggregate mass is near the threshold, wetting and fouling are inevitable, suggesting that initial conditions are paramount for process stability and membrane longevity.

Chapter 8

Conclusions and future outlook

8.1 Summary of the current research

This dissertation has undertaken an in-depth investigation into the performance and challenges of MD technology for treating high-strength wastewater. The study initially focused on identifying the performance limitations of MD using commercial hydrophobic membranes (PVDF with mean pore sizes of 0.2 µm and 0.45 µm, and PTFE with a mean pore size of 0.5 µm). The objective was to determine the operational limits influencing the performance of MD systems. Subsequently, the research extended to integrating sulphate radical-based advanced oxidation processes (SR-AOPs) into MD, as well as developing hydrophilic surface modifications using PDA to address fouling and wetting issues in the treatment of high-salinity streams with a fixed initial MB concentration solution in MD utilizing commercial PVDF membranes. Furthermore, the research explored the impact of high salinity and the salting-out effect on MD performance. The following key findings and contributions were made through extensive experimental work and analysis:

Process intensification with reactive membrane distillation: Chapter 2 reviewed the integration of MD with oxidation processes, categorizing them into "hybrid" and "integrated" approaches. In hybrid processes, reactive materials are loaded into the feed tank, while in integrated processes, they are incorporated into/onto the membrane. The review highlighted that oxidation of organics significantly enhances MD performance, though its application has primarily been limited to scenarios with low salinity and organic concentrations. To extend the application of reactive MD to high-strength wastewater, further studies were identified as necessary, including the efficiency of reactive MD in highly concentrated streams, the role of membrane surface properties on fouling and wetting, and the interactions between ions, solvents, and non-electrolytes, specifically the solubility effects of organics in high-salt solutions.

MD performance limitations: Detailed experiments with commercial PVDF and PTFE membranes under various salt and dye concentrations revealed critical sensitivities related to the MD setup. These included inconsistencies in wetting behaviour and potential contamination from previous usage of heating coils. By establishing consistent experimental conditions, valid testing of PVDF membranes was achieved. The MD tests under high salinity conditions showed fouling and wetting occurring at NaCl concentrations of 100 g/L and MB concentrations of 3750 mg/L. These findings provided a foundation for understanding and extending the performance limits of MD membranes.

The study investigated the integration of SR-AOPs using Oxone as the oxidant in conjunction with MD employing commercial PVDF membrane. Experiments were conducted with a fixed concentration of Oxone (500 ppm) and MB (3750 mg/L) as the model organic dye pollutant. Results indicated that while Oxone delayed the onset of membrane wetting, its low concentration relative to the pollutant limited its overall effectiveness. Marginal enhancement in MD performance was observed when pH was adjusted to neutral with NaOH. Adjusting the solution pH with HCl with the use of oxidant did not also yield substantial improvements, suggesting other factors beyond pH or oxidation play a critical role in MD performance. Therefore, while SR-AOPs offer a promising approach for enhancing MD, the findings suggest that the oxidation process, as tested in this study, does not provide a significant benefit to MD when dealing with high concentrations of organic pollutants, even with partial reactions involving MB.

Surface modification of MD membranes with PDA:

Commercial PVDF membrane were modified with PDA to enhance its hydrophilicity and resistance to fouling and wetting. Characterization techniques such as FTIR and contact angle measurements confirmed successful modification, introducing hydrophilic functional groups like carboxyl, amine, and hydroxyl onto the membrane surface. Testing with high salinity solutions (NaCl concentrations up to 100 g/L) and MB (3750 mg/L) demonstrated that PDA-modified membranes exhibited a delayed onset of wetting compared to unmodified PVDF membranes. However, surface modification alone was insufficient to completely prevent wetting, indicating the need for further enhancements.

Impact of high salinity and salting-out effect:

The study extensively examined the salting-out phenomenon, where high concentrations of NaCl reduced the solubility of the model organic compound, MB, leading to flux decline and increased wetting. Experiments across a range of NaCl concentrations (35 to 100 g/L) and a fixed initial MB concentration of 3750 mg/L revealed that the salting-out effect is a critical factor influencing MD performance. This effect was studied through the Setschenow equation, providing insights into the solubility and behaviour of MB in the MD process. A critical threshold for MB aggregate mass was identified, beyond which membrane wetting and breakthrough occurred in all studied cases. The PVDF membrane demonstrated more stable performance in terms of flux and wetting in continuous operation compared to batch processes, as long as the solution was not concentrating, thereby ruling out the effect of time on fouling and wetting. These findings highlight the significance of the initial mass of MB aggregates. If the initial aggregate mass is near the threshold, wetting and fouling are inevitable, suggesting that initial conditions are paramount for process stability and membrane longevity.

8.2 Future outlook

Building on the findings of this research, future work should focus on several key areas to further advance MD technology for high-strength wastewater treatment:

Further investigating the reactive MD processes: In considering the potential for reactive MD processes in industrial applications, it is important to recognise the need for an economic evaluation, which was beyond the scope of this study. Given the limited availability of economic studies in this area, a separate analysis would be necessary to accurately assess the economic feasibility of reactive MD systems. Future work could build on the technical findings presented here by developing economic models to evaluate their potential in industrial applications.

Further investigation into reactive MD processes is also necessary. The current study showed that adding Oxone to the feed solution did not significantly improve MD performance under the tested conditions. Future research should explore alternative oxidants that might offer a better performance than Oxone, especially in high-organic-load and high-salinity scenarios. Partial oxidation can sometimes enhance MD performance by transforming pollutants into less hydrophobic compounds. Detailed studies are needed to determine whether integrated MD processes, using catalysts for surface modification, can simultaneously increase membrane hydrophilicity and improve oxidant performance to circumvent fouling. This approach could protect the membrane and achieve higher removal efficiency in treating high-strength wastewater without compromising MD performance.

Enhancing surface modifications with advanced materials: This study demonstrated that PDA-modified PVDF membranes enhanced hydrophilicity and delayed the onset of wetting in high salinity dye solutions. However, it also highlighted that this modification alone is not sufficient to fully prevent wetting. Focusing future work on developing and testing surface modifications using advanced materials such as superhydrophilic coatings or mixed-matrix membranes is expected to further enhance the hydrophilicity and fouling resistance of MD membranes. Additionally, investigating the use of nanomaterials, such as graphene oxide or titanium dioxide nanoparticles in surface modifications could further improve membrane performance and longevity.

Comprehensive study of the salting-out effect: The current study demonstrated the effects of salting-out on a model organic dye, MB, using NaCl as the salt. However, each organic compound can exhibit unique behaviour at high salinities. Therefore, performing a series of experiments to further understand the salting-out effect on a variety of organic and inorganic compounds beyond MB is crucial. Additionally, some salts, such as $NaClO_4$, can induce salting-in, the opposite effect of salting-out. Future studies should focus on investigating the effects of high concentrations of different salts to develop a comprehensive model for describing the impact of salting-out (and/or salting-in) on MD processes. Further research is also needed to develop analytical methods for accurately quantifying changes in solubility and aggregation behaviour of organic compounds in high-salinity conditions. Also, comprehensive evaluation of real wastewater with complex matrix should be conducted to further apply and adjusted the developed strategies.

Appendix A:

Determination of MB solubility using the solubility ratio analysis in chapter 7

To determine the solubility of MB in various conditions, Setschenow equation [45] was employed (**Equation A-1**). The MB solubility was evaluated by fitting the data to the Setschenow equation [45] where the *log* (S_0/S) was graphed against molar NaCl concentration.

$$\log\left({}^{S_0}\!/_{S}\right) = K_s C_s \qquad \text{A-1}$$

Where S_0 (g/L) and S (g/L) represent the solubilities of MB in deionized water and in a salt solution, respectively, Ks is the salting-out constant, and Cs (mol/L) is the molar concentration of the salt solution. Initially, the MB solubility in pure water (S_0) was determined using the Arrhenius equation, using data from Salimi et al. [229] for MB solubility at various temperatures. The natural logarithm of these solubility values was then plotted against the reciprocal of temperature ($1/T$), as shown in **Figure A-1.** Through linear fitting of these points, the solubility of MB in pure water was extrapolated across a range of temperatures.

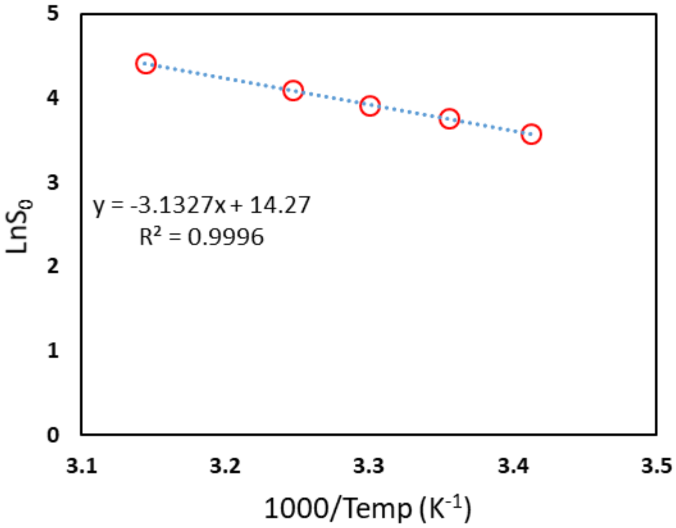

Figure. A-1. Correlation of natural logarithm of solubility in water and inverse temperature and linear regression indicating Arrhenius behaviour

Subsequently, MB solubility was measured in salt solutions of varying NaCl concentrations, as detailed above. Then, by comparing these solubility values (S) to the baseline solubility in pure water (S_0), the corresponding values of *log* (S_0/S) was calculated. The obtained data was then used to plot *log* (S_0/S) against NaCl concentration at temperature of 35°C to 20°C as depicted in **Figure A-2**. Linear fitting of this plot yielded the slope and intercept, from which the constant K_S was derived. Notably, in the absence of salinity, S_0 equates to S, though the linear equations may still exhibit an intercept [230–232]. Our analysis focused on high salinity levels (>35g/L NaCl), relevant to the salinity spectrum of the MD solutions under study, while disregarding lower salinities due to their potentially divergent behaviour [230–232].

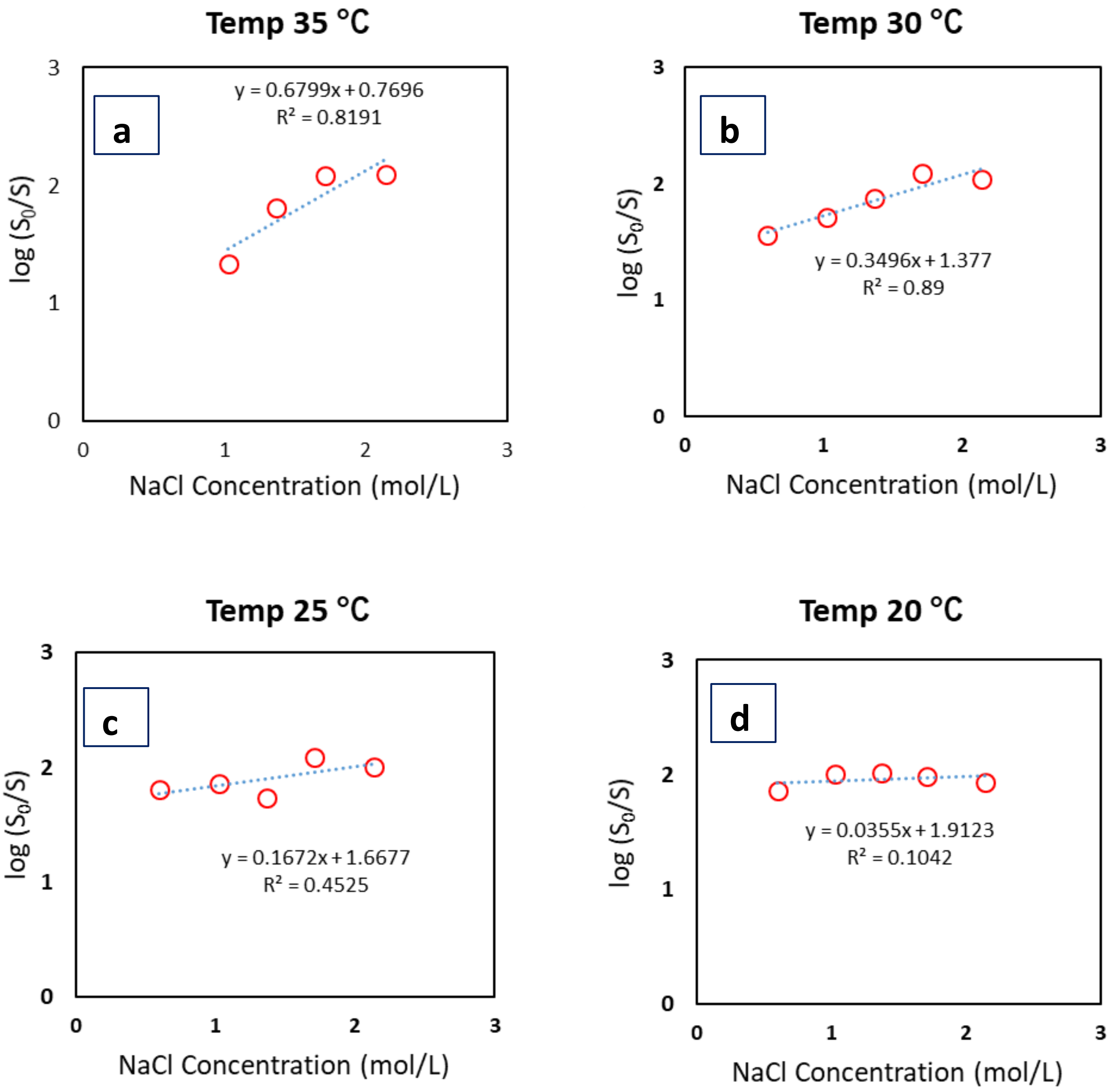

Figure. A-2 Solubility ratio of MB (expressed as *log* (S_0/S) where S_0 is solubility of MB in deionized water, and *S* is MB solubility in salt solution) versus NaCl concentrations at temperatures of 35 ° to 20 °C.

Subsequently, the slope and intercept obtained from the solubility plots were used to predict the solubility at 60°C, relevant to the feed temperature in MD operations. The relationship between slope, intercept, and temperature in solubility measurements (**equation A-2 and A-3**) is shown in **Figure A-3.** By applying the fitted data, solubility at specific temperatures and NaCl concentrations was determined using the following formula:

$$log\left({}^{S_0}/_{S}\right) = (0.043 * T\ - 0.86)C_s + (-0.073 * T + 3.44) \qquad \text{A-2}$$

Here, S_0 (g/L) denotes the solubility of MB in deionized water, while S (g/L) indicates its solubility in a salt solution. Cs (mol/L) represents the molar concentration of the salt solution, and T (k) refers to the temperature.

Therefore, at the temperature of 60°C, the **Equation A-2** can be written as:

$$log\left({}^{S_0}/_{S}\right) = 1.7C_s - 0.96 \tag{A-3}$$

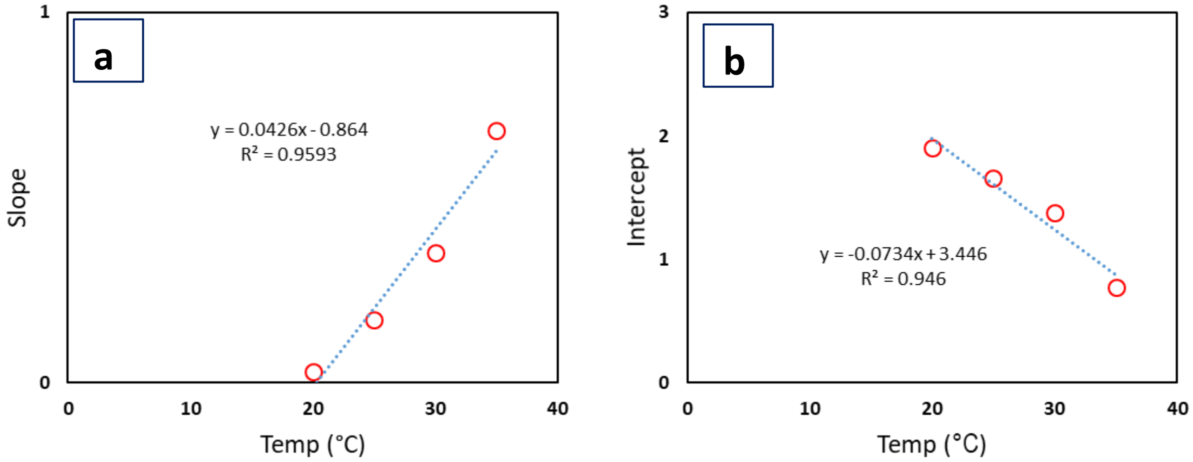

Figure. A-3 Correlation between slope, intercept, and temperature for solubility measurements

Reference:

[1] N. Hamzah, C.P. Leo, Membrane distillation of saline with phenolic compound using superhydrophobic PVDF membrane incorporated with TiO 2 nanoparticles: Separation, fouling and self-cleaning evaluation, Desalination 418 (2017) 79–88. https://doi.org/10.1016/j.desal.2017.05.029.

[2] Q.-L. Huang, Y. Huang, C.-F. Xiao, Y.-W. You, C.-X. Zhang, Electrospun ultrafine fibrous PTFE-supported ZnO porous membrane with self-cleaning function for vacuum membrane distillation, J. Memb. Sci. 534 (2017) 73–82. https://doi.org/10.1016/j.memsci.2017.04.015.

[3] J. Guo, D.Y.S. Yan, F.L.-Y. Lam, B.J. Deka, X. Lv, Y.H. Ng, A.K. An, Self-cleaning BiOBr/Ag photocatalytic membrane for membrane regeneration under visible light in membrane distillation, Chem. Eng. J. 378 (2019) 122137. https://doi.org/10.1016/j.cej.2019.122137.

[4] A. Yadav, R.V. Patel, P. Awasthi, N. Sinha, P.K. Labhasetwar, Hexagonal boron nitride nanosheets incorporated photocatalytic polyvinylidene fluoride mixed matrix membranes for textile wastewater treatment via vacuum-assisted distillation, Colloids Surfaces A Physicochem. Eng. Asp. 653 (2022) 129955. https://doi.org/10.1016/j.colsurfa.2022.129955.

[5] Y. Li, S. Dong, L. Zhu, Preparation of novel poly(vinylidene fluoride)/TiO2 photocatalysis membranes for use in direct contact membrane distillation, J. Nanoparticle Res. 20 (2018) 63. https://doi.org/10.1007/s11051-018-4167-9.

[6] Y. Li, L. Zhu, Evaluation of the antifouling and photocatalytic properties of novel poly(vinylidene fluoride) membranes with a reduced graphene oxide-Bi 2 WO 6 active layer, J. Appl. Polym. Sci. 134 (2017) 45426. https://doi.org/10.1002/app.45426.

[7] R. Ning, Z. Yan, Z. Lu, Q. Wang, Z. Wu, W. Dai, G. Fan, X. Fu, Photocatalytic membrane for in situ enhanced removal of semi-volatile organic compounds in membrane distillation under visible light, Sep. Purif. Technol. 292 (2022) 121068. https://doi.org/10.1016/j.seppur.2022.121068.

[8] J. Sun, M.U. Farid, M.W. Boey, Y. Sato, G. Chen, A.K. An, MXene-PVA-TiO2-based photothermal-catalytic membrane with high structural stability for efficient desalination and photodegradation, Chem. Eng. J. 468 (2023) 143744. https://doi.org/10.1016/j.cej.2023.143744.

[9] N. Hamzah, C.P. Leo, Fouling prevention in the membrane distillation of phenolic-rich solution using superhydrophobic PVDF membrane incorporated with TiO2 nanoparticles, Sep. Purif. Technol. 167 (2016) 79–87. https://doi.org/10.1016/j.seppur.2016.05.005.

[10] L.A. Hoover, W.A. Phillip, A. Tiraferri, N.Y. Yip, M. Elimelech, Forward with Osmosis: Emerging Applications for Greater Sustainability, Environ. Sci. Technol. 45 (2011) 9824–9830. https://doi.org/10.1021/es202576h.

[11] T. Distefano, S. Kelly, Are we in deep water? Water scarcity and its limits to economic growth, Ecol. Econ. 142 (2017) 130–147. https://doi.org/10.1016/j.ecolecon.2017.06.019.

[12] L.N. Nthunya, L. Gutierrez, S. Derese, E.N. Nxumalo, A.R. Verliefde, B.B. Mamba, S.D. Mhlanga, A review of nanoparticle-enhanced membrane distillation membranes: membrane synthesis and applications in water treatment, J. Chem.

Technol. Biotechnol. 94 (2019) 2757–2771. https://doi.org/10.1002/jctb.5977.

[13] K.M. Lee, C.W. Lai, K.S. Ngai, J.C. Juan, Recent developments of zinc oxide based photocatalyst in water treatment technology: A review, Water Res. 88 (2016) 428–448. https://doi.org/10.1016/j.watres.2015.09.045.

[14] X.-R. Xu, X.-Z. Li, Degradation of azo dye Orange G in aqueous solutions by persulfate with ferrous ion, Sep. Purif. Technol. 72 (2010) 105–111. https://doi.org/10.1016/j.seppur.2010.01.012.

[15] X. Yang, A.G. Fane, R. Wang, Membrane Distillation: Now and Future, in: Desalination, John Wiley & Sons, Inc., Hoboken, NJ, USA, 2014: pp. 373–424. https://doi.org/10.1002/9781118904855.ch8.

[16] L.D. Tijing, Y.C. Woo, J.-S. Choi, S. Lee, S.-H. Kim, H.K. Shon, Fouling and its control in membrane distillation—A review, J. Memb. Sci. 475 (2015) 215–244. https://doi.org/10.1016/j.memsci.2014.09.042.

[17] A. CRISCUOLI, J. ZHONG, A. FIGOLI, M. CARNEVALE, R. HUANG, E. DRIOLI, Treatment of dye solutions by vacuum membrane distillation, Water Res. 42 (2008) 5031–5037. https://doi.org/10.1016/j.watres.2008.09.014.

[18] N.G.P. Chew, S. Zhao, C.H. Loh, N. Permogorov, R. Wang, Surfactant effects on water recovery from produced water via direct-contact membrane distillation, J. Memb. Sci. 528 (2017) 126–134. https://doi.org/10.1016/j.memsci.2017.01.024.

[19] G. Naidu, L. Tijing, M.A.H. Johir, H. Shon, S. Vigneswaran, Hybrid membrane distillation: Resource, nutrient and energy recovery, J. Memb. Sci. 599 (2020) 117832. https://doi.org/10.1016/j.memsci.2020.117832.

[20] T. Horseman, Y. Yin, K.S. Christie, Z. Wang, T. Tong, S. Lin, Wetting, Scaling, and Fouling in Membrane Distillation: State-of-the-Art Insights on Fundamental Mechanisms and Mitigation Strategies, ACS ES&T Eng. 1 (2021) 117–140. https://doi.org/10.1021/acsestengg.0c00025.

[21] Z. Wang, S. Lin, Membrane fouling and wetting in membrane distillation and their mitigation by novel membranes with special wettability, Water Res. 112 (2017) 38–47. https://doi.org/10.1016/j.watres.2017.01.022.

[22] Y. Liao, R. Wang, A.G. Fane, Fabrication of Bioinspired Composite Nanofiber Membranes with Robust Superhydrophobicity for Direct Contact Membrane Distillation, Environ. Sci. Technol. 48 (2014) 6335–6341. https://doi.org/10.1021/es405795s.

[23] Y.-U. Shin, E.-T. Yun, J. Kim, H. Lee, S. Hong, J. Lee, Electrochemical Oxidation–Membrane Distillation Hybrid Process: Utilizing Electric Resistance Heating for Distillation and Membrane Defouling through Thermal Activation of Anodically Formed Persulfate, Environ. Sci. Technol. 54 (2020) 1867–1877. https://doi.org/10.1021/acs.est.9b05141.

[24] H. Wu, X. Xu, L. Shi, Y. Yin, L.-C. Zhang, Z. Wu, X. Duan, S. Wang, H. Sun, Manganese oxide integrated catalytic ceramic membrane for degradation of organic pollutants using sulfate radicals, Water Res. 167 (2019) 115110. https://doi.org/10.1016/j.watres.2019.115110.

[25] Z. Yang, D. Dai, Y. Yao, L. Chen, Q. Liu, L. Luo, Extremely enhanced generation of reactive oxygen species for oxidation of pollutants from peroxymonosulfate induced by a supported copper oxide catalyst, Chem. Eng. J. 322 (2017) 546–

555. https://doi.org/10.1016/j.cej.2017.04.018.

[26] W.-D. Oh, Z. Dong, T.-T. Lim, Generation of sulfate radical through heterogeneous catalysis for organic contaminants removal: Current development, challenges and prospects, Appl. Catal. B Environ. 194 (2016) 169–201. https://doi.org/10.1016/j.apcatb.2016.04.003.

[27] E. Saputra, S. Muhammad, H. Sun, H.-M. Ang, M.O. Tadé, S. Wang, Manganese oxides at different oxidation states for heterogeneous activation of peroxymonosulfate for phenol degradation in aqueous solutions, Appl. Catal. B Environ. 142–143 (2013) 729–735. https://doi.org/10.1016/j.apcatb.2013.06.004.

[28] P. Hu, M. Long, Cobalt-catalyzed sulfate radical-based advanced oxidation: A review on heterogeneous catalysts and applications, Appl. Catal. B Environ. 181 (2016) 103–117. https://doi.org/10.1016/j.apcatb.2015.07.024.

[29] P. Zhang, W. Liu, S. Rajabzadeh, Y. Jia, Q. Shen, C. Fang, N. Kato, H. Matsuyama, Modification of PVDF hollow fiber membrane by co-deposition of PDA/MPC-co-AEMA for membrane distillation application with anti-fouling and anti-scaling properties, J. Memb. Sci. 636 (2021) 119596. https://doi.org/10.1016/j.memsci.2021.119596.

[30] N.G.P. Chew, S. Zhao, C. Malde, R. Wang, Polyvinylidene fluoride membrane modification via oxidant-induced dopamine polymerization for sustainable direct-contact membrane distillation, J. Memb. Sci. 563 (2018) 31–42. https://doi.org/10.1016/j.memsci.2018.05.035.

[31] K. Wang, D. Hou, P. Qi, K. Li, Z. Yuan, J. Wang, Development of a composite membrane with underwater-oleophobic fibrous surface for robust anti-oil-fouling membrane distillation, J. Colloid Interface Sci. 537 (2019) 375–383. https://doi.org/10.1016/j.jcis.2018.11.040.

[32] Y. Chen, K.-J. Lu, S. Japip, T.-S. Chung, Can Composite Janus Membranes with an Ultrathin Dense Hydrophilic Layer Resist Wetting in Membrane Distillation?, Environ. Sci. Technol. 54 (2020) 12713–12722. https://doi.org/10.1021/acs.est.0c04242.

[33] Z. Wang, H.-C. Yang, F. He, S. Peng, Y. Li, L. Shao, S.B. Darling, Mussel-Inspired Surface Engineering for Water-Remediation Materials, Matter 1 (2019) 115–155. https://doi.org/10.1016/j.matt.2019.05.002.

[34] C. Zhang, L. Gong, L. Xiang, Y. Du, W. Hu, H. Zeng, Z.-K. Xu, Deposition and Adhesion of Polydopamine on the Surfaces of Varying Wettability, ACS Appl. Mater. Interfaces 9 (2017) 30943–30950. https://doi.org/10.1021/acsami.7b09774.

[35] R. Bahamonde Soria, J. Zhu, I. Gonza, B. Van der Bruggen, P. Luis, Effect of (TiO2: ZnO) ratio on the anti-fouling properties of bio-inspired nanofiltration membranes, Sep. Purif. Technol. 251 (2020) 117280. https://doi.org/10.1016/j.seppur.2020.117280.

[36] S.-C. Li, L.-N. Chu, X.-Q. Gong, U. Diebold, Hydrogen Bonding Controls the Dynamics of Catechol Adsorbed on a TiO2(110) Surface, Science (80-.). 328 (2010) 882–884. https://doi.org/10.1126/science.1188328.

[37] J. Yu, W. Wei, M.S. Menyo, A. Masic, J.H. Waite, J.N. Israelachvili, Adhesion of Mussel Foot Protein-3 to TiO 2 Surfaces: the Effect of pH, Biomacromolecules 14 (2013) 1072–1077. https://doi.org/10.1021/bm301908y.

[38] J. Yu, Y. Kan, M. Rapp, E. Danner, W. Wei, S. Das, D.R. Miller, Y. Chen, J.H. Waite, J.N. Israelachvili, Adaptive hydrophobic and hydrophilic interactions of mussel foot proteins with organic thin films, Proc. Natl. Acad. Sci. 110 (2013) 15680–15685. https://doi.org/10.1073/pnas.1315015110.

[39] N.G.P. Chew, Y. Zhang, K. Goh, J.S. Ho, R. Xu, R. Wang, Hierarchically Structured Janus Membrane Surfaces for Enhanced Membrane Distillation Performance, ACS Appl. Mater. Interfaces 11 (2019) 25524–25534. https://doi.org/10.1021/acsami.9b05967.

[40] F. Ponzio, J. Barthès, J. Bour, M. Michel, P. Bertani, J. Hemmerlé, M. D'Ischia, V. Ball, Oxidant Control of Polydopamine Surface Chemistry in Acids: A Mechanism-Based Entry to Superhydrophilic-Superoleophobic Coatings, Chem. Mater. 28 (2016) 4697–4705. https://doi.org/10.1021/acs.chemmater.6b01587.

[41] Q. Wei, F. Zhang, J. Li, B. Li, C. Zhao, Oxidant-induced dopamine polymerization for multifunctional coatings, Polym. Chem. 1 (2010) 1430. https://doi.org/10.1039/c0py00215a.

[42] M.R. Choudhury, N. Anwar, D. Jassby, M.S. Rahaman, Fouling and wetting in the membrane distillation driven wastewater reclamation process – A review, Adv. Colloid Interface Sci. 269 (2019) 370–399. https://doi.org/10.1016/j.cis.2019.04.008.

[43] C.Y. Tang, T.H. Chong, A.G. Fane, Colloidal interactions and fouling of NF and RO membranes: A review, Adv. Colloid Interface Sci. 164 (2011) 126–143. https://doi.org/10.1016/j.cis.2010.10.007.

[44] J. Lin, C.Y. Tang, W. Ye, S.-P. Sun, S.H. Hamdan, A. Volodin, C. Van Haesendonck, A. Sotto, P. Luis, B. Van der Bruggen, Unraveling flux behavior of superhydrophilic loose nanofiltration membranes during textile wastewater treatment, J. Memb. Sci. 493 (2015) 690–702. https://doi.org/10.1016/j.memsci.2015.07.018.

[45] W.-H. Xie, W.-Y. Shiu, D. Mackay, A review of the effect of salts on the solubility of organic compounds in seawater, Mar. Environ. Res. 44 (1997) 429–444. https://doi.org/10.1016/S0141-1136(97)00017-2.

[46] I.M. Valente, L.M. Gonçalves, J.A. Rodrigues, Another glimpse over the salting-out assisted liquid–liquid extraction in acetonitrile/water mixtures, J. Chromatogr. A 1308 (2013) 58–62. https://doi.org/10.1016/j.chroma.2013.08.014.

[47] N.A. Moringo, L.D.C. Bishop, H. Shen, A. Misiura, N.C. Carrejo, R. Baiyasi, W. Wang, F. Ye, J.T. Robinson, C.F. Landes, A mechanistic examination of salting out in protein–polymer membrane interactions, Proc. Natl. Acad. Sci. 116 (2019) 22938–22945. https://doi.org/10.1073/pnas.1909860116.

[48] J. Cho, J.K. Cho, J. Lee, D. Lee, C. Park, S. Kim, Optimization of salting-out crystallization for an efficient in situ separation of synthetic anthraquinone- and azo-type reactive dyes, Sep. Purif. Technol. 68 (2009) 138–144. https://doi.org/10.1016/j.seppur.2009.04.015.

[49] J. Lin, W. Ye, H. Zeng, H. Yang, J. Shen, S. Darvishmanesh, P. Luis, A. Sotto, B. Van der Bruggen, Fractionation of direct dyes and salts in aqueous solution using loose nanofiltration membranes, J. Memb. Sci. 477 (2015) 183–193. https://doi.org/10.1016/j.memsci.2014.12.008.

[50] B. Van der Bruggen, E. Curcio, E. Drioli, Process intensification in the textile industry: the role of membrane technology, J. Environ. Manage. 73 (2004) 267–

274. https://doi.org/10.1016/j.jenvman.2004.07.007.

[51] M. Afsari, H.K. Shon, L.D. Tijing, Janus membranes for membrane distillation: Recent advances and challenges, Adv. Colloid Interface Sci. 289 (2021) 102362. https://doi.org/10.1016/j.cis.2021.102362.

[52] R. Vinoth Kumar, M.O. Barbosa, A.R. Ribeiro, S. Morales-Torres, M.F.R. Pereira, A.M.T. Silva, Advanced oxidation technologies combined with direct contact membrane distillation for treatment of secondary municipal wastewater, Process Saf. Environ. Prot. 140 (2020) 111–123. https://doi.org/10.1016/j.psep.2020.03.008.

[53] W. Liang, G. Chen, M. Huang, Performance and membrane fouling mitigation for bio-treated coking wastewater treatment via membrane distillation: Effect of pre-treatment, J. Water Process Eng. 46 (2022) 102647. https://doi.org/10.1016/j.jwpe.2022.102647.

[54] L. Chen, Z. Chen, Y. Wang, Y. Mao, Z. Cai, Effective treatment of leachate concentrate using membrane distillation coupled with electrochemical oxidation, Sep. Purif. Technol. 267 (2021) 118679. https://doi.org/10.1016/j.seppur.2021.118679.

[55] C. Li, W. Deng, C. Gao, X. Xiang, X. Feng, B. Batchelor, Y. Li, Membrane distillation coupled with a novel two-stage pretreatment process for petrochemical wastewater treatment and reuse, Sep. Purif. Technol. 224 (2019) 23–32. https://doi.org/10.1016/j.seppur.2019.05.007.

[56] M. Ding, H. Xu, C. Yao, W. Chen, N. Song, Q. Zhang, T. Lin, Z. Xie, Understanding the membrane fouling control process at molecular level in the heated persulfate activation- membrane distillation hybrid system, Water Res. 229 (2023) 119465. https://doi.org/10.1016/j.watres.2022.119465.

[57] C.B. Alvim, V.R. Moreira, Y.A.R. Lebron, A.V. Santos, L.C. Lange, R.P.M. Moreira, L.V. de S. Santos, M.C.S. Amaral, Comparison of UV, UV/H2O2 and ozonation processes for the treatment of membrane distillation concentrate from surface water treatment: PhACs removal and environmental and human health risk assessment, Chem. Eng. J. 397 (2020) 125482. https://doi.org/10.1016/j.cej.2020.125482.

[58] L. Jiang, L. Chen, L. Zhu, In-situ electric-enhanced membrane distillation for simultaneous flux-increasing and anti-wetting, J. Memb. Sci. 630 (2021) 119305. https://doi.org/10.1016/j.memsci.2021.119305.

[59] J. Schneider, M. Matsuoka, M. Takeuchi, J. Zhang, Y. Horiuchi, M. Anpo, D.W. Bahnemann, Understanding TiO 2 Photocatalysis: Mechanisms and Materials, Chem. Rev. 114 (2014) 9919–9986. https://doi.org/10.1021/cr5001892.

[60] K.P. Gopinath, N.V. Madhav, A. Krishnan, R. Malolan, G. Rangarajan, Present applications of titanium dioxide for the photocatalytic removal of pollutants from water: A review, J. Environ. Manage. 270 (2020) 110906. https://doi.org/10.1016/j.jenvman.2020.110906.

[61] H. Dong, G. Zeng, L. Tang, C. Fan, C. Zhang, X. He, Y. He, An overview on limitations of TiO2-based particles for photocatalytic degradation of organic pollutants and the corresponding countermeasures, Water Res. 79 (2015) 128–146. https://doi.org/10.1016/j.watres.2015.04.038.

[62] M. Nadimi, A. Ziarati Saravani, M.A. Aroon, A. Ebrahimian Pirbazari, Photodegradation of methylene blue by a ternary magnetic

TiO2/Fe3O4/graphene oxide nanocomposite under visible light, Mater. Chem. Phys. 225 (2019) 464–474. https://doi.org/10.1016/j.matchemphys.2018.11.029.

[63] S. Mozia, D. Darowna, J. Przepiórski, A.W. Morawski, Evaluation of Performance of Hybrid Photolysis-DCMD and Photocatalysis-DCMD Systems Utilizing UV-C Radiation for Removal of Diclofenac Sodium Salt From Water, Polish J. Chem. Technol. 15 (2013) 51–60. https://doi.org/10.2478/pjct-2013-0010.

[64] S. Mozia, A.W. Morawski, Integration of Photocatalysis with Ultrafiltration or Membrane Distillation for Removal of Azo Dye Direct Green 99 from Water, J. Adv. Oxid. Technol. 12 (2009). https://doi.org/10.1515/jaots-2009-0114.

[65] S. Mozia, Application of temperature modified titanate nanotubes for removal of an azo dye from water in a hybrid photocatalysis-MD process, Catal. Today 156 (2010) 198–207. https://doi.org/10.1016/j.cattod.2010.02.026.

[66] S. Mozia, A.W. Morawski, M. Toyoda, M. Inagaki, Effectiveness of photodecomposition of an azo dye on a novel anatase-phase TiO2 and two commercial photocatalysts in a photocatalytic membrane reactor (PMR), Sep. Purif. Technol. 63 (2008) 386–391. https://doi.org/10.1016/j.seppur.2008.05.029.

[67] D. Qu, Z. Qiang, S. Xiao, Q. Liu, Y. Lei, T. Zhou, Degradation of Reactive Black 5 in a submerged photocatalytic membrane distillation reactor with microwave electrodeless lamps as light source, Sep. Purif. Technol. 122 (2014) 54–59. https://doi.org/10.1016/j.seppur.2013.11.004.

[68] J. Wang, X. Sun, Y. Yuan, H. Chen, H. Wang, D. Hou, A novel microwave assisted photo-catalytic membrane distillation process for treating the organic wastewater containing inorganic ions, J. Water Process Eng. 9 (2016) 1–8. https://doi.org/10.1016/j.jwpe.2015.11.004.

[69] Y. Huo, Z. Xie, X. Wang, H. Li, M. Hoang, R.A. Caruso, Methyl orange removal by combined visible-light photocatalysis and membrane distillation, Dye. Pigment. 98 (2013) 106–112. https://doi.org/10.1016/j.dyepig.2013.02.009.

[70] S. Mozia, R. Rajakumaran, K. Szymański, M. Gryta, Removal of ketoprofen from surface water in a submerged photocatalytic membrane reactor utilizing membrane distillation: effect of process parameters and evaluation of long-term performance, J. Chem. Technol. Biotechnol. 98 (2023) 1125–1136. https://doi.org/10.1002/jctb.7313.

[71] K. Szymański, M. Gryta, D. Darowna, S. Mozia, A new submerged photocatalytic membrane reactor based on membrane distillation for ketoprofen removal from various aqueous matrices, Chem. Eng. J. 435 (2022) 134872. https://doi.org/10.1016/j.cej.2022.134872.

[72] S. Mozia, M. Tomaszewska, A.W. Morawski, A new photocatalytic membrane reactor (PMR) for removal of azo-dye Acid Red 18 from water, Appl. Catal. B Environ. 59 (2005) 131–137. https://doi.org/10.1016/j.apcatb.2005.01.011.

[73] S. Mozia, M. Toyoda, T. Tsumura, M. Inagaki, A.W. Morawski, Comparison of effectiveness of methylene blue decomposition using pristine and carbon-coated TiO2 in a photocatalytic membrane reactor, Desalination 212 (2007) 141–151. https://doi.org/10.1016/j.desal.2006.10.007.

[74] S. Mozia, A.W. Morawski, The performance of a hybrid photocatalysis–MD system for the treatment of tap water contaminated with ibuprofen, Catal. Today 193 (2012) 213–220. https://doi.org/10.1016/j.cattod.2012.03.016.

[75] S. Mozia, M. Tomaszewska, A.W. Morawski, Photocatalytic membrane reactor (PMR) coupling photocatalysis and membrane distillation—Effectiveness of removal of three azo dyes from water, Catal. Today 129 (2007) 3–8. https://doi.org/10.1016/j.cattod.2007.06.043.

[76] S. Mozia, A.W. Morawski, Hybridization of photocatalysis and membrane distillation for purification of wastewater, Catal. Today 118 (2006) 181–188. https://doi.org/10.1016/j.cattod.2005.12.003.

[77] D. Darowna, S. Grondzewska, A.W. Morawski, S. Mozia, Removal of non-steroidal anti-inflammatory drugs from primary and secondary effluents in a photocatalytic membrane reactor, J. Chem. Technol. Biotechnol. 89 (2014) 1265–1273. https://doi.org/10.1002/jctb.4386.

[78] J. Grzechulska-Damszel, A. Morawski, Removal of organic dye in the hybrid photocatalysis/membrane processes system, Polish J. Chem. Technol. 9 (2007). https://doi.org/10.2478/v10026-007-0036-5.

[79] S. Mozia, A.W. Morawski, M. Toyoda, T. Tsumura, Integration of photocatalysis and membrane distillation for removal of mono- and poly-azo dyes from water, Desalination 250 (2010) 666–672. https://doi.org/10.1016/j.desal.2009.06.075.

[80] S. Mozia, A.W. Morawski, M. Toyoda, T. Tsumura, Effect of process parameters on photodegradation of Acid Yellow 36 in a hybrid photocatalysis–membrane distillation system, Chem. Eng. J. 150 (2009) 152–159. https://doi.org/10.1016/j.cej.2008.12.012.

[81] S. Mozia, M. Toyoda, M. Inagaki, B. Tryba, A.W. Morawski, Application of carbon-coated TiO2 for decomposition of methylene blue in a photocatalytic membrane reactor, J. Hazard. Mater. 140 (2007) 369–375. https://doi.org/10.1016/j.jhazmat.2006.10.016.

[82] S. Mozia, A.W. Morawski, M. Toyoda, T. Tsumura, Effect of process parameters on photodegradation of Acid Yellow 36 in a hybrid photocatalysis–membrane distillation system, Chem. Eng. J. 150 (2009) 152–159. https://doi.org/10.1016/j.cej.2008.12.012.

[83] S. Mozia, D. Darowna, K. Szymański, S. Grondzewska, K. Borchert, R. Wróbel, A.W. Morawski, Performance of two photocatalytic membrane reactors for treatment of primary and secondary effluents, Catal. Today 236 (2014) 135–145. https://doi.org/10.1016/j.cattod.2013.12.049.

[84] S.. Tsui, W. Chu, Quantum yield study of the photodegradation of hydrophobic dyes in the presence of acetone sensitizer, Chemosphere 44 (2001) 17–22. https://doi.org/10.1016/S0045-6535(00)00379-9.

[85] B. Neppolian, H.C. Choi, S. Sakthivel, B. Arabindoo, V. Murugesan, Solar light induced and TiO2 assisted degradation of textile dye reactive blue 4, Chemosphere 46 (2002) 1173–1181. https://doi.org/10.1016/S0045-6535(01)00284-3.

[86] M. Laqbaqbi, M.C. García-Payo, M. Khayet, J. El Kharraz, M. Chaouch, Application of direct contact membrane distillation for textile wastewater treatment and fouling study, Sep. Purif. Technol. 209 (2019) 815–825. https://doi.org/10.1016/j.seppur.2018.09.031.

[87] Y.-H. Hsien, C.-F. Chang, Y.-H. Chen, S. Cheng, Photodegradation of aromatic pollutants in water over TiO2 supported on molecular sieves, Appl. Catal. B Environ. 31 (2001) 241–249. https://doi.org/10.1016/S0926-3373(00)00283-6.

[88] Q. Wang, C. Chen, D. Zhao, W. Ma, J. Zhao, Change of Adsorption Modes of Dyes on Fluorinated TiO 2 and Its Effect on Photocatalytic Degradation of Dyes under Visible Irradiation, Langmuir 24 (2008) 7338–7345. https://doi.org/10.1021/la800313s.

[89] H. Park, W. Choi, Effects of TiO 2 Surface Fluorination on Photocatalytic Reactions and Photoelectrochemical Behaviors, J. Phys. Chem. B 108 (2004) 4086–4093. https://doi.org/10.1021/jp036735i.

[90] H. Zhou, X. Sheng, J. Xiao, Z. Ding, D. Wang, X. Zhang, J. Liu, R. Wu, X. Feng, L. Jiang, Increasing the Efficiency of Photocatalytic Reactions via Surface Microenvironment Engineering, J. Am. Chem. Soc. 142 (2020) 2738–2743. https://doi.org/10.1021/jacs.9b12247.

[91] N. Bao, Y. Li, Z. Wei, G. Yin, J. Niu, Adsorption of Dyes on Hierarchical Mesoporous TiO 2 Fibers and Its Enhanced Photocatalytic Properties, J. Phys. Chem. C 115 (2011) 5708–5719. https://doi.org/10.1021/jp1100939.

[92] A.K. An, J. Guo, E.-J. Lee, S. Jeong, Y. Zhao, Z. Wang, T. Leiknes, PDMS/PVDF hybrid electrospun membrane with superhydrophobic property and drop impact dynamics for dyeing wastewater treatment using membrane distillation, J. Memb. Sci. 525 (2017) 57–67. https://doi.org/10.1016/j.memsci.2016.10.028.

[93] A.K. An, J. Guo, S. Jeong, E.-J. Lee, S.A.A. Tabatabai, T. Leiknes, High flux and antifouling properties of negatively charged membrane for dyeing wastewater treatment by membrane distillation, Water Res. 103 (2016) 362–371. https://doi.org/10.1016/j.watres.2016.07.060.

[94] S. Mozia, A.W. Morawski, M. Toyoda, The Influence of Solution Composition on the Effectiveness of Degradation of Ibuprofen Sodium Salt in a Hybrid Photocatalysis – Membrane Distillation System, J. Adv. Oxid. Technol. 15 (2012). https://doi.org/10.1515/jaots-2012-0102.

[95] C. Hu, J.C. Yu, Z. Hao, P.. Wong, Effects of acidity and inorganic ions on the photocatalytic degradation of different azo dyes, Appl. Catal. B Environ. 46 (2003) 35–47. https://doi.org/10.1016/S0926-3373(03)00139-5.

[96] J.N. Meegoda, S.A. Hewage, J.H. Batagoda, Application of the Diffused Double Layer Theory to Nanobubbles, Langmuir 35 (2019) 12100–12112. https://doi.org/10.1021/acs.langmuir.9b01443.

[97] X. Yang, A.G. Fane, R. Wang, Membrane Distillation: Now and Future, in: Desalination, John Wiley & Sons, Inc., Hoboken, NJ, USA, 2014: pp. 373–424. https://doi.org/10.1002/9781118904855.ch8.

[98] L.D. Tijing, Y.C. Woo, J.-S. Choi, S. Lee, S.-H. Kim, H.K. Shon, Fouling and its control in membrane distillation—a review, J. Memb. Sci. 475 (2015) 215–244. https://doi.org/10.1016/j.memsci.2014.09.042.

[99] S. Hong, M. Elimelech, Chemical and physical aspects of natural organic matter (NOM) fouling of nanofiltration membranes, J. Memb. Sci. 132 (1997) 159–181. https://doi.org/10.1016/S0376-7388(97)00060-4.

[100] K.M. Reza, A. Kurny, F. Gulshan, Parameters affecting the photocatalytic degradation of dyes using TiO2: a review, Appl. Water Sci. 7 (2017) 1569–1578. https://doi.org/10.1007/s13201-015-0367-y.

[101] R.G. Nair, S. Paul, S.K. Samdarshi, High UV/visible light activity of mixed phase

titania: A generic mechanism, Sol. Energy Mater. Sol. Cells 95 (2011) 1901–1907. https://doi.org/10.1016/j.solmat.2011.02.017.

[102] D. Zhang, S. Dong, Challenges in band alignment between semiconducting materials: A case of rutile and anatase TiO2, Prog. Nat. Sci. Mater. Int. 29 (2019) 277–284. https://doi.org/10.1016/j.pnsc.2019.03.012.

[103] H. He, C. Liu, K.D. Dubois, T. Jin, M.E. Louis, G. Li, Enhanced charge separation in nanostructured TiO 2 materials for photocatalytic and photovoltaic applications, Ind. Eng. Chem. Res. 51 (2012) 11841–11849. https://doi.org/10.1021/ie300510n.

[104] D.O. Scanlon, C.W. Dunnill, J. Buckeridge, S.A. Shevlin, A.J. Logsdail, S.M. Woodley, C.R.A. Catlow, M.J. Powell, R.G. Palgrave, I.P. Parkin, G.W. Watson, T.W. Keal, P. Sherwood, A. Walsh, A.A. Sokol, Band alignment of rutile and anatase TiO2, Nat. Mater. 12 (2013) 798–801. https://doi.org/10.1038/nmat3697.

[105] M. Anpo, T. Shima, S. Kodama, Y. Kubokawa, Photocatalytic hydrogenation of propyne with water on small-particle titania: size quantization effects and reaction intermediates, J. Phys. Chem. 91 (1987) 4305–4310. https://doi.org/10.1021/j100300a021.

[106] Z. Zhang, C. Wang, R. Zakaria, J.Y. Ying, Role of Particle Size in Nanocrystalline TiO 2 -Based Photocatalysts, (1998) 10871–10878. https://doi.org/10.1021/jp982948+.

[107] H. He, C. Liu, K.D. Dubois, T. Jin, M.E. Louis, G. Li, Enhanced Charge Separation in Nanostructured TiO 2 Materials for Photocatalytic and Photovoltaic Applications, Ind. Eng. Chem. Res. 51 (2012) 11841–11849. https://doi.org/10.1021/ie300510n.

[108] C. Wang, Z. Zhang, J.Y. Ying, Photocatalytic decomposition of halogenated organics over nanocrystalline titania, Nanostructured Mater. 9 (1997) 583–586. https://doi.org/10.1016/S0965-9773(97)00130-X.

[109] T. Peng, D. Zhao, K. Dai, W. Shi, K. Hirao, Synthesis of Titanium Dioxide Nanoparticles with Mesoporous Anatase Wall and High Photocatalytic Activity, J. Phys. Chem. B 109 (2005) 4947–4952. https://doi.org/10.1021/jp044771r.

[110] C.-C. Wang, Z. Zhang, J.Y. Ying, Photocatalytic decomposition of halogenated organics over nanocrystalline titania, Nanostructured Mater. 9 (1997) 583–586. https://doi.org/10.1016/S0965-9773(97)00130-X.

[111] K. Dai, D. Li, J. Lv, L. Lu, C. Liang, G. Zhu, A scalable synthesis technique of hierarchical BiOBr microspheres for advanced visible light photocatalyst, Mater. Lett. 136 (2014) 438–440. https://doi.org/10.1016/j.matlet.2014.08.105.

[112] L. Ye, Y. Su, X. Jin, H. Xie, F. Cao, Z. Guo, Which affect the photoreactivity of BiOBr single-crystalline nanosheets with different hydrothermal pH value: Size or facet?, Appl. Surf. Sci. 311 (2014) 858–863. https://doi.org/10.1016/j.apsusc.2014.05.191.

[113] Y. Sun, W. Zhang, T. Xiong, Z. Zhao, F. Dong, R. Wang, W.-K. Ho, Growth of BiOBr nanosheets on C3N4 nanosheets to construct two-dimensional nanojunctions with enhanced photoreactivity for NO removal, J. Colloid Interface Sci. 418 (2014) 317–323. https://doi.org/10.1016/j.jcis.2013.12.037.

[114] Z. Jiang, F. Yang, G. Yang, L. Kong, M.O. Jones, T. Xiao, P.P. Edwards, The hydrothermal synthesis of BiOBr flakes for visible-light-responsive photocatalytic

degradation of methyl orange, J. Photochem. Photobiol. A Chem. 212 (2010) 8–13. https://doi.org/10.1016/j.jphotochem.2010.03.004.

[115] R. Hou, Y. Gao, H. Zhu, G. Yang, W. Liu, Y. Huo, Z. Xie, H. Li, Coupling system of Ag/BiOBr photocatalysis and direct contact membrane distillation for complete purification of N-containing dye wastewater, Chem. Eng. J. 317 (2017) 386–393. https://doi.org/10.1016/j.cej.2017.02.085.

[116] L.T. Nyamutswa, B. Hanson, D. Navaratna, S.F. Collins, K.G. Linden, M.C. Duke, Sunlight-Transmitting Photocatalytic Membrane for Reduced Maintenance Water Treatment, ACS ES&T Water 1 (2021) 2001–2011. https://doi.org/10.1021/acsestwater.1c00073.

[117] C. Xue, Y. Mao, W. Wang, Z. Song, X. Zhao, J. Sun, Y. Wang, Current status of applying microwave-associated catalysis for the degradation of organics in aqueous phase – A review, J. Environ. Sci. (China) 81 (2019) 119–135. https://doi.org/10.1016/j.jes.2019.01.019.

[118] A.L. Garcia-Costa, J.A. Zazo, J.J. Rodriguez, J.A. Casas, Microwave-assisted catalytic wet peroxide oxidation. Comparison of Fe catalysts supported on activated carbon and Γ-alumina, Appl. Catal. B Environ. 218 (2017) 637–642. https://doi.org/10.1016/j.apcatb.2017.06.058.

[119] M.J. Hülsey, C.W. Lim, N. Yan, Promoting heterogeneous catalysis beyond catalyst design, Chem. Sci. 11 (2020) 1456–1468. https://doi.org/10.1039/C9SC05947D.

[120] C. Xue, Y. Mao, W. Wang, Z. Song, X. Zhao, J. Sun, Y. Wang, Current status of applying microwave-associated catalysis for the degradation of organics in aqueous phase – A review, J. Environ. Sci. 81 (2019) 119–135. https://doi.org/10.1016/j.jes.2019.01.019.

[121] G.B. Dudley, R. Richert, A.E. Stiegman, On the existence of and mechanism for microwave-specific reaction rate enhancement, Chem. Sci. 6 (2015) 2144–2152. https://doi.org/10.1039/C4SC03372H.

[122] C.O. Kappe, B. Pieber, D. Dallinger, Microwave Effects in Organic Synthesis: Myth or Reality?, Angew. Chemie Int. Ed. 52 (2013) 1088–1094. https://doi.org/10.1002/anie.201204103.

[123] J. Staehelin, J. Hoigne, Decomposition of ozone in water: rate of initiation by hydroxide ions and hydrogen peroxide, Environ. Sci. Technol. 16 (1982) 676–681. https://doi.org/10.1021/es00104a009.

[124] J. Hoigné, H. Bader, The role of hydroxyl radical reactions in ozonation processes in aqueous solutions, Water Res. 10 (1976) 377–386. https://doi.org/10.1016/0043-1354(76)90055-5.

[125] S. Wacławek, H. V. Lutze, K. Grübel, V.V.T. Padil, M. Černík, D.D. Dionysiou, Chemistry of persulfates in water and wastewater treatment: A review, Chem. Eng. J. 330 (2017) 44–62. https://doi.org/10.1016/j.cej.2017.07.132.

[126] I.A. Ike, J.D. Orbell, M. Duke, Feasibility, mechanisms, and optimisation of organic pollutant degradation by thermally activated persulphate, Chem. Eng. Res. Des. 136 (2018) 304–314. https://doi.org/10.1016/j.cherd.2018.05.041.

[127] I. Woodard & Curran, Methods for Treating Wastewaters from Industry, in: Ind. Waste Treat. Handb., Elsevier, 2006: pp. 149–334. https://doi.org/10.1016/B978-075067963-3/50009-6.

[128] B. Aftab, H.B. Truong, J. Cho, J. Hur, Enhanced performance of a direct contact membrane distillation system via in-situ thermally activated H2O2 oxidation for the treatment of landfill leachate, J. Memb. Sci. 652 (2022) 120478. https://doi.org/10.1016/j.memsci.2022.120478.

[129] Y. Zhang, P. Zhao, J. Li, D. Hou, J. Wang, H. Liu, A hybrid process combining homogeneous catalytic ozonation and membrane distillation for wastewater treatment, Chemosphere 160 (2016) 134–140. https://doi.org/10.1016/j.chemosphere.2016.06.070.

[130] M.B. Asif, Z. Fida, A. Tufail, J.P. van de Merwe, F.D.L. Leusch, B.K. Pramanik, W.E. Price, F.I. Hai, Persulfate oxidation-assisted membrane distillation process for micropollutant degradation and membrane fouling control, Sep. Purif. Technol. 222 (2019) 321–331. https://doi.org/10.1016/j.seppur.2019.04.035.

[131] M.B. Asif, W.E. Price, Z. Fida, A. Tufail, T. Ren, F.I. Hai, Acid mine drainage and sewage impacted groundwater treatment by membrane distillation: Organic micropollutant and metal removal and membrane fouling, J. Environ. Manage. 291 (2021) 112708. https://doi.org/10.1016/j.jenvman.2021.112708.

[132] M. Han, R. Zhao, J. Shi, X. Li, D. He, L. Liu, L. Han, Membrane Distillation Hybrid Peroxydisulfate Activation toward Mitigating the Membrane Wetting by Sodium Dodecyl Sulfate, Membranes (Basel). 12 (2022) 164. https://doi.org/10.3390/membranes12020164.

[133] F.R. Omi, M. Rastgar, M. Sadrzadeh, Synergistic effect of thermal dehydrating on the emerging contaminants removal via Electro-Fenton, J. Clean. Prod. 356 (2022) 131880. https://doi.org/10.1016/j.jclepro.2022.131880.

[134] B. Ji, Y. Li, Z. Zhang, Electrochemically activated peroxymonosulfate (PMS) pretreatment for fouling remediation during membrane distillation of surface water: Role of PMS concentration and dosing mode, Sep. Purif. Technol. 322 (2023) 124308. https://doi.org/10.1016/j.seppur.2023.124308.

[135] M.M. Rokni, Power to Hydrogen Through Polygeneration Systems Based on Solid Oxide Cell Systems, Energies 12 (2019) 4793. https://doi.org/10.3390/en12244793.

[136] T.N.-D. Cao, S.-S. Chen, H.-M. Chang, T.X. Bui, I.-C. Chien, A promising bioelectrochemical reactor integrating membrane distillation and microbial fuel cell for dual advantages of power generation and water recovery, Environ. Sci. Water Res. Technol. 6 (2020) 2776–2788. https://doi.org/10.1039/D0EW00379D.

[137] Q. Zhao, H. Zhang, Z. Hu, Y. Li, An alkaline fuel cell/direct contact membrane distillation hybrid system for cogenerating electricity and freshwater, Energy 225 (2021) 120303. https://doi.org/10.1016/j.energy.2021.120303.

[138] W. Zhu, Y. Ge, X. Zhu, J. Han, Performance of proton exchange membrane fuel cell integrated with direct contact membrane distillation for electricity and fresh water productions, Desalination 529 (2022) 115642. https://doi.org/10.1016/j.desal.2022.115642.

[139] X. Lai, R. Long, Z. Liu, W. Liu, A hybrid system using direct contact membrane distillation for water production to harvest waste heat from the proton exchange membrane fuel cell, Energy 147 (2018) 578–586. https://doi.org/10.1016/j.energy.2018.01.065.

[140] Y. Qin, H. Zhang, F. Wang, J. Zhao, C. Zhang, L. Xiao, H. Miao, J. Yuan,

Integration of high-temperature PEMFC with air gap membrane distillation for simultaneous electricity generation and seawater desalination: A theoretical investigation, Desalination 543 (2022) 116100. https://doi.org/10.1016/j.desal.2022.116100.

[141] W. Zhu, J. Han, Y. Ge, J. Yang, W. Liang, Performance analysis and multi-objective optimization of a poly-generation system based on PEMFC, DCMD and heat pump, Desalination 555 (2023) 116542. https://doi.org/10.1016/j.desal.2023.116542.

[142] J. Li, C. Lai, H. Zhang, L. Xiao, J. Zhao, F. Wang, C. Zhang, L. Xia, H. Miao, J. Yuan, A combined phosphoric acid fuel cell and direct contact membrane distillation hybrid system for electricity generation and seawater desalination, Energy Convers. Manag. 267 (2022) 115916. https://doi.org/10.1016/j.enconman.2022.115916.

[143] Y. Qin, H. Zhang, S. Hou, F. Wang, J. Zhao, C. Zhang, H. Miao, J. Yuan, An efficient high-temperature PEMFC/membrane distillation hybrid system for simultaneous production of electricity and freshwater, Int. J. Hydrogen Energy 47 (2022) 11998–12014. https://doi.org/10.1016/j.ijhydene.2022.01.224.

[144] Y.-H. Liu, V.S.K. Adi, S.-Y. Suen, Heat-Integration of Solar-Heated Membrane Distillation and Fuel Cell for Desalination System Based on the Dynamic Optimization Approach, Processes 10 (2022) 663. https://doi.org/10.3390/pr10040663.

[145] B.B.A. Al Mahri, H.A. Balogun, A. Yusuf, A. Giwa, Electro-osmotic thermal process model for performance enhancement of forward osmosis integrated with membrane distillation, Sep. Purif. Technol. 238 (2020) 116494. https://doi.org/10.1016/j.seppur.2019.116494.

[146] B.P. Chaplin, Critical review of electrochemical advanced oxidation processes for water treatment applications, Environ. Sci. Process. Impacts 16 (2014) 1182–1203. https://doi.org/10.1039/C3EM00679D.

[147] F.C. Moreira, R.A.R. Boaventura, E. Brillas, V.J.P. Vilar, Electrochemical advanced oxidation processes: A review on their application to synthetic and real wastewaters, Appl. Catal. B Environ. 202 (2017) 217–261. https://doi.org/10.1016/j.apcatb.2016.08.037.

[148] S. Dharmalingam, V. Kugarajah, M. Sugumar, Membranes for Microbial Fuel Cells, in: Microb. Electrochem. Technol., Elsevier, 2019: pp. 143–194. https://doi.org/10.1016/B978-0-444-64052-9.00007-8.

[149] U. Lucia, Overview on fuel cells, Renew. Sustain. Energy Rev. 30 (2014) 164–169. https://doi.org/10.1016/j.rser.2013.09.025.

[150] S. Mateo, P. Cañizares, F.J. Fernandez-Morales, M.A. Rodrigo, A Critical View of Microbial Fuel Cells: What Is the Next Stage?, ChemSusChem 11 (2018) 4183–4192. https://doi.org/10.1002/cssc.201802187.

[151] A.J. Slate, K.A. Whitehead, D.A.C. Brownson, C.E. Banks, Microbial fuel cells: An overview of current technology, Renew. Sustain. Energy Rev. 101 (2019) 60–81. https://doi.org/10.1016/j.rser.2018.09.044.

[152] M.H. Do, H.H. Ngo, W.S. Guo, Y. Liu, S.W. Chang, D.D. Nguyen, L.D. Nghiem, B.J. Ni, Challenges in the application of microbial fuel cells to wastewater treatment and energy production: A mini review, Sci. Total Environ. 639 (2018) 910–920. https://doi.org/10.1016/j.scitotenv.2018.05.136.

[153] Y.-Z. Wang, Y.-K. Wang, C.-S. He, H.-Y. Yang, G.-P. Sheng, J.-Y. Shen, Y. Mu, H.-Q. Yu, Hydrodynamics of an Electrochemical Membrane Bioreactor, Sci. Rep. 5 (2015) 10387. https://doi.org/10.1038/srep10387.

[154] Y.-K. Wang, G.-P. Sheng, W.-W. Li, Y.-X. Huang, Y.-Y. Yu, R.J. Zeng, H.-Q. Yu, Development of a Novel Bioelectrochemical Membrane Reactor for Wastewater Treatment, Environ. Sci. Technol. 45 (2011) 9256–9261. https://doi.org/10.1021/es2019803.

[155] K.C. de F. Araújo, J.P. de P. Barreto, J.C. Cardozo, E.V. dos Santos, D.M. de Araújo, C.A. Martínez-Huitle, Sulfate pollution: evidence for electrochemical production of persulfate by oxidizing sulfate released by the surfactant sodium dodecyl sulfate, Environ. Chem. Lett. 16 (2018) 647–652. https://doi.org/10.1007/s10311-017-0703-6.

[156] H.M. Nguyen, C.M. Phan, T. Sen, Degradation of sodium dodecyl sulfate by photoelectrochemical and electrochemical processes, Chem. Eng. J. 287 (2016) 633–639. https://doi.org/10.1016/j.cej.2015.11.074.

[157] J.A. Kharraz, N.K. Khanzada, M.U. Farid, J. Kim, S. Jeong, A.K. An, Membrane distillation bioreactor (MDBR) for wastewater treatment, water reuse, and resource recovery: A review, J. Water Process Eng. 47 (2022) 102687. https://doi.org/10.1016/j.jwpe.2022.102687.

[158] S. Goh, J. Zhang, Y. Liu, A.G. Fane, Membrane Distillation Bioreactor (MDBR) – A lower Green-House-Gas (GHG) option for industrial wastewater reclamation, Chemosphere 140 (2015) 129–142. https://doi.org/10.1016/j.chemosphere.2014.09.003.

[159] F. Meng, S. Zhang, Y. Oh, Z. Zhou, H.-S. Shin, S.-R. Chae, Fouling in membrane bioreactors: An updated review, Water Res. 114 (2017) 151–180. https://doi.org/10.1016/j.watres.2017.02.006.

[160] F. Meng, S.-R. Chae, A. Drews, M. Kraume, H.-S. Shin, F. Yang, Recent advances in membrane bioreactors (MBRs): Membrane fouling and membrane material, Water Res. 43 (2009) 1489–1512. https://doi.org/10.1016/j.watres.2008.12.044.

[161] N.S.A. Mutamim, Z.Z. Noor, M.A.A. Hassan, A. Yuniarto, G. Olsson, Membrane bioreactor: Applications and limitations in treating high strength industrial wastewater, Chem. Eng. J. 225 (2013) 109–119. https://doi.org/10.1016/j.cej.2013.02.131.

[162] M. Alshabib, S.A. Onaizi, A review on phenolic wastewater remediation using homogeneous and heterogeneous enzymatic processes: Current status and potential challenges, Sep. Purif. Technol. 219 (2019) 186–207. https://doi.org/10.1016/j.seppur.2019.03.028.

[163] W. Zhou, W. Zhang, Y. Cai, Laccase immobilization for water purification: A comprehensive review, Chem. Eng. J. 403 (2021) 126272. https://doi.org/10.1016/j.cej.2020.126272.

[164] N.A. Daronch, M. Kelbert, C.S. Pereira, P.H.H. de Araújo, D. de Oliveira, Elucidating the choice for a precise matrix for laccase immobilization: A review, Chem. Eng. J. 397 (2020) 125506. https://doi.org/10.1016/j.cej.2020.125506.

[165] M. Asif, F. Hai, J. Kang, J. van de Merwe, F. Leusch, K. Yamamoto, W. Price, L. Nghiem, Degradation of Trace Organic Contaminants by a Membrane Distillation—Enzymatic Bioreactor, Appl. Sci. 7 (2017) 879.

https://doi.org/10.3390/app7090879.

[166] M.B. Asif, F.I. Hai, J. Kang, J.P. van de Merwe, F.D.L. Leusch, W.E. Price, L.D. Nghiem, Biocatalytic degradation of pharmaceuticals, personal care products, industrial chemicals, steroid hormones and pesticides in a membrane distillation-enzymatic bioreactor, Bioresour. Technol. 247 (2018) 528–536. https://doi.org/10.1016/j.biortech.2017.09.129.

[167] M.B. Asif, L.N. Nguyen, F.I. Hai, W.E. Price, L.D. Nghiem, Integration of an enzymatic bioreactor with membrane distillation for enhanced biodegradation of trace organic contaminants, Int. Biodeterior. Biodegradation 124 (2017) 73–81. https://doi.org/10.1016/j.ibiod.2017.06.012.

[168] A. Tufail, S. Alharbi, J. Alrifai, A. Ansari, W.E. Price, F.I. Hai, Combining enzymatic membrane bioreactor and ultraviolet photolysis for enhanced removal of trace organic contaminants: Degradation efficiency and by-products formation, Process Saf. Environ. Prot. 145 (2021) 110–119. https://doi.org/10.1016/j.psep.2020.08.001.

[169] S. Goh, J. Zhang, Y. Liu, A.G. Fane, Fouling and wetting in membrane distillation (MD) and MD-bioreactor (MDBR) for wastewater reclamation, Desalination 323 (2013) 39–47. https://doi.org/10.1016/j.desal.2012.12.001.

[170] J. Phattaranawik, A.G. Fane, A.C.S. Pasquier, W. Bing, A novel membrane bioreactor based on membrane distillation, Desalination 223 (2008) 386–395. https://doi.org/10.1016/j.desal.2007.02.075.

[171] P. Jacob, P. Phungsai, K. Fukushi, C. Visvanathan, Direct contact membrane distillation for anaerobic effluent treatment, J. Memb. Sci. 475 (2015) 330–339. https://doi.org/10.1016/j.memsci.2014.10.021.

[172] D. Kwon, W. Bae, J. Kim, Hybrid Forward Osmosis/Membrane Distillation Integrated with Anaerobic Fluidized Bed Bioreactor for Advanced Wastewater Treatment, J. Hazard. Mater. (2020) 124160. https://doi.org/10.1016/j.jhazmat.2020.124160.

[173] M. Tomaszewska, L. Białończyk, Production of ethanol from lactose in a bioreactor integrated with membrane distillation, Desalination 323 (2013) 114–119. https://doi.org/10.1016/j.desal.2013.01.026.

[174] H.-C. Kim, J. Shin, S. Won, J.-Y. Lee, S.K. Maeng, K.G. Song, Membrane distillation combined with an anaerobic moving bed biofilm reactor for treating municipal wastewater, Water Res. 71 (2015) 97–106. https://doi.org/10.1016/j.watres.2014.12.048.

[175] J. Li, W. Zhou, S. Fan, Z. Xiao, Y. Liu, J. Liu, B. Qiu, Y. Wang, Bioethanol production in vacuum membrane distillation bioreactor by permeate fractional condensation and mechanical vapor compression with polytetrafluoroethylene (PTFE) membrane, Bioresour. Technol. 268 (2018) 708–714. https://doi.org/10.1016/j.biortech.2018.08.055.

[176] X. Song, W. Luo, J. McDonald, S.J. Khan, F.I. Hai, W.E. Price, L.D. Nghiem, An anaerobic membrane bioreactor – membrane distillation hybrid system for energy recovery and water reuse: Removal performance of organic carbon, nutrients, and trace organic contaminants, Sci. Total Environ. 628–629 (2018) 358–365. https://doi.org/10.1016/j.scitotenv.2018.02.057.

[177] M. Tomaszewska, L. Białończyk, Ethanol production from whey in a bioreactor coupled with direct contact membrane distillation, Catal. Today 268 (2016) 156–

163. https://doi.org/10.1016/j.cattod.2016.01.059.

[178] G. Lewandowicz, W. Białas, B. Marczewski, D. Szymanowska, Application of membrane distillation for ethanol recovery during fuel ethanol production, J. Memb. Sci. 375 (2011) 212–219. https://doi.org/10.1016/j.memsci.2011.03.045.

[179] M. Gryta, A.W. Morawski, M. Tomaszewska, Ethanol production in membrane distillation bioreactor, Catal. Today 56 (2000) 159–165. https://doi.org/10.1016/S0920-5861(99)00272-2.

[180] M. Yao, Y.C. Woo, J. Ren, L.D. Tijing, J.-S. Choi, S.-H. Kim, H.K. Shon, Volatile fatty acids and biogas recovery using thermophilic anaerobic membrane distillation bioreactor for wastewater reclamation, J. Environ. Manage. 231 (2019) 833–842. https://doi.org/10.1016/j.jenvman.2018.11.009.

[181] C.C. Duong, S.-S. Chen, H.Q. Le, H.-M. Chang, N.C. Nguyen, D.T.N. Cao, I.-C. Chien, A novel thermophilic anaerobic granular sludge membrane distillation bioreactor for wastewater reclamation, Environ. Sci. Pollut. Res. (2020). https://doi.org/10.1007/s11356-020-09987-4.

[182] K.C. Wijekoon, F.I. Hai, J. Kang, W.E. Price, W. Guo, H.H. Ngo, T.Y. Cath, L.D. Nghiem, A novel membrane distillation–thermophilic bioreactor system: Biological stability and trace organic compound removal, Bioresour. Technol. 159 (2014) 334–341. https://doi.org/10.1016/j.biortech.2014.02.088.

[183] Q. Huang, H. Liu, Y. Wang, C. Xiao, A hybrid electric field assisted vacuum membrane distillation method to mitigate membrane fouling, RSC Adv. 8 (2018) 18084–18092. https://doi.org/10.1039/C8RA02304B.

[184] L. Jiang, L. Chen, L. Zhu, Electrically conductive membranes for anti-biofouling in membrane distillation with two novel operation modes: Capacitor mode and resistor mode, Water Res. 161 (2019) 297–307. https://doi.org/10.1016/j.watres.2019.06.015.

[185] H. Liu, Q. Huang, Y. Wang, C. Xiao, PTFE conductive membrane for EVMD process and the application of electro-catalysis, Sep. Purif. Technol. 187 (2017) 327–333. https://doi.org/10.1016/j.seppur.2017.06.067.

[186] J. Kim, E.-T. Yun, L. Tijing, H.K. Shon, S. Hong, Mitigation of fouling and wetting in membrane distillation by electrical repulsion using a multi-layered single-wall carbon nanotube/polyvinylidene fluoride membrane, J. Memb. Sci. 653 (2022) 120519. https://doi.org/10.1016/j.memsci.2022.120519.

[187] M. Lou, X. Zhu, X. Fang, Y. Liu, F. Li, Interception of volatile organic compounds through CNT electrochemistry of electrified membrane surface during membrane distillation, Sep. Purif. Technol. 297 (2022) 121380. https://doi.org/10.1016/j.seppur.2022.121380.

[188] F. Han, J. Mao, S. Liu, Preparation of reduced graphene oxide-carbon nanotubes membranes for conductive heating membrane distillation treatment of humic acid, Sep. Purif. Technol. 302 (2022) 122181. https://doi.org/10.1016/j.seppur.2022.122181.

[189] Y. Dong, L. Ma, C.Y. Tang, F. Yang, X. Quan, D. Jassby, M.J. Zaworotko, M.D. Guiver, Stable Superhydrophobic Ceramic-Based Carbon Nanotube Composite Desalination Membranes, Nano Lett. 18 (2018) 5514–5521. https://doi.org/10.1021/acs.nanolett.8b01907.

[190] Y. Si, C. Sun, D. Li, F. Yang, C.Y. Tang, X. Quan, Y. Dong, M.D. Guiver, Flexible

Superhydrophobic Metal-Based Carbon Nanotube Membrane for Electrochemically Enhanced Water Treatment, Environ. Sci. Technol. 54 (2020) 9074–9082. https://doi.org/10.1021/acs.est.0c01084.

[191] X. Fan, Y. Liu, X. Quan, H. Zhao, S. Chen, G. Yi, L. Du, High desalination permeability, wetting and fouling resistance on superhydrophobic carbon nanotube hollow fiber membrane under self-powered electrochemical assistance, J. Memb. Sci. 514 (2016) 501–509. https://doi.org/10.1016/j.memsci.2016.05.003.

[192] A. V. Dudchenko, J. Rolf, K. Russell, W. Duan, D. Jassby, Organic fouling inhibition on electrically conducting carbon nanotube–polyvinyl alcohol composite ultrafiltration membranes, J. Memb. Sci. 468 (2014) 1–10. https://doi.org/10.1016/j.memsci.2014.05.041.

[193] N.A. Zakaria, S.Q. Zaliman, C.P. Leo, A.L. Ahmad, B.S. Ooi, P.E. Poh, Electrochemical cleaning of superhydrophobic polyvinylidene fluoride/polymethyl methacrylate/carbon black membrane after membrane distillation, J. Taiwan Inst. Chem. Eng. 138 (2022) 104448. https://doi.org/10.1016/j.jtice.2022.104448.

[194] N.A. Zakaria, S.Q. Zaliman, C.P. Leo, A.L. Ahmad, B.S. Ooi, P.E. Poh, 3D imprinted superhydrophobic polyvinylidene fluoride/carbon black membrane for membrane distillation with electrochemical cleaning evaluation, J. Environ. Chem. Eng. 10 (2022) 107346. https://doi.org/10.1016/j.jece.2022.107346.

[195] S.J.W. D.Y. Cheng, Composite membrane for a membrane distillation system, In Google Patents (1983).

[196] J. Nambikkattu, N.J. Kaleekkal, Development of Janus membranes with asymmetric wettability for desalination of impaired seawater by direct contact membrane distillation, J. Environ. Chem. Eng. 11 (2023) 111396. https://doi.org/10.1016/j.jece.2023.111396.

[197] Z. Zhu, Y. Liu, H. Hou, W. Shi, F. Qu, F. Cui, W. Wang, Dual-Bioinspired Design for Constructing Membranes with Superhydrophobicity for Direct Contact Membrane Distillation, Environ. Sci. Technol. 52 (2018) 3027–3036. https://doi.org/10.1021/acs.est.7b06227.

[198] Y. Chen, K.-J. Lu, W. Gai, T.-S. Chung, Nanofiltration-Inspired Janus Membranes with Simultaneous Wetting and Fouling Resistance for Membrane Distillation, Environ. Sci. Technol. 55 (2021) 7654–7664. https://doi.org/10.1021/acs.est.1c01269.

[199] A.M. Hyde, S.L. Zultanski, J.H. Waldman, Y.-L. Zhong, M. Shevlin, F. Peng, General Principles and Strategies for Salting-Out Informed by the Hofmeister Series, Org. Process Res. Dev. 21 (2017) 1355–1370. https://doi.org/10.1021/acs.oprd.7b00197.

[200] D.L. Shaffer, L.H. Arias Chavez, M. Ben-Sasson, S. Romero-Vargas Castrillón, N.Y. Yip, M. Elimelech, Desalination and Reuse of High-Salinity Shale Gas Produced Water: Drivers, Technologies, and Future Directions, Environ. Sci. Technol. 47 (2013) 9569–9583. https://doi.org/10.1021/es401966e.

[201] B. Muster-Slawitsch, N. Dow, D. Desai, D. Pinches, C. Brunner, M. Duke, Membrane distillation for concentration of protein-rich waste water from meat processing, J. Water Process Eng. 44 (2021) 102285. https://doi.org/10.1016/j.jwpe.2021.102285.

[202] J.M. Moreira Barradas, B. Dida, S. Matula, F. Dolezal, A model to formulate

nutritive solutions for fertigation with customized electrical conductivity and nutrient ratios, Irrig. Sci. 36 (2018) 133–142. https://doi.org/10.1007/s00271-018-0569-9.

[203] Sudaryanto, W. Naily, Ratio of Major Ions in Groundwater to Determine Saltwater Intrusion in Coastal Areas, IOP Conf. Ser. Earth Environ. Sci. 118 (2018) 012021. https://doi.org/10.1088/1755-1315/118/1/012021.

[204] J. Zhang, N. Dow, M. Duke, E. Ostarcevic, J.-D. Li, S. Gray, Identification of material and physical features of membrane distillation membranes for high performance desalination, J. Memb. Sci. 349 (2010) 295–303. https://doi.org/10.1016/j.memsci.2009.11.056.

[205] F. Banat, S. Al-Asheh, M. Qtaishat, Treatment of waters colored with methylene blue dye by vacuum membrane distillation, Desalination 174 (2005) 87–96. https://doi.org/10.1016/j.desal.2004.09.004.

[206] F. Li, J. Huang, Q. Xia, M. Lou, B. Yang, Q. Tian, Y. Liu, Direct contact membrane distillation for the treatment of industrial dyeing wastewater and characteristic pollutants, Sep. Purif. Technol. 195 (2018) 83–91. https://doi.org/10.1016/j.seppur.2017.11.058.

[207] J.J. Salazar-Rabago, R. Leyva-Ramos, J. Rivera-Utrilla, R. Ocampo-Perez, F.J. Cerino-Cordova, Biosorption mechanism of Methylene Blue from aqueous solution onto White Pine (Pinus durangensis) sawdust: Effect of operating conditions, Sustain. Environ. Res. 27 (2017) 32–40. https://doi.org/10.1016/j.serj.2016.11.009.

[208] H.V. Le, N.T. Dao, H.T. Bui, P.T. Kim Le, K.A. Le, A.T. Tuong Tran, K.D. Nguyen, H.H. Mai Nguyen, P.H. Ho, Bacterial Cellulose Aerogels Derived from Pineapple Peel Waste for the Adsorption of Dyes, ACS Omega 8 (2023) 33412–33425. https://doi.org/10.1021/acsomega.3c03130.

[209] J. Cai, M. Zhou, W. Yang, Y. Pan, X. Lu, K.G. Serrano, Degradation and mechanism of 2,4-dichlorophenoxyacetic acid (2,4-D) by thermally activated persulfate oxidation, Chemosphere 212 (2018) 784–793. https://doi.org/10.1016/j.chemosphere.2018.08.127.

[210] A. Alkhatib, M.A. Ayari, A.H. Hawari, Fouling mitigation strategies for different foulants in membrane distillation, Chem. Eng. Process. - Process Intensif. 167 (2021) 108517. https://doi.org/10.1016/j.cep.2021.108517.

[211] G. Egabaierdi, H.-B. Yu, Y. Li, X.-Q. Zhang, H.-O. Song, M.-X. Du, Effect of dye aggregation and salting-out on membrane fouling and control measures during nanofiltration of saline dye wastewater, J. Water Process Eng. 50 (2022) 103285. https://doi.org/10.1016/j.jwpe.2022.103285.

[212] D. Wang, X. Luo, S. Yang, G. Xue, Tourmaline/Perovskite composite material as heterogeneous catalysts for activation peroxymonosulfate to remove organic dye in water, J. Environ. Chem. Eng. 9 (2021) 105221. https://doi.org/10.1016/j.jece.2021.105221.

[213] H. Li, Z. Yang, S. Lu, L. Su, C. Wang, J. Huang, J. Zhou, J. Tang, M. Huang, Nano-porous bimetallic CuCo-MOF-74 with coordinatively unsaturated metal sites for peroxymonosulfate activation to eliminate organic pollutants: Performance and mechanism, Chemosphere 273 (2021) 129643. https://doi.org/10.1016/j.chemosphere.2021.129643.

[214] K. Zhang, D. Sun, C. Ma, G. Wang, X. Dong, X. Zhang, Activation of

peroxymonosulfate by CoFe2O4 loaded on metal-organic framework for the degradation of organic dye, Chemosphere 241 (2020) 125021. https://doi.org/10.1016/j.chemosphere.2019.125021.

[215] X. Pan, R. Zhu, L. Zhao, H. Ma, Z. Qiu, X. Gong, M. Sun, Peroxymonosulfate activation by iron-cobalt bimetallic phosphide modified nickel foam for efficient dye degradation, Environ. Res. 258 (2024) 119420. https://doi.org/10.1016/j.envres.2024.119420.

[216] Y. Gao, W. Cao, K. Wang, H. Shi, S. Wang, Q. Meng, K. Du, C. Wang, J. Lin, Performance and mechanism of magnetic Fe3O4@MnO2 catalyst for rapid degradation of methylene blue by activation of peroxymonosulfate, J. Alloys Compd. 987 (2024) 174144. https://doi.org/10.1016/j.jallcom.2024.174144.

[217] G. Cao, J. Zhao, G. Zhao, D. Wan, Z. Wu, R. Li, Q. He, Determination of the Acute and Chronic Toxicity of Sulfate from the Sulfur Autotrophic Denitrification Process to Juvenile Zebrafish (Danio rerio), ACS Omega 7 (2022) 47165–47173. https://doi.org/10.1021/acsomega.2c06320.

[218] D. Breite, M. Went, A. Prager, A. Schulze, Tailoring Membrane Surface Charges: A Novel Study on Electrostatic Interactions during Membrane Fouling, Polymers (Basel). 7 (2015) 2017–2030. https://doi.org/10.3390/polym7101497.

[219] L. Meng, Y. Lv, P. Deng, N. Li, M. Huang, J. Mansouri, V. Chen, Novel PVDF membrane with sandwich structure for enhanced membrane distillation, Chem. Eng. J. 415 (2021) 128960. https://doi.org/10.1016/j.cej.2021.128960.

[220] C. Luo, Q. Liu, Oxidant-Induced High-Efficient Mussel-Inspired Modification on PVDF Membrane with Superhydrophilicity and Underwater Superoleophobicity Characteristics for Oil/Water Separation, ACS Appl. Mater. Interfaces 9 (2017) 8297–8307. https://doi.org/10.1021/acsami.6b16206.

[221] M. Bhadra, S. Roy, S. Mitra, Enhanced desalination using carboxylated carbon nanotube immobilized membranes, Sep. Purif. Technol. 120 (2013) 373–377. https://doi.org/10.1016/j.seppur.2013.10.020.

[222] M. Bhadra, S. Roy, S. Mitra, Flux enhancement in direct contact membrane distillation by implementing carbon nanotube immobilized PTFE membrane, Sep. Purif. Technol. 161 (2016) 136–143. https://doi.org/10.1016/j.seppur.2016.01.046.

[223] J.E. Gordon, R.L. Thorne, Salt effects on the activity coefficient of naphthalene in mixed aqueous electrolyte solutions. I. Mixtures of two salts, J. Phys. Chem. 71 (1967) 4390–4399. https://doi.org/10.1021/j100872a035.

[224] W.E. May, S.P. Wasik, D.H. Freeman, Determination of the solubility behavior of some polycyclic aromatic hydrocarbons in water, Anal. Chem. 50 (1978) 997–1000. https://doi.org/10.1021/ac50029a042.

[225] G. Gold, S. Rodriguez, The effect of temperature and salinity on the Setschenow parameters of naphthalene in seawater, Can. J. Chem. 67 (1989) 822–826. https://doi.org/10.1139/v89-127.

[226] M. Aquan-Yuen, D. Mackay, W.Y. Shiu, Solubility of hexane, phenanthrene, chlorobenzene and p-dichlorobenzene in aqueous electrolyte solutions, J. Chem. Eng. Data 24 (1979) 30–34. https://doi.org/10.1021/je60080a009.

[227] J. Guo, P.W. Wong, B.J. Deka, B. Zhang, S. Jeong, A.K. An, Investigation of fouling mechanism in membrane distillation using in-situ optical coherence

tomography with green regeneration of fouled membrane, J. Memb. Sci. 641 (2022) 119894. https://doi.org/10.1016/j.memsci.2021.119894.

[228] P.W. Wong, J. Guo, N.K. Khanzada, V.M.W. Yim, A. Kyoungjin, In-situ 3D fouling visualization of membrane distillation treating industrial textile wastewater by optical coherence tomography imaging, Water Res. 205 (2021) 117668. https://doi.org/10.1016/j.watres.2021.117668.

[229] A. Salimi, A. Roosta, Experimental solubility and thermodynamic aspects of methylene blue in different solvents, Thermochim. Acta 675 (2019) 134–139. https://doi.org/10.1016/j.tca.2019.03.024.

[230] A. Burant, G. V. Lowry, A.K. Karamalidis, Measurement of Setschenow constants for six hydrophobic compounds in simulated brines and use in predictive modeling for oil and gas systems, Chemosphere 144 (2016) 2247–2256. https://doi.org/10.1016/j.chemosphere.2015.10.115.

[231] B. Yang, Z. Li, L. Lei, F. Sun, J. Zhu, Prediction of Setschenow constants of N-heteroaromatics in NaCl solutions based on the partial charge on the heterocyclic nitrogen atom, Environ. Sci. Pollut. Res. 23 (2016) 3399–3405. https://doi.org/10.1007/s11356-015-5544-x.

[232] A. Burant, G. V. Lowry, A.K. Karamalidis, Measurement and Modeling of Setschenow Constants for Selected Hydrophilic Compounds in NaCl and CaCl 2 Simulated Carbon Storage Brines, Acc. Chem. Res. 50 (2017) 1332–1341. https://doi.org/10.1021/acs.accounts.6b00567.